

# Information on Technical Impracticability for Remediation of Iodine- 129 Contamination

Summary of Data and Modeling for  
Hanford Site 200-UP-1 Operable Unit

September 2019

ML Rockhold  
SR Waichler  
JL Downs  
X He  
JD Tagestad  
Y Fang  
VL Freedman  
MJ Truex  
CMR Yonkofski

## DISCLAIMER

This report was prepared as an account of work sponsored by an agency of the United States Government. Neither the United States Government nor any agency thereof, nor Battelle Memorial Institute, nor any of their employees, makes **any warranty, express or implied, or assumes any legal liability or responsibility for the accuracy, completeness, or usefulness of any information, apparatus, product, or process disclosed, or represents that its use would not infringe privately owned rights.** Reference herein to any specific commercial product, process, or service by trade name, trademark, manufacturer, or otherwise does not necessarily constitute or imply its endorsement, recommendation, or favoring by the United States Government or any agency thereof, or Battelle Memorial Institute. The views and opinions of authors expressed herein do not necessarily state or reflect those of the United States Government or any agency thereof.

PACIFIC NORTHWEST NATIONAL LABORATORY  
*operated by*  
BATTELLE  
*for the*  
UNITED STATES DEPARTMENT OF ENERGY  
*under Contract DE-AC05-76RL01830*

Printed in the United States of America

Available to DOE and DOE contractors from the  
Office of Scientific and Technical Information,  
P.O. Box 62, Oak Ridge, TN 37831-0062;  
ph: (865) 576-8401  
fax: (865) 576-5728  
email: [reports@adonis.osti.gov](mailto:reports@adonis.osti.gov)

Available to the public from the National Technical Information Service  
5301 Shawnee Rd., Alexandria, VA 22312  
ph: (800) 553-NTIS (6847)  
email: [orders@ntis.gov](mailto:orders@ntis.gov) <<https://www.ntis.gov/about>>  
Online ordering: <http://www.ntis.gov>

# **Information on Technical Impracticability for Remediation of Iodine-129 Contamination**

Summary of Data and Modeling for Hanford Site 200-UP-1 Operable Unit

September 2019

ML Rockhold  
SR Waichler  
JL Downs  
X He  
JD Tagestad  
Y Fang  
VL Freedman  
MJ Truex  
CMR Yonkofski

Prepared for  
the U.S. Department of Energy  
under Contract DE-AC05-76RL01830

Pacific Northwest National Laboratory  
Richland, Washington 99354

## Summary

Groundwater in the 200-UP-1 operable unit (OU) is contaminated with carbon tetrachloride, uranium, nitrate, chromium (total and hexavalent), iodine-129, technetium-99, and tritium, associated with past nuclear weapons production activities at Hanford. The preferred alternative described in the 2012 Record of Decision (ROD) for the 200-UP-1 OU Interim Remedial Action includes 35 years of active remediation using a combination of groundwater pump-and-treat and monitored natural attenuation (MNA) for portions of the contaminated groundwater, followed by institutional controls until cleanup levels are met for unrestricted use. As noted in the 200-UP-1 OU interim ROD, no treatment technology for iodine-129 had been found that could achieve the drinking water standard (DWS) of 1 pCi/L for the iodine-129 concentrations present in the 200-UP-1 OU groundwater. Therefore, the 200-UP-1 OU interim ROD specified hydraulic containment of the iodine-129 plume, update of the conceptual model for iodine-129, and further evaluation of potentially applicable iodine-129 treatment technologies. The 200-UP-1 OU interim ROD further stated that in the event a viable treatment technology is not available, the use of a technical impracticability (TI) waiver may need to be considered as part of the final remedy and that this information be gathered concurrently with the technology evaluation. Hence, this report provides information relevant to a TI waiver consideration on the current federal 1 pCi/L DWS for iodine-129 in the 200-UP-1 groundwater OU of the Hanford Site.

The 200-UP-1 OU is expected to be under institutional controls, with no withdrawals of groundwater for drinking in the foreseeable future.<sup>1</sup> Long-term monitoring data show that iodine-129 groundwater concentrations are declining slowly over time and the plume area is shrinking. The injection wells used for hydraulic containment appear to be effective in limiting, or eliminating, migration of the plume, although the hydraulic containment wells have only been operating since 2015 and their effects are still being evaluated. Mechanisms that may be responsible for iodine plume attenuation, including volatilization, sorption, and incorporation into carbonate or iron-oxide precipitates, have been identified in laboratory studies supporting an update of the iodine-129 plume conceptual site model. The attenuation mechanisms associated with iodine-129 transport under the oxidizing conditions in the 200-UP-1 aquifer have been demonstrated to be well represented by a kinetic Langmuir model. This was demonstrated in simulations of both column experiments and iodine-129 transport at the field-scale.

The information provided in this report is based on the U.S. Environmental Protection Agency's (EPA's) recommended summary checklist for Superfund site groundwater TI evaluation. The checklist was developed by the EPA to assist regions in evaluating whether they have sufficient information to support a TI evaluation for the administrative record. Categories of information in the checklist include (1) the specific applicable or relevant and appropriate requirements (ARARs) or media cleanup standards that are being addressed, (2) the spatial extent of TI decisions, (3) the development and purpose of the site conceptual model, (4) evaluation of restoration potential, (5) cost estimates, (6) alternative remedial strategies, and (7) additional remedy selection considerations. The EPA checklist is included as Appendix A to this report, with links to specific locations in this document that provide supporting information, including a summary of site hydrogeology, time-histories of measured iodine-129 concentrations in groundwater, and the changes in plume area over time. Appendix B provides a compendium of publications that support the iodine conceptual model, iodine technology evaluation, and data and parameter evaluations. Collectively, these publications support the information required in the EPA checklist.

---

<sup>1</sup> DOE. 2013. *Hanford Site Cleanup Completion Framework*. DOE/RL-2009-10, Rev. 1, U.S. Department of Energy, Richland Operations Office, Richland, Washington.

Although the iodine-129 plume footprint is shrinking over time, model projections suggest that iodine-129 concentrations will remain above the DWS beyond the hydraulic containment period specified in the ROD as an interim remedial action. Hence, to achieve site closure, a TI waiver may be necessary for recalcitrant regions of the plume that remain above the DWS within this timeframe. The information provided in this report addresses the technical basis needed for TI waiver consideration for iodine-129.

## Acknowledgments

This document was prepared by the Deep Vadose Zone – Applied Field Research Initiative at Pacific Northwest National Laboratory. Funding for this work was provided by the U.S. Department of Energy (DOE) Richland Operations Office. We thank Mary Hartman and Margo Aye of CH2M Hill Plateau Remediation Company (CHPRC) for their assistance in providing the most current information regarding iodine-129 contamination in the 200-UP-1 Operable Unit. We also extend our appreciation to Art Lee and Sally Simmons (CHPRC) for providing operational and monitoring data for the 200 West Area pump-and-treat system.

## Acronyms and Abbreviations

ARAR	applicable or relevant and appropriate requirement
CCU	Cold Creek Unit
CERCLA	<i>Comprehensive Environmental Response, Compensation, and Liability Act</i>
CHPRC	CH2M Hill Plateau Remediation Company
DOC	dissolved organic carbon
DOE	U.S. Department of Energy
DWS	drinking water standard
EPA	U.S. Environmental Protection Agency
ERDF	Environmental Restoration Disposal Facility
GFM	Geologic Framework Model
GIS	geographic information system
HF	Hanford formation
HSU	hydrostratigraphic units
K <sub>d</sub>	distribution coefficient
LOWESS	locally-weighted regression
MCL	maximum contaminant level
MNA	monitored natural attenuation
NQAP	Nuclear Quality Assurance Program
Organo-I	organo-iodine
OU	operable unit
P&T	pump-and treat
RAWP	Remedial Action Work Plan
RCRA	Resource Conservation and Recovery Act
REDOX	reduction oxidation
RI/FS	remedial investigation/feasibility study
Rlm	Ringold Formation Lower Mud
ROD	record of decision
Rtf	Ringold Formation Taylor Flats Unit
Rwia	Ringold Formation Wooded Island Unit A
Rwie	Ringold Formation Wooded Island Unit E
SOM	soil organic matter
STOMP	Subsurface Transport Over Multiple Phase
TI	technical impracticability
WMA	Waste Management Area

# Contents

Summary .....	iii
Acknowledgments.....	v
Acronyms and Abbreviations .....	vi
Contents .....	vii
1.0 Introduction.....	1.1
1.1 Background.....	1.2
2.0 Status of Iodine-129 in the 200-UP-1 Operable Unit .....	2.1
2.1 Sources of I-129 .....	2.1
2.2 Areal Extent of Iodine-129 Groundwater Plume .....	2.2
2.3 Vertical Extent of I-129 Plume .....	2.6
2.4 I-129 Trends in Monitoring Wells .....	2.12
3.0 Site Conceptual Model.....	3.1
3.1 Geologic and Hydrologic Features of the 200-UP-1 OU.....	3.2
3.1.1 Physical and Hydraulic Properties of Subsurface Materials.....	3.5
3.1.2 Depth to Groundwater .....	3.6
3.1.3 Hydraulic Gradients (Horizontal and Vertical) .....	3.6
3.1.4 Temporal Variability in Hydrologic Conditions and Contaminant Concentrations .....	3.9
3.1.5 Groundwater Recharge and Discharge Information .....	3.9
3.1.6 Groundwater Withdrawal and Potential Receptors .....	3.11
3.2 Geochemical and Biological Processes Affecting Iodine-129 in Soils and Groundwater .....	3.12
3.2.1 Iodine Speciation .....	3.13
3.2.2 Iodine Sorption .....	3.15
3.2.3 Iodine Transformation Processes.....	3.17
3.3 Iodine-129 Source and Release Information.....	3.18
3.4 Simulation of Iodine-129 Transport and Fate .....	3.19
4.0 Evaluation of Restoration Potential .....	4.1
4.1 Remedial Action Performance Analysis .....	4.1
4.1.1 Hydraulic Containment Remedy for Iodine-129 .....	4.2
4.1.2 Trends in Subsurface Iodine-129 Concentrations.....	4.3
4.2 Restoration Timeframe Analysis .....	4.4
4.3 Other Applicable Technologies .....	4.4
5.0 Summary and Conclusions .....	5.1
6.0 Quality Assurance.....	6.1
7.0 References.....	7.1
Appendix A Summary Checklist for Groundwater Technical Impracticability Evaluation .....	A.1



Appendix B Compendium of References on Iodine-129 at Hanford.....	B.1
---	-----

## Figures

Figure 1.1. Location of 200-UP-1 Operable Unit on the Central Plateau at the Hanford Site (from DOE 2013a) .....	1.4
Figure 1.2. Groundwater Contaminant Plumes in 200-UP-1 Operable Unit (DOE 2019) .....	1.6
Figure 2.1. Key Iodine-129 Source Areas within 200-UP-1 OU in Relation to the 2018 Iodine-129 Plume. Light and dark plume colors denote 1 and 10 pCi/L contour levels, respectively. ....	2.2
Figure 2.2. Detailed Map of Iodine-129 Plume from Hanford Site Groundwater Monitoring Report for 2018, DOE/RL-2018-66 (DOE 2019a). (Groundwater monitoring wells are shown with iodine-129 concentration data (pCi/L) as of publication of that report, followed by the well identifier.) .....	2.3
Figure 2.3. Estimated Extent of the 200-UP-1 OU Iodine-129 Plume for 1993 to 2008 with 1, 5, and 20 pCi/L contours.....	2.4
Figure 2.4. Estimated Extent of the 200-UP-1 OU Iodine-129 Plume for the Period from 2007 through 2017 for the 1 and 10 pCi/L Contour Levels.....	2.5
Figure 2.5. Trend in Estimated Areal Extent of the Iodine-129 Plume in 200-UP-1 Operable Unit.....	2.6
Figure 2.6. Location Map Showing Groundwater Plumes and Conception Cross Section Orientations within 200-UP-1 (Figure A-1 from DOE 2013a). Cross sections corresponding to lines A-A' and F-F' are shown in Figure 2.7 and Figure 2.8.....	2.9
Figure 2.7. Iodine-129 Conceptual Cross Section A-A' (Figure A-6 in DOE 2013a). ....	2.10
Figure 2.8. Iodine-129 Conceptual Cross Section F-F' (Figure A-7 in DOE 2013a).....	2.11
Figure 2.9. Iodine-129 Plume for 2018 (Hanford Site Groundwater Monitoring Program) and Selected Wells, Color-Coded by Their Maximum Lifetime Iodine-129 Concentration Value (pCi/L). Light and dark plume colors denote 1 and 10 pCi/L contour levels, respectively.....	2.12
Figure 2.10. Iodine-129 Concentration versus Time at Selected Wells—Set 1. Solid blue dots represent measured values and open circles represent non-detects (which are reported with a value). The locally-weighted regression (LOWESS) line (black) suggests the approximate trend over time (fit excludes non-detects). The well location in relation to the 2017 plume is shown as a black dot in the panel strip. Wells are arranged in order of decreasing value of the most recent point in time of the trend line. ....	2.13
Figure 2.11. Iodine-129 Concentration versus Time at Selected Wells—Set 2. Solid blue dots are measured values, open circles are non-detects (which are reported with a value). Black line is a locally-weighted regression (LOWESS) line to suggest an approximate trend over time (fit excludes non-detects). Well location in relation to the 2017 plume is shown as a black dot in the panel strip. Wells are arranged in order of decreasing value of the most recent point in time of the trend line, continuing from set 1 wells in Figure 2.10. ....	2.14
Figure 3.1. System-Level Depiction of Elements Affecting Iodine Fate and Transport. ....	3.1
Figure 3.2. Hydrostratigraphic Units and Generalized Hanford Site Stratigraphy for 200-UP-1 Groundwater OU (Hammond and Lupton 2015).....	3.3

Figure 3.3. Cross Sections of Geologic Framework Model (GFM), West to East (a) (left to right) and South to North (b) through the 1 pCi/L Plume Center of the 2017 Iodine-129. Red ticks under the blue water table line mark the lateral extent of the plume. The extent of GFM and its discretization shown here are for the eSTOMP model domain. Grid blocks are 50 m in x- and y-directions and 5 m in the z-direction. Vertical exaggeration of the figure is 10x.....	3.4
Figure 3.4. Conceptual Vertical Cross Section Showing the Extent of Contaminant Plumes with Respect to Hydrostratigraphic Units (from DOE 2013a).....	3.5
Figure 3.5. Water Table Elevation in 200-UP Interest Area from March 2016 (Figure 11-2 from DOE 2017b).....	3.7
Figure 3.6. Water Level Monitoring Network and Water Table Elevations as Influenced by Iodine-129 Plume Hydraulic Containment Remedy as of December 2018 (DOE/RL-2018-66; DOE 2019a).....	3.8
Figure 3.7. Measured Water Table Elevations Over Time at Selected Wells. Water level data are from the Hanford Environmental Information System. The well location in relation to the 2017 plume is shown as a black dot in the panel strip.....	3.10
Figure 3.8. Conceptual Overview of Subsurface Biogeochemical Processes Affecting Iodine Fate and Transport (from Truex et al. 2017). Processes include biotic (bacteria) transformations between iodine species and potential transformations to other iodine species. Iodate reduction may also occur abiotically (e.g., by reactions with sediment-associated iron/manganese at the Hanford Site). Iodine species adsorb to sediment surfaces (e.g., on iron oxide deposits or phyllosilicates), with greater adsorption expected in fine-textured sediment zones (Fines). Natural organic matter may facilitate sorption and accumulation of iodine or, as a dissolved organic carbon (DOC), may form mobile Organo-I. Iodate may co-precipitate with calcium carbonate. The figure does not distinguish between iodine-129 and iodine-127 because the processes are the same for both isotopes.....	3.13
Figure 3.9. Reference Map Showing eSTOMP Model Domain. Transect lines A-A' and F-F' are same as those in Figure 2.6.....	3.21
Figure 3.10. Simulation results and observed iodate breakthrough curve data for the Column 1 experiment from Qafoku et al. (2018). ....	3.22
Figure 3.11. eSTOMP Simulation Results (filled contours) Using a One-Site Kinetic Langmuir Sorption Model, and Geographic Information System (GIS) Maps of Field Data (contour lines) for Years 2009-2018. Green filled and open circles are the centers of the 1 pCi/L contours for the simulated and GIS-based plumes, respectively.....	3.23
Figure 3.12. eSTOMP Simulation Results (filled contours) Using a One-Site Kinetic Langmuir Sorption Model, and Geographic Information System (GIS) Maps of Field Data (contour lines) for Years 2015-2100.....	3.24
Figure 4.1. Water Table for the Iodine 129 Plume Hydraulic Containment Remedy, December 2018 (from DOE 2019b).....	4.3

## Tables

Table 2.1. Iodine-129 Sample Results by Depth for New Wells Drilled in 2016 in 200-UP-1. (Data for well 299-W21-3, well 299-W22-114, well 699-36-63B, well 299-W19-115, and well 299-W19-116 as reported in Tables 11.2 through 11.6 in DOE 2017b; <i>Hanford Site Groundwater Monitoring Report for 2016</i> .) .....	2.8
--	-----

Table 3.1. Estimated Long-Term Recharge Rates for Use in Hanford Assessments (Table 6.1 from Fayer and Keller 2007).....	3.11
Table 3.2. Chemistry and Iodine-127 Speciation in Filtered Hanford Site Groundwater Samples (from Zhang et al. 2013) .....	3.14
Table 3.3. Iodine Speciation in Groundwater Samples During Drilling Monitoring Well 299-W22-114 (August 2016) (from Truex et al. 2017).....	3.15
Table 3.4. Iodine Speciation in Groundwater Samples Collected Over the Length of the 200-UP-1 Plume (from Truex et al. 2017).....	3.15
Table 3.5. Primary Waste Sites with Highest Iodine-129 Activity and Liquid Effluent Releases in 200-UP-1 (Eslinger et al. 2006a,b). ....	3.18
Table 3.6. Characteristics of the Iodine-129 Plume Within 200-UP-1 (from 200-UP-1 RAWP; DOE 2013a) .....	3.19
Table 3.7. Estimated and Modeled Migration of Iodine-129 Groundwater Plume. Movement of the plume as documented by the Groundwater Monitoring Program (DOE 2018a) is calculated from the centroids of the GIS polygons representing the 1 pCi/L plume. Movement of the plume is calculated from the center of mass for dissolved iodine-129 in the z = 110-120 m horizon.....	3.25

# 1.0 Introduction

The 200-UP-1 groundwater operable unit (OU), located on the U.S. Department of Energy (DOE) Hanford Site in southeastern Washington State, consists of the groundwater beneath the southern portion of the 200 West Area within the Central Plateau, as shown in Figure 1.1. Groundwater in the 200-UP-1 OU is contaminated with carbon tetrachloride, uranium, nitrate, chromium (total and hexavalent), iodine-129, technetium-99, and tritium. The DOE Richland Operations Office is the lead agency for remediation of the 200-UP-1 OU and the U.S. Environmental Protection Agency (EPA) is the lead regulatory agency, as identified in Section 5.6 and Appendix C of the Tri-Party Agreement.<sup>1</sup> In accordance with the Tri-Party Agreement, Article XIV, Paragraph 54, DOE developed and proposed remedial action for the 200-UP-1 OU through completion and approval of a remedial investigation/feasibility study (RI/FS) (DOE 2012a). The *Record of Decision for Interim Remedial Action, Hanford 200 Area Superfund Site, 200-UP-1 Operable Unit* (hereafter referred to as the 200-UP-1 OU ROD) (EPA et al. 2012) was signed by EPA, DOE, and the Washington State Department of Ecology on September 27, 2012. The selected interim remedy was chosen in accordance with the *Comprehensive Environmental Response, Compensation, and Liability Act* (CERCLA), as amended by the *Superfund Amendments and Reauthorization Act of 1986*, the Tri-Party Agreement, and, to the extent practicable, the National Contingency Plan (40 CFR 300). This decision is based on the Administrative Record file for the 200-UP-1 OU.

The preferred alternative described in the 200-UP-1 OU ROD includes 35 years of active remediation using a combination of groundwater pump-and-treat (P&T) and monitored natural attenuation (MNA) for portions of the contaminated groundwater, followed by institutional controls until cleanup levels are met for unrestricted use (EPA et al. 2012; DOE 2012c). The selected interim remedy stipulates groundwater P&T for parts of the carbon tetrachloride plume, technetium-99 plumes, uranium plume, high-concentration nitrate plume area, and chromium (total and hexavalent) plumes, remedy performance monitoring for all plumes, followed by institutional controls. However, as noted in the 200-UP-1 OU ROD, no current treatment technology for iodine-129 had been identified that could achieve the federal drinking water standard (DWS) of 1 pCi/L for the iodine-129 concentrations present in the 200-UP-1 OU groundwater. The 200-UP-1 OU interim ROD specified hydraulic containment of the iodine-129 plume and further evaluation of potentially applicable iodine-129 treatment technologies. An assessment of potential remediation technologies is provided by Truex et al. (2019). The 200-UP-1 OU ROD further stated that the interim remedial action:

“is only a part of the expected total remedial action for the 200-UP-1 OU, that will attain or otherwise waive the ARAR for iodine-129 upon completion of remedial action, as required by CERCLA Section 121(d)(4), “Cleanup Standards,” “Degree of Cleanup. A subsequent ROD will be needed to complete the total remedial action for the 200-UP-1 OU. In the event a viable treatment technology is not available, the use of a technical impracticable waiver under 40 CFR 300.430(f)(1)(ii)(c) may need to be considered as part of the final remedy.”

This document provides information relevant to future consideration of a technical impracticability (TI) waiver for iodine-129 in the 200-UP-1 OU if the evaluation of potential treatment options does not identify feasible remediation technologies. The technology evaluation plan for iodine-129 specified in the interim ROD has been prepared, and updates to the conceptual model for the plume, reviews of current literature, and a feasibility analysis of potential treatment options have been published (DOE 2017a;

<sup>1</sup> Hanford Federal Facility Agreement and Consent Order by Washington State Department of Ecology, United States Environmental Protection Agency, United States Department of Energy, as Amended Through March 28, 2018, 89-10 Rev. 8.

Truex et al. 2017; Truex et al. 2019). In situ technologies that have been evaluated include contaminant sequestration via co-precipitation and enhanced sorption processes, and treatments that would enhance iodine mobility for capture in the P&T facility. Efficient materials for ex situ removal of iodine from groundwater have also been evaluated. The outcome of these technology evaluations is documented in Truex et al. (2019).

This report is an update (Rev. 1) to an earlier draft TI evaluation report for iodine-129 in the 200-UP-1 OU. Updates include the following. Figures and associated text were revised to address the most recent interpretation of the iodine-129 plume (DOE 2019a). Time-series plots were updated to include more recent (2018-2019) well monitoring data. Modeling results are from a revised subsurface flow and transport model that represents a smaller domain (200-UP-1 OU only, instead of the combined 200-UP-1 and 200-ZP-1 OUs). The revised model is also based on a Central Plateau Vadose Zone Geologic Framework Model (Springer et al. 2018), instead of a Hanford South Geologic Framework Model (Hammond and Lupton, 2015). Physical and hydraulic properties were updated based on aquifer test results for wells in the 200-UP-1 OU. Lateral boundary conditions for the model were updated to use field-measured water level data through 2018. The groundwater iodine-129 plume from 1993 was used as an initial condition, instead of propagating uncertain historical liquid effluent and iodine-129 release estimates through the vadose zone. Finally, iodine-129 transport was modeled using a kinetic Langmuir sorption model instead of an equilibrium linear-Freundlich isotherm (a.k.a.  $K_d$ ) model.

The report is organized as follows. The remainder of Section 1 provides background information on the Hanford 200 West Area and the 200-UP-1 OU. Section 2 provides information on the distribution and extent of the iodine-129 plume. Section 3 describes the components considered in the conceptual model for iodine-129 including the waste disposal history for 200-UP-1 OU, hydrogeological features affecting iodine-129 distribution and movement, and the biogeochemical processes affecting fate and transport of iodine-129. Section 3 includes simulation results from an updated flow and I-129 transport model for the 200-UP-1 OU. Implementation of hydraulic containment as the interim remedy for iodine-129 is described in Section 4, along with brief descriptions of alternative iodine-129 remedy technologies that are being considered. Appendix A contains the EPA's checklist for groundwater TI evaluation.

## 1.1 Background

The iodine-129 plume lies within the 200-UP-1 OU, which encompasses the groundwater contaminant plumes beneath the southern portion of the 200 West Area and adjacent portions of the surrounding area (Figure 1.1) (DOE 2017b). The 200 West Area is approximately 8 km<sup>2</sup> (3 mi<sup>2</sup>) in size and is located near the middle of the Hanford Site on an elevated, flat area that is often referred to as the Central Plateau. The Central Plateau contains no perennial streams, wetlands, or floodplains (DOE 2013a). The 200-UP-1 OU is bounded on the eastern side by the 200-PO-1 groundwater OU and to the north by the 200-ZP-1 groundwater OU. The 200-UP-1 OU lies about 8 km (5 mi) from the Columbia River and 11.3 km (7 mi) from the nearest Hanford Site boundary (Figure 1.1) (DOE 2013a).

Contamination of groundwater in the 200-UP-1 OU has resulted primarily from historical operations and disposal of liquid wastes associated with uranium and plutonium recovery processes. Bulk liquid waste discharges contributing to the majority of the contamination in the subsurface occurred from 1944 to the early 1990s. No liquid waste discharges currently occur to the ground above the OU (with the exception of septic drain fields) (DOE 2013a). The extent of the iodine-129 plume is shown in context with the other contaminant plumes in 200-UP-1 groundwater in Figure 1.2.

The remedies selected in the interim ROD for 200-UP-1 contaminants are outlined in the remedial action work plan for the 200-UP-1 OU (DOE 2013a). P&T remedies combined with MNA are expected to achieve cleanup levels for technetium-99 within 15 years, for uranium within 25 years, for chromium

(total and hexavalent) within 25 years, and for nitrate within 35 years. MNA is the selected remedy for the tritium plume, which is expected to achieve cleanup levels within 25 years. Active restoration and MNA are anticipated to take approximately 125 years to reach the cleanup level for carbon tetrachloride, which is consistent with the time frame for cleanup of carbon tetrachloride in the adjacent 200-ZP-1 OU. Institutional controls will be implemented to prevent exposure and groundwater use until cleanup levels are achieved for these contaminants.

The RI/FS determined that mature, demonstrated, ex situ treatment processes were not available at that time to achieve the federal DWS of 1 pCi/L for iodine-129 in the groundwater in 200-UP-1 OU. Therefore, the 200-UP-1 interim ROD (EPA et al. 2012) specified that hydraulic containment of the iodine-129 plume would be implemented until a subsequent remedial decision is made regarding the iodine-129 plume. In addition, the interim ROD specified a technology evaluation plan for iodine-129 be prepared to provide an update to the conceptual model for the plume, a review of current literature, and a feasibility analysis of potential treatment options (DOE 2017a). That report fulfilled the associated Tri-Party Agreement milestone, M-016-192, “Submit I-129 Technology Evaluation Plan Draft A to EPA as defined in the 200-UP-1 RD/RA WP.”

Remediating the iodine-129 plume in the 200-UP-1 OU is technically challenging. The plume is large but dilute. However, the DWS is also very low. Iodine is typically very mobile in the environment, but its mobility varies with environmental conditions. Various forms are soluble in water and/or volatile, and iodine speciation affects their mobility, phase partitioning, and reactivity. Minerals such as iron and manganese may mediate iodine transformation processes, either directly or coupled with microbial processes. Iodine may also interact with organic materials in the subsurface to form (1) immobile, sediment-associated organo-iodine (Organo-I) compounds, (2) mobile soluble Organo-I compounds, or (3) volatile Organo-I compounds. Organic materials can also affect iodine fate and transport through microbially-mediated reduction reactions that directly or indirectly affect iodine speciation or by providing adsorption capacity for iodine species.

Another key challenge in remediating the iodine-129 is that naturally occurring, stable iodine-127 also exists in the plume and is present at much greater concentrations than iodine-129. For most strong sorbents to work effectively to lower iodine-129 concentrations, they would also have to lower natural iodine concentrations by about two orders of magnitude (Kaplan et al. 2012). As natural stable iodine concentrations in groundwater are decreased by treatment, Hanford sediments could potentially release additional iodine in response to the altered adsorption/desorption and solubility equilibrium in the subsurface system. Together, the large size of the iodine-129 plume, the very low target concentration, and the presence of relatively high concentrations of the stable iodine isotope significantly limit practical remediation options for iodine-129. A current assessment of potentially viable remediation technologies for iodine-129 in the 200-UP-1 OU is provided by Truex et al. (2019).

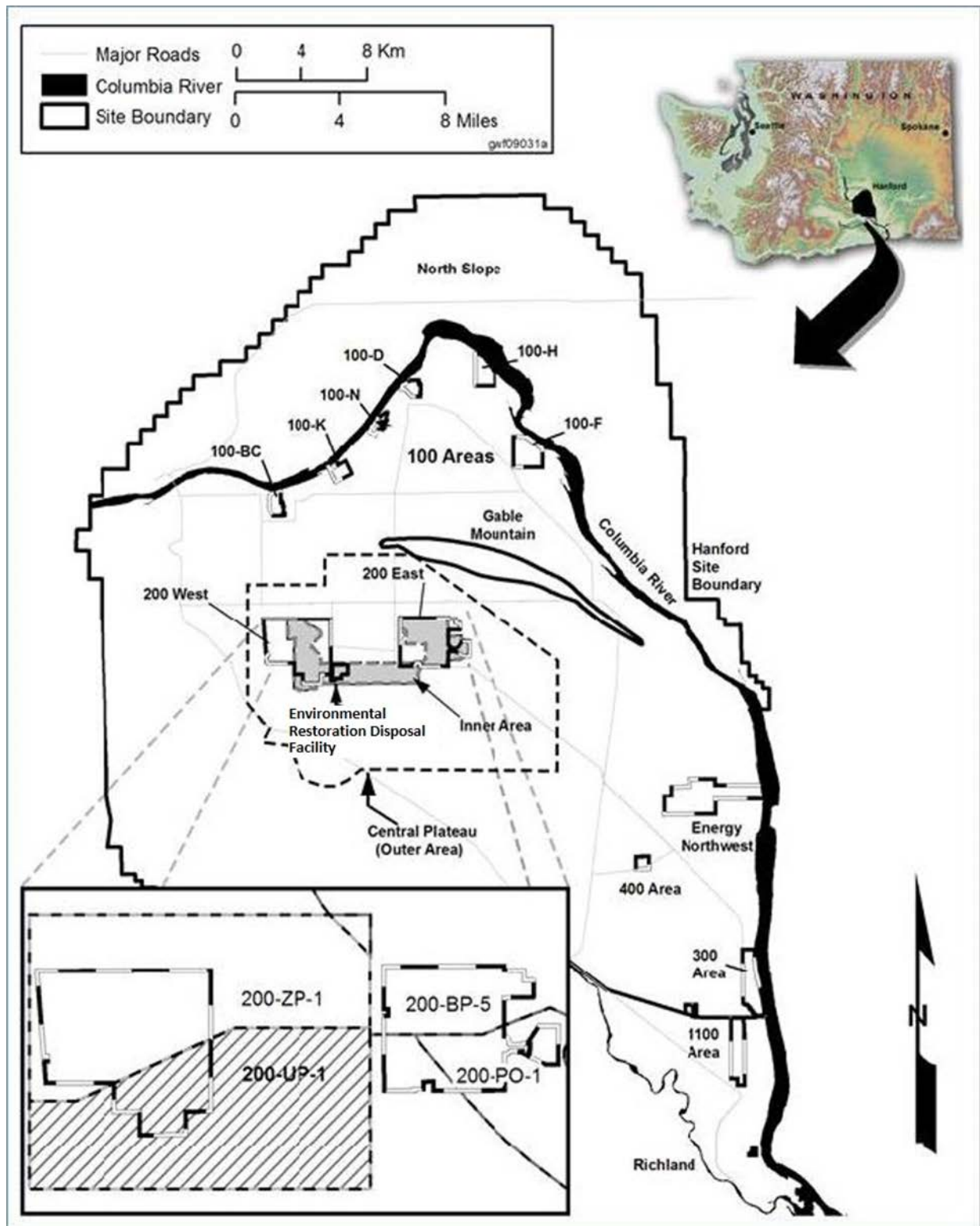


Figure 1.1. Location of 200-UP-1 Operable Unit on the Central Plateau at the Hanford Site (from DOE 2013a)

Potential remediation options for iodine-129 are being evaluated as specified in the 200-UP-1 ROD (DOE 2017a). The remediation technology evaluation will compile sufficient information about the technology options to demonstrate whether they are viable with respect to meeting the 200-UP-1 OU remedial action objectives for iodine-129. Based on the technology evaluation results, the OU can either pursue a TI or other applicable or relevant and appropriate requirements (ARAR) waiver or conduct a focused feasibility study to select an iodine-129 remedy other than the hydraulic control remedy identified in the 200-UP-1 OU ROD.

In addition to the iodine-129 plume in 200-UP-1, the contaminant plumes and sources within the 200-UP-1 OU include the following (Figure 1.2):

- A uranium plume originating from the U Plant cribs
- A widespread nitrate plume originating from U Plant and S Plant cribs and Waste Management Area (WMA) S-SX
- A chromium (total and hexavalent) plume associated with WMA S-SX, and a dispersed chromium (total and hexavalent) plume in the southeast corner of the OU that originated from an S Plant crib
- Four separate technetium-99 plumes associated with WMA U, U Plant cribs, and WMA S-SX
- A widespread tritium plume originating from S Plant cribs
- In addition to the plumes that formed within the 200-UP-1 OU, a widespread carbon tetrachloride plume exists over a large portion of the 200 West Area. This plume originated from operation of the Plutonium Finishing Plant (Z Plant) facilities and has spread south and east from the 200-ZP-1 OU and into the 200-UP-1 OU.

Some of these contaminant plumes overlap portions of the iodine-129 plume, as shown in Figure 1.2, but are not explicitly considered in this evaluation of the TI for remediating iodine. Any remedy applied to address iodine-129 will need to consider the effects of the remedy on other contaminants within the 200-UP-1 OU. The nitrate plume currently has the largest overlap with the iodine-129 plume in the 200-UP-1 OU.



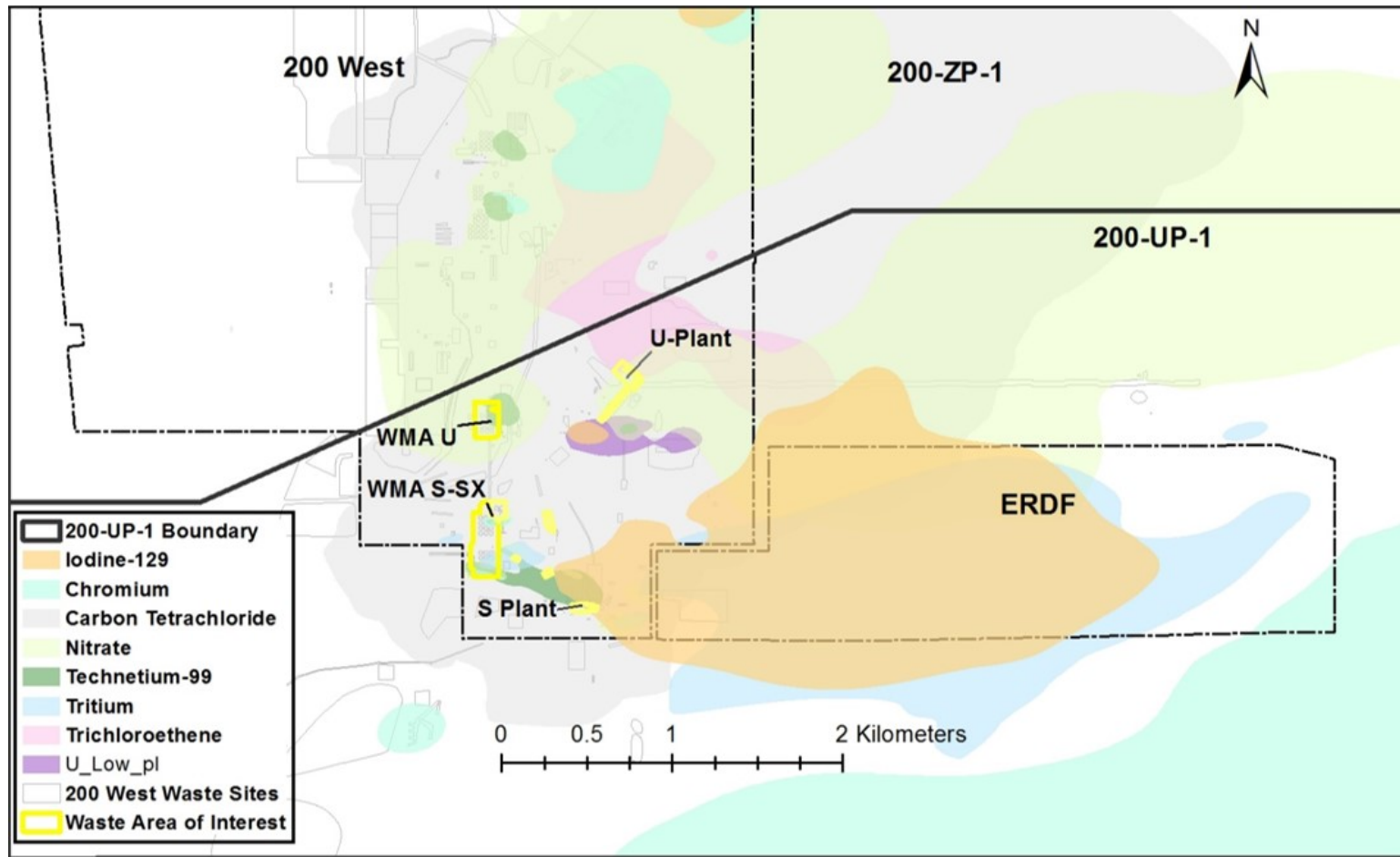


Figure 1.2. Groundwater Contaminant Plumes in 200-UP-1 Operable Unit (DOE 2019a)

## 2.0 Status of Iodine-129 in the 200-UP-1 Operable Unit

The sources of contaminants currently observed in groundwater at 200-UP-1 were primarily planned releases of the process liquid wastes and wastewater to the soil via discharge to engineered structures (cribs, trenches, ditches, ponds, leach fields, or injection wells). Releases to these engineered structures occurred during the 1940s through the 1990s, and there are no current liquid discharges within the OU. The iodine-129 groundwater contaminant plume resulting from the historical discharge is well defined, occurring within the unconfined aquifer beneath, and east of, the 200 West Area (DOE 2012a). The 200-UP-1 iodine-129 plume extends less than 5 km to the east of the originating waste sources and does not interact with any surface waters within or adjacent to its boundaries.

Withdrawal of groundwater from 200-UP-1 OU is prohibited by DOE institutional controls placed on groundwater use. The existing institutional controls (specifically, prohibitions against use of groundwater for a source of drinking water) prevent human exposure. The plume currently does not extend past the OU boundary and does not extend to the groundwater discharge areas along the Columbia River to the east; thus, no ecological receptors are exposed. Estimates of groundwater travel times indicate that the current institutional controls should remain effective at preventing exposure to human and ecological receptors for the foreseeable future. Current land use on the Central Plateau is industrial, and public access to the site is restricted. The OU is anticipated to continue as an industrial area under institutional control for ongoing waste disposal operations and infrastructure services (DOE 2013b).

Based on an analysis of recent groundwater monitoring data from the HEIS, all iodine-129 concentrations measured in monitoring wells in the vicinity of 200-UP-1 were less than 25 pCi/L in 2019 (data after 9/12/2018). Of the 75 iodine-129 values measured in the vicinity of 200-UP-1, 48% were non-detectable, 11% were between 0 and 1 pCi/L, 32% were between 1 and 10 pCi/L, and 9% were greater than 10 pCi/L. The DWS and presumed cleanup level for iodine-129 is 1 pCi/L. The maximum concentration measured during 2019 was 23.7 pCi/L in well 299-W21-3. Among the 15 wells located within the mapped 1 pCi/L plume boundary and sampled for iodine-129 in 2019, the DWS was exceeded in all of them except 699-38-70C, which had a single reported value, 0.841 pCi/L. The mean measured iodine-129 concentration across all data points for wells located within the mapped plume was 6.45 pCi/L.

### 2.1 Sources of I-129

The main waste sites that contributed to iodine-129 contamination in groundwater within the 200-UP-1 OU included ponds, cribs, and trenches receiving liquid waste from the 202-S Reduction Oxidation (REDOX) Facility (S Plant) and U Plant operations, and unplanned releases from WMA S-SX (DOE 2012a). The REDOX Plant conducted plutonium separations from 1952 through 1967; U Plant conducted uranium recovery from 1952 through 1957. Unplanned releases resulted from inadvertent releases of the same or similar waste materials from tanks, pipelines, or other waste storage or conveyance components. Most of the liquid waste and wastewater migrated downward through the soil column by gravity to reach the underlying groundwater. Downward flux through the vadose zone may continue to contribute contaminants to the groundwater at a low rate, but most groundwater monitoring well data suggest that there are no significant, ongoing sources of iodine-129 to the water table.

As described in the 2018 Hanford Groundwater Monitoring Report (DOE 2019a), the iodine-129 groundwater plume in 200-UP-1 OU emanates primarily from disposal cribs located near U Plant and S Plant (Figure 2.1). The waste sites believed to be the most important contributors to the plume are 216-S-1&2, 216-S-7, and 216-U-1&2 (Truex et al. 2017). Other sites such as 216-A-10 and 216-S-9 had either very dilute iodine-129 solutions or much smaller total iodine-129 mass disposed in them.

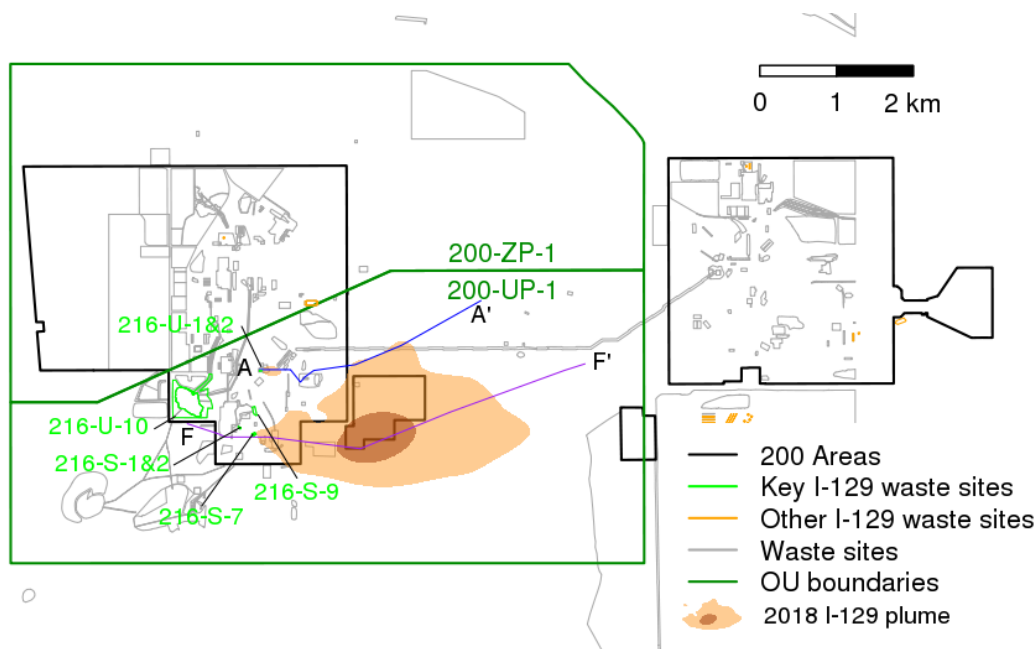


Figure 2.1. Key Iodine-129 Source Areas within 200-UP-1 OU in Relation to the 2018 Iodine-129 Plume. Light and dark plume colors denote 1 and 10 pCi/L contour levels, respectively.

The highest iodine-129 concentrations in 200-UP-1 OU, greater than 10 times the 1 pCi/L cleanup level, probably originated from the 216-S waste sites, but the 216-U-1&2 cribs also produced a plume that was locally significant in the past. East of the 200 West Area, the plumes merged, forming a larger comingled plume extending across the OU, which generally follows the same groundwater flow path across the OU as tritium. Additional information on releases and volumes of iodine-129 and water is provided in Section 3.3.

## 2.2 Areal Extent of Iodine-129 Groundwater Plume

Plume locations and extents are inferred from the well sample data collected by the Hanford Groundwater Monitoring Program and reported annually (DOE 2018a). The areal extent of the iodine-129 plume from groundwater concentrations in the 200-UP-1 OU (as defined by the 1 pCi/L contour) is approximately 4 km<sup>2</sup> as estimated in 2018 (DOE 2019a). The plume extends approximately 3 km (1.9 mi) east from the REDOX Plant waste sites into the 600 Area (Figure 2.2). Figure 2.3 and Figure 2.4 depict the plume extent over the past several decades based on well sample data. These plots show that the plume has declined in areal extent.

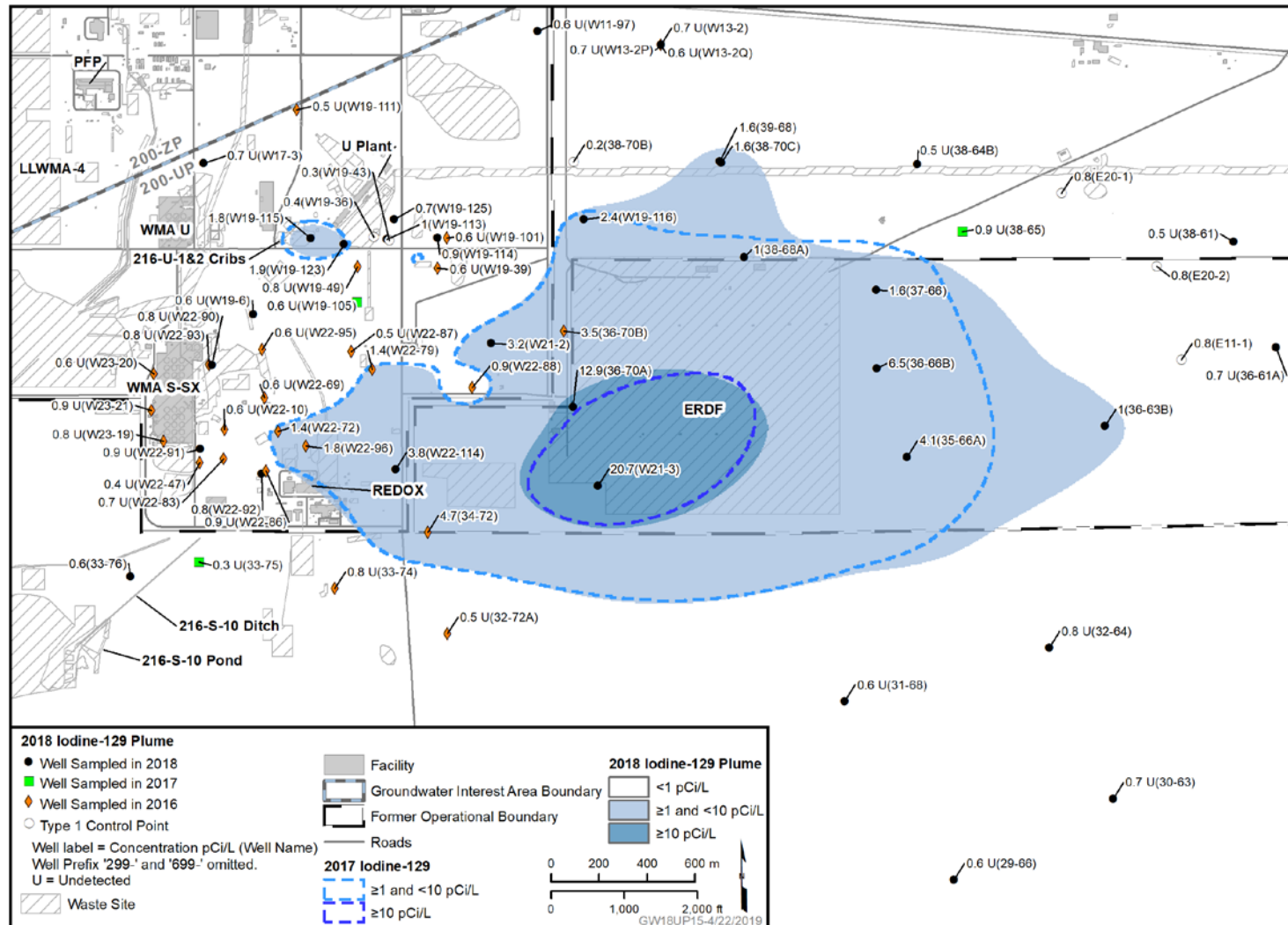


Figure 2.2. Detailed Map of Iodine-129 Plume from Hanford Site Groundwater Monitoring Report for 2018, DOE/RL-2018-66 (DOE 2019a). (Groundwater monitoring wells are shown with iodine-129 concentration data (pCi/L) as of publication of that report, followed by the well identifier.)

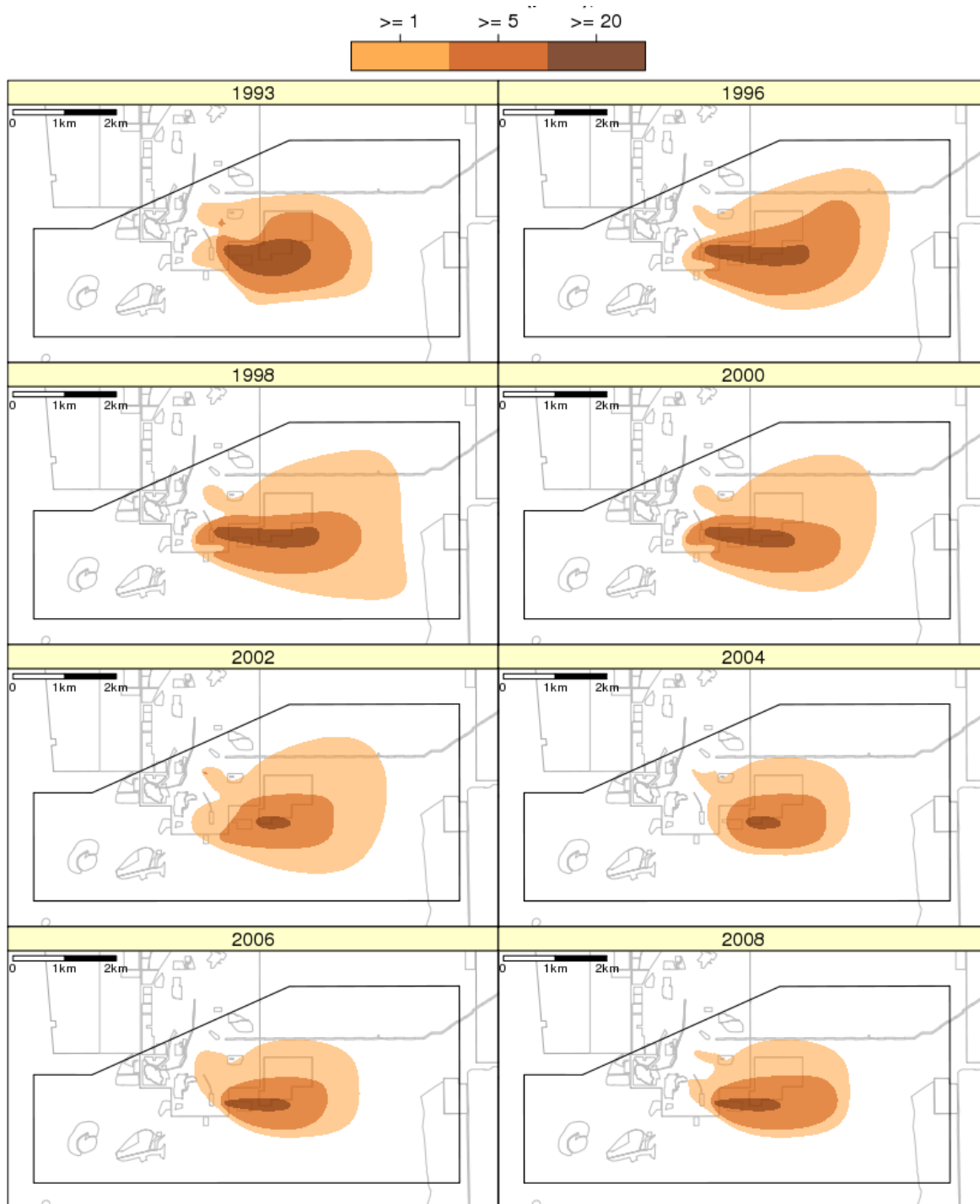


Figure 2.3. Estimated Extent of the 200-UP-1 OU Iodine-129 Plume from 1993 to 2008 with 1, 5, and 20 pCi/L Contours (Rockhold et al. 2018b).

The maximum distance between 1 pCi/L plume centers is about 760 m (between years 1994 and 2006), and location of the 2017 plume center is only about 55 m from the 1993 location.

Since 2008, estimation of the 5 and 20 pCi/L contour levels was discontinued; instead, a 10 pCi/L contour level is calculated and reported by the Hanford Groundwater Monitoring Program as shown in Figure 2.4. The most recent plume estimations indicate that the interior plume area above 10 pCi/L may also be declining.

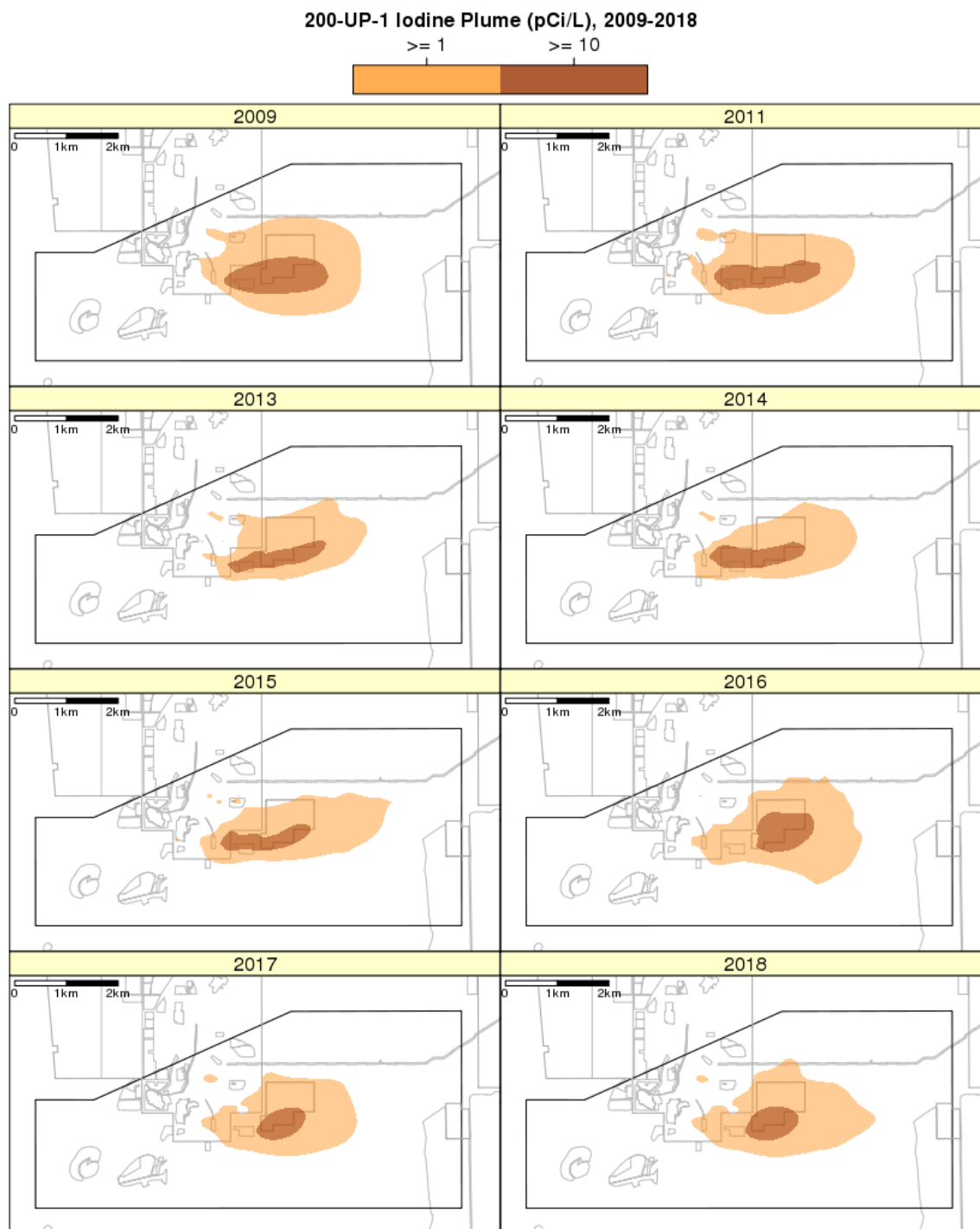


Figure 2.4. Estimated Extent of the 200-UP-1 OU Iodine-129 Plume for the Period from 2009 through 2018 for the 1 and 10 pCi/L Contour Levels (updated from Rockhold et al. 2018b).

Changes in the inferred plume shape and boundary are due in part to changes in well status and sampling variability in time. Iodine-129 was previously found to occur beneath the SX Tank Farm (WMA S-SX) at concentrations slightly above the 1 pCi/L cleanup level, and the estimated areal extent of the plume before 2014 reflects that. The iodine-129 concentration was 2.0 pCi/L in a December 2011 sample from well 299-W23-19, located within the SX Tank Farm (as indicated on Figure 2.2). Concentrations in the WMA S-SX area have declined since startup of groundwater extraction in the area during July 2012. In June 2015, the iodine-129 concentration in well 299-W23-19 was 1.6 pCi/L. During 2016, no sample results from wells in the WMA S-SX area exceeded the 1 pCi/L cleanup level. Iodine-129 was detected above the cleanup level at 299-W22-26 (downgradient from the S Tank Farm) before this well became dry (2.8 pCi/L in 2011), but the source was considered to be the 216-S-9 Crib. Iodine concentrations measured in two new wells drilled in 2016 to replace wells that had gone dry also influence the current plume extent. Well 299-W21-3 replaced dry well 699-35-70, and well 299-W22-114 replaced dry well 299-W22-9. Before the new wells were drilled and sampled, groundwater sample data from 2005 were used to represent the data at the locations of the dry wells for plume plotting. After data from the new wells became available, the plume area with concentrations greater than 10 pCi/L decreased compared to previous years. Plume size overall generally has decreased over time as shown in Figure 2.5.

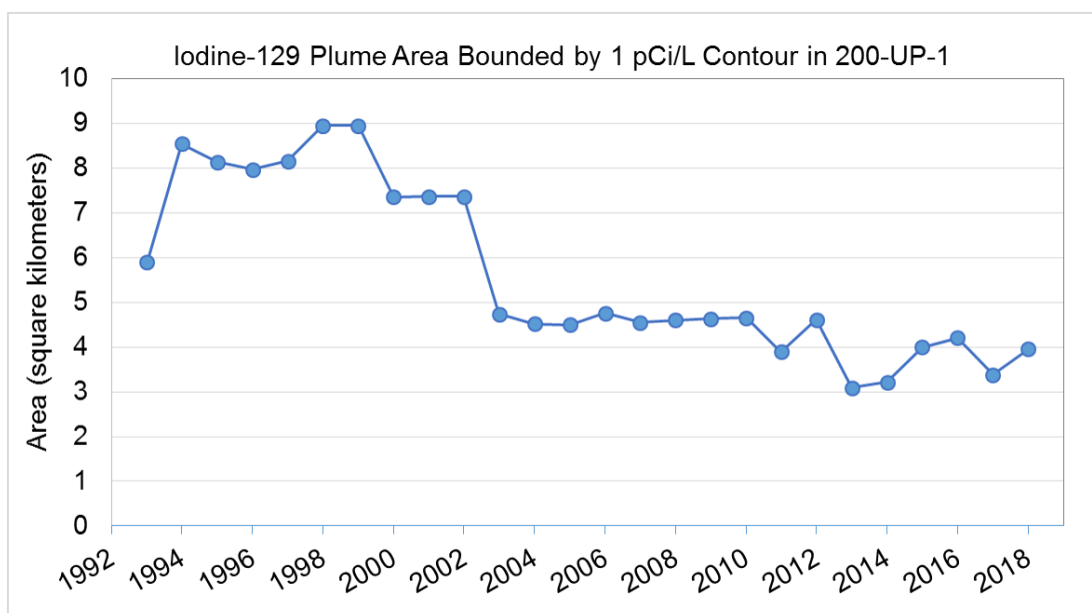


Figure 2.5. Trend in Estimated Areal Extent of the Iodine-129 Plume in 200-UP-1 Operable Unit.

## 2.3 Vertical Extent of I-129 Plume

The known vertical extent of the iodine-129 plume is limited to the unconfined aquifer above the Ringold Lower Mud formation. Depending on location within the plume, the portion of the unconfined aquifer contaminated at the 1 pCi/L level ranges from just the upper part of the aquifer to the full thickness.

Two conceptual cross sections were made along transect lines A-A' and F-F' in Figure 2.6 as part of the Remedial Action Work Plan (RAWP) for 200-UP-1 (DOE 2013a), based on data collected through 2011. The iodine-129 conceptual cross section for each of these locations, including depth-specific concentration data and an interpretation of the vertical extent of iodine-129 at 1 pCi/L or above, are shown in Figure 2.7 and Figure 2.8. The cross section along A-A' (Figure 2.7) indicates that the extent of the iodine-129 plume remains localized downgradient of 216-U-1&2, and the contamination is limited to the upper portion of the unconfined aquifer. Cross section F-F' (Figure 2.8) extends from a location

upgradient of the S Plant sources, downgradient approximately along the center of the current plume, to near the eastern boundary of 200-UP-1. This figure illustrates two separate plumes: (1) a small, emerging plume beneath the WMA S-SX (which is coincident with the WMA technetium-99, nitrate, and chromium plumes from that source); and (2) the much larger iodine-129 plume that formed from multiple smaller plumes merging downgradient from the 216-S-1&2, 216-S-7, and 216-S-9 crib sources. Figure 2.8 interprets the iodine-129 contamination as extending through the total thickness of the unconfined aquifer below the area where concentrations exceed 10 pCi/L. This is a conservative interpretation because there are no depth-discrete data available in this area to validate the vertical extent of the iodine-129.

Depth-discrete profiles of iodine-129 measured in five wells drilled in 2016 are given in Table 2.1 and the well locations are shown in Figure 2.2 and Figure 2.9. At well 299-W22-114, the maximum concentration observed during drilling was 4.03 pCi/L in the uppermost sample collected 3.4 m (11 ft) below the water table. The plume is interpreted to occur at a shallow depth near the source to well 299-W19-116 but deepens farther eastward. The plume is fully mixed vertically at well 699-38-70C, 1.8 km (1.1 mi) east of the cribs—this well is screened just above the Ringold Lower Mud unit and had a concentration of 1.51 pCi/L during 2016 (DOE 2017b). However, iodine-129 has not been measured in wells that are only screened below the Ringold Lower Mud, which indicates that only the upper unconfined aquifer has been contaminated above the 1 pCi/L level. Concentrations above 1 pCi/L occur in approximately the upper 20 m (70 ft) of the aquifer at well 299-W22-114 (DOE 2017b). Data for well 299-W21-3, drilled in 2016, indicate that iodine-129 occurs above the 1 pCi/L cleanup level throughout the aquifer thickness (Table 2.1)



Table 2.1. Iodine-129 Sample Results by Depth for New Wells Drilled in 2016 in 200-UP-1. (Data for well 299-W21-3, well 299-W22-114, well 699-36-63B, well 299-W19-115, and well 299-W19-116 as reported in Tables 11.2 through 11.6 in DOE 2017b; *Hanford Site Groundwater Monitoring Report for 2016.*)

Well 299-W21-3			Well 299-W22-114			Well 699-36-63B			Well 299-W19-115			Well 299-W19-116		
Depth Below Water Table (m)	Depth Below Water Table (ft)	I-129 (pCi/L)	Depth Below Water Table (m)	Depth Below Water Table (ft)	I-129 (pCi/L)	Depth Below Water Table (m)	Depth Below Water Table (ft)	I-129 (pCi/L)	Depth Below Water Table (m)	Depth Below Water Table (ft)	I-129 (pCi/L)	Depth Below Water Table (m)	Depth Below Water Table (ft)	I-129 (pCi/L)
1.5	4.8	14.1	3.2	10.6	4.01	2.3	7.4	0.678	4.3	14.2	0.93	2.8	9.1	2.75
14.9	48.9	38.9	10.4	34.1	1.73	5.2	17.2	<0.695	10.3	33.9	<0.834	11.9	39.3	2.25
21.2	69.6	7.14	20.5	67.4	1.49	11.5	37.6	0.848	15.7	51.6	0.642	21.3	69.9	<0.63
30.4	99.9	14.5	29.8	97.7	<0.663	17.6	57.6	<0.53	21.7	71.5	<0.616	30.1	98.8	<0.928
39.2	128.7	3.70	39.8	127.6	<0.763	23.7	77.8	<0.867	27.7	90.8	<0.511	36.3	119.0	<0.542
45.4	149.0	2.31	54.1	177.6	<0.613							45.3	148.6	<0.609
			60.1	197.3	<0.422							50.2	164.7	<0.789
Well 299-W21-3: screened interval depth from 11.6 to 17.7 m (38.1 to 58.1) ft below the water table														
Well 299-W22-114: screened interval depth from 0.04 to 10.7 m (0.13 to 35.1) ft below the water table														
Well 299-699-36-63B: screened interval depth from 0 to 20.9 m (0 to 68.7 ft) below the water table														
Well 299-W19-115: screened interval depth from 1.6 to 12.2 m (5.1 to 40.1 ft) below the water table														
Well 299-W19-116: screened interval depth from 0 to 9.7 m (0 to 31.7 ft) below the water table														

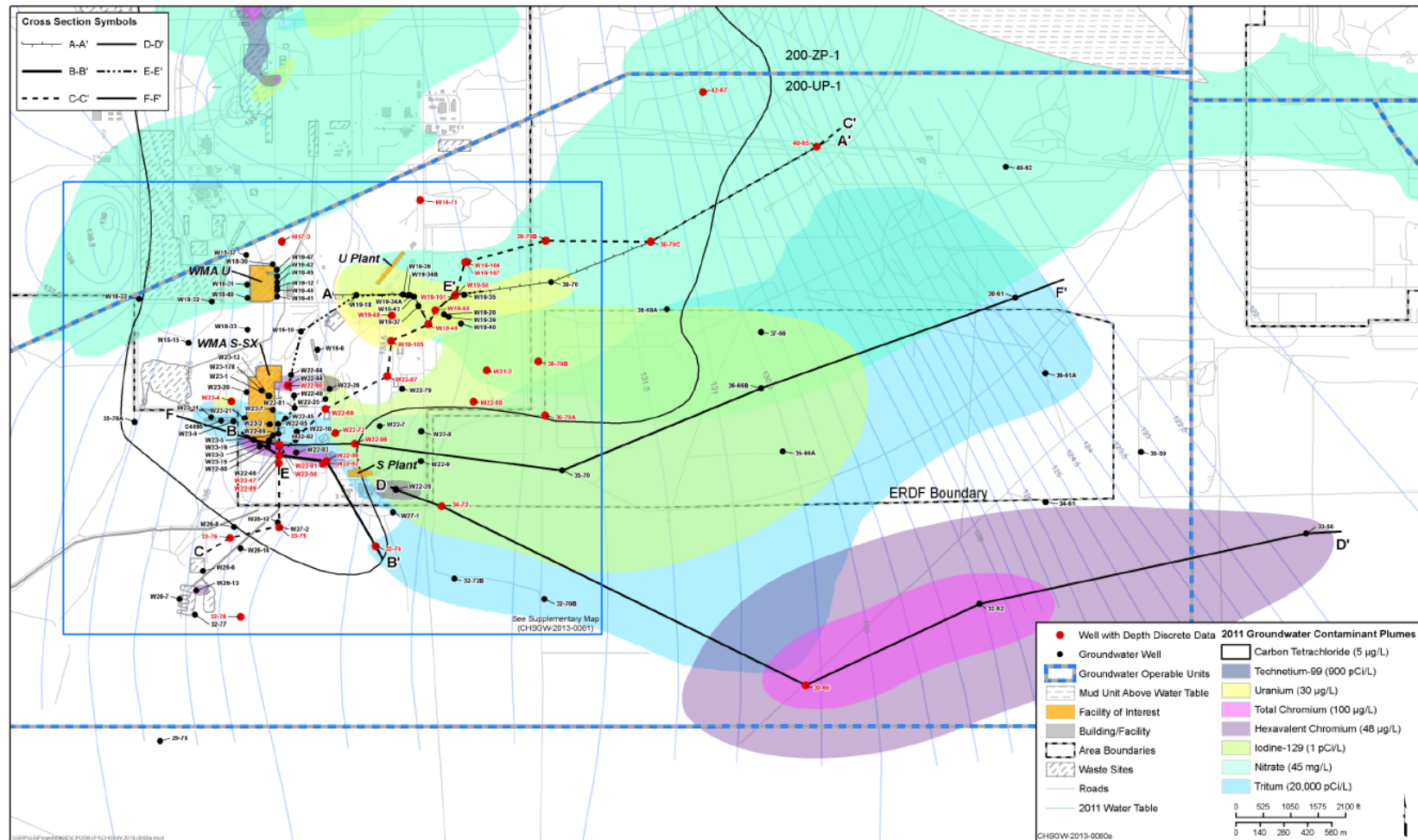


Figure 2.6. Location Map Showing Groundwater Plumes and Conception Cross Section Orientations within 200-UP-1 (Figure A-1 from DOE 2013a). Cross sections corresponding to lines A-A' and F-F' are shown in Figure 2.7 and Figure 2.8.

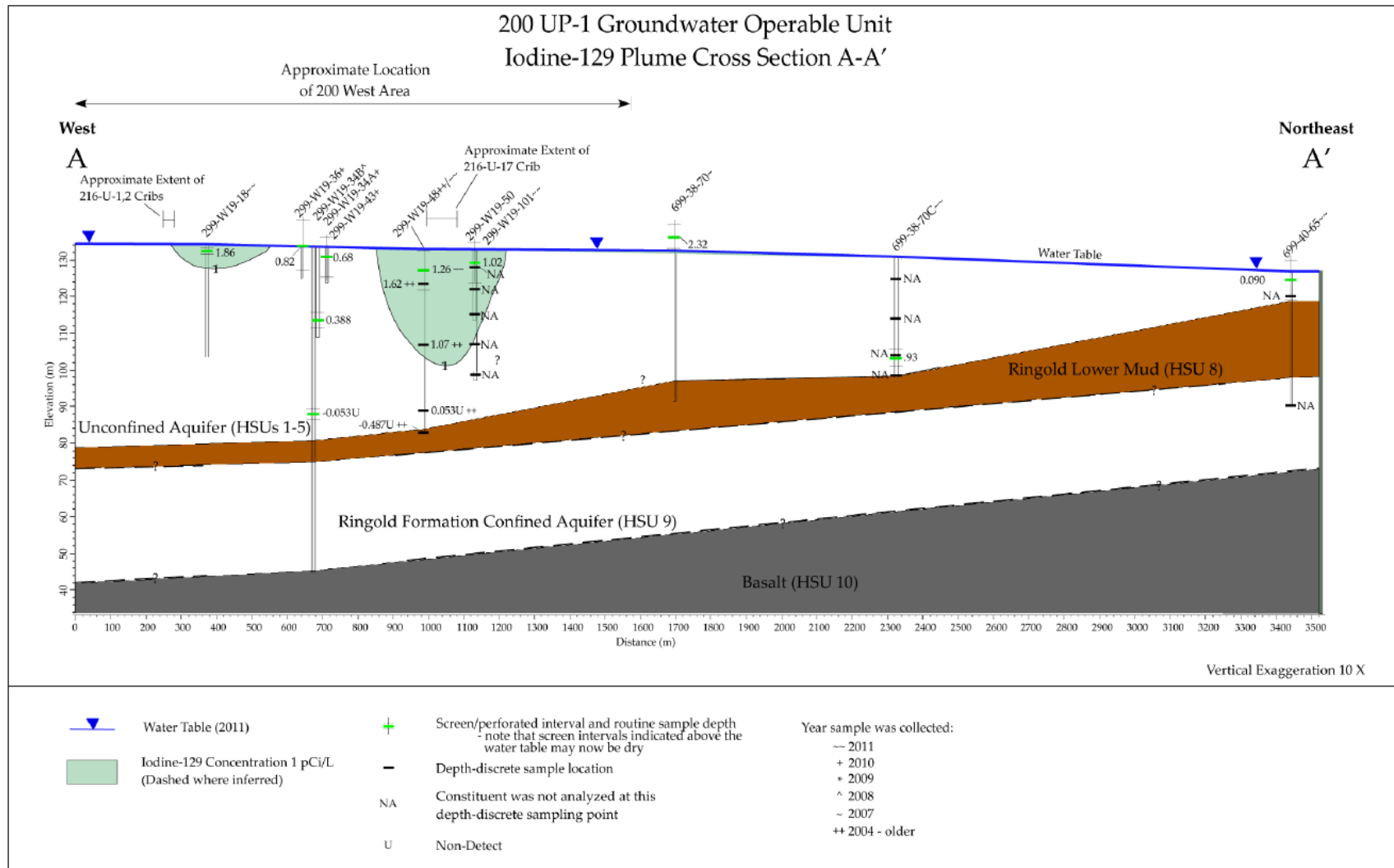


Figure 2.7. Iodine-129 Conceptual Cross Section A-A' (Figure A-6 in DOE 2013a).

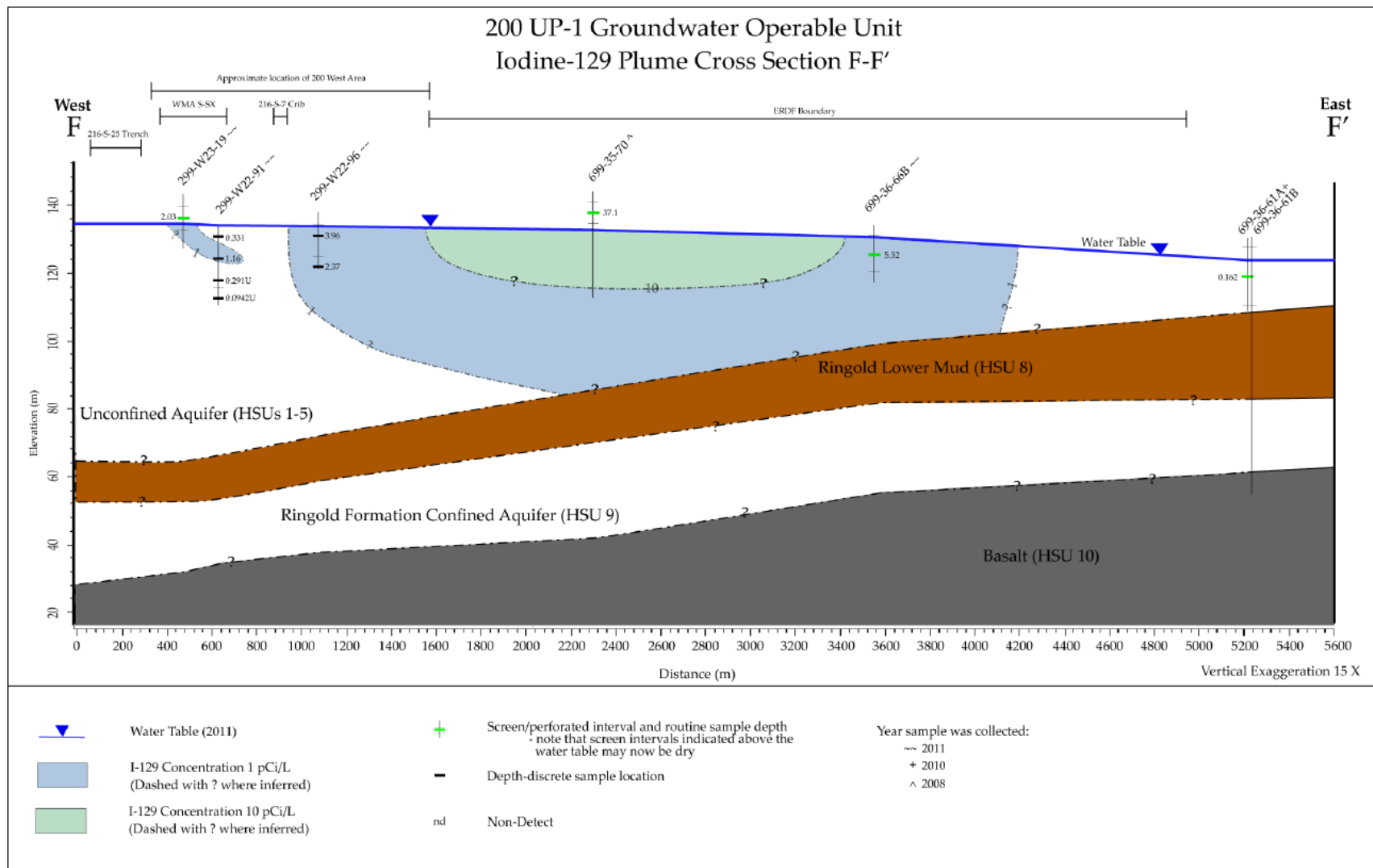


Figure 2.8. Iodine-129 Conceptual Cross Section F-F' (Figure A-7 in DOE 2013a).

## 2.4 I-129 Trends in Monitoring Wells

Iodine-129 concentrations in most of the groundwater wells sampled around the iodine-129 plume are stable and/or decreasing. The estimated boundary of the 2018 plume and the locations of 36 representative wells are shown in Figure 2.9 with color coding indicating the maximum concentration measured over the lifetime of each well. These data provide further indication that the plume has decreased in size and that lateral movement of the plume has not been significant. Time-series concentration data for 12 of these wells are shown in Figure 2.10 and Figure 2.11. Most of the wells exhibit declining trends, and none of the wells exhibit large increases compared to the recent past.

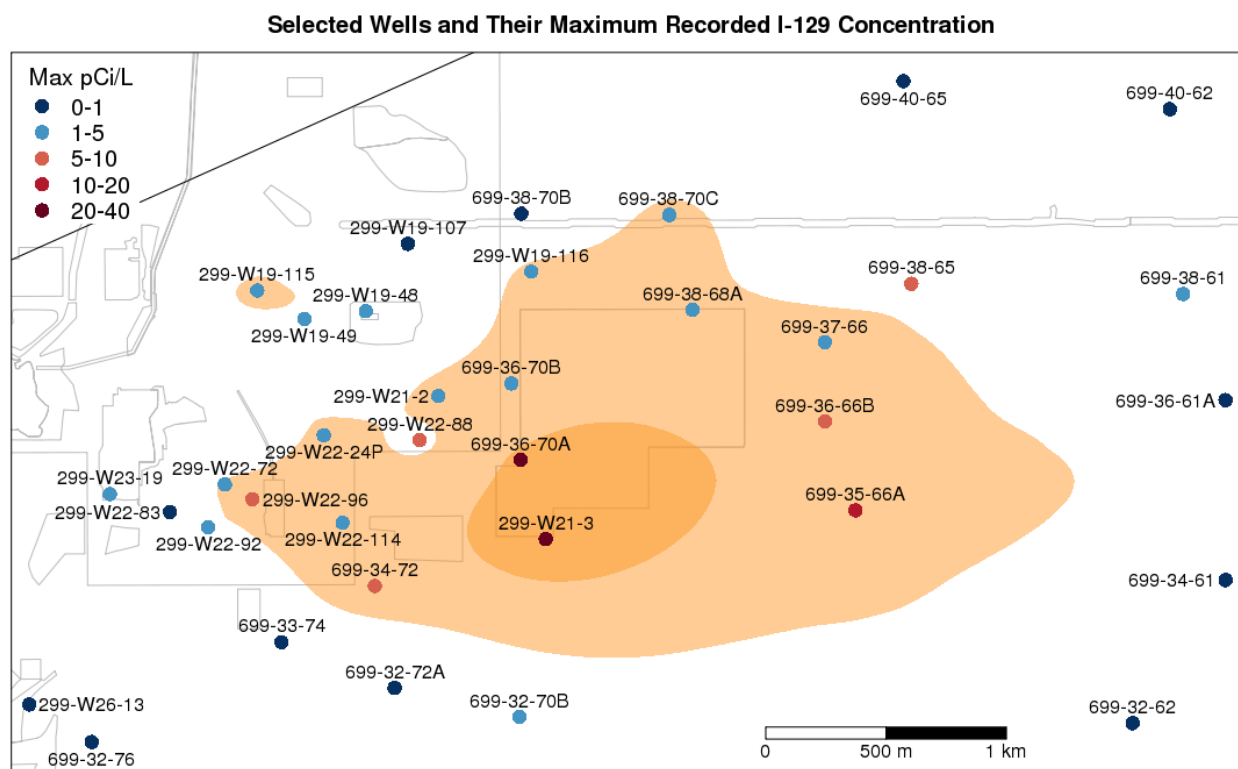


Figure 2.9. Iodine-129 Plume for 2018 (Hanford Site Groundwater Monitoring Program) and Selected Wells, Color-Coded by Their Maximum Lifetime Iodine-129 Concentration Value (pCi/L). Light and dark plume colors denote 1 and 10 pCi/L contour levels, respectively.

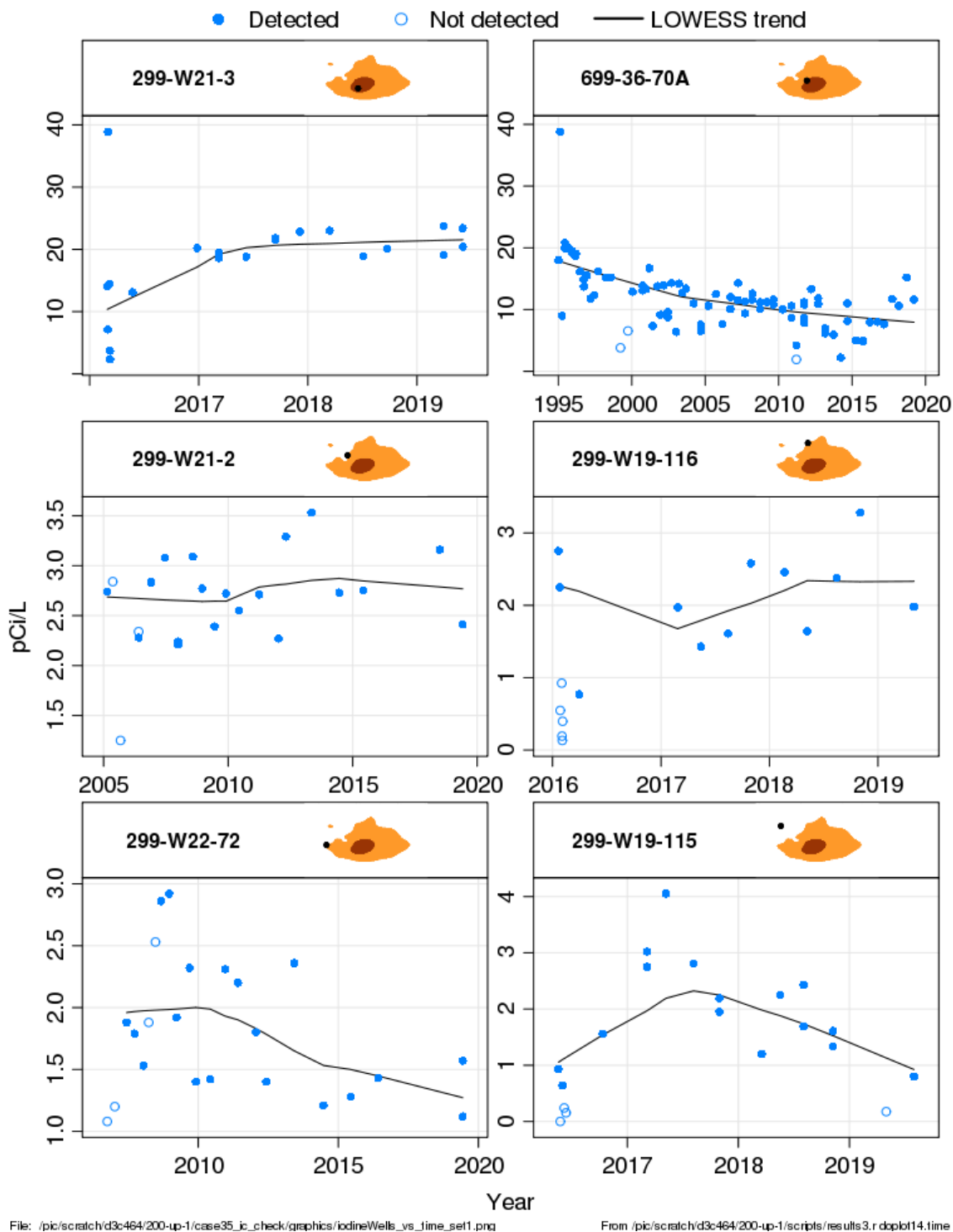


Figure 2.10. Iodine-129 Concentration versus Time at Selected Wells—Set 1. Solid blue dots represent measured values and open circles represent non-detects (which are reported with a value). The locally-weighted regression (LOWESS) line (black) suggests the approximate trend over time (fit excludes non-detects). The well location in relation to the 2018 plume is shown as a black dot in the panel strip. Wells are arranged in order of decreasing value of the most recent point in time of the trend line.

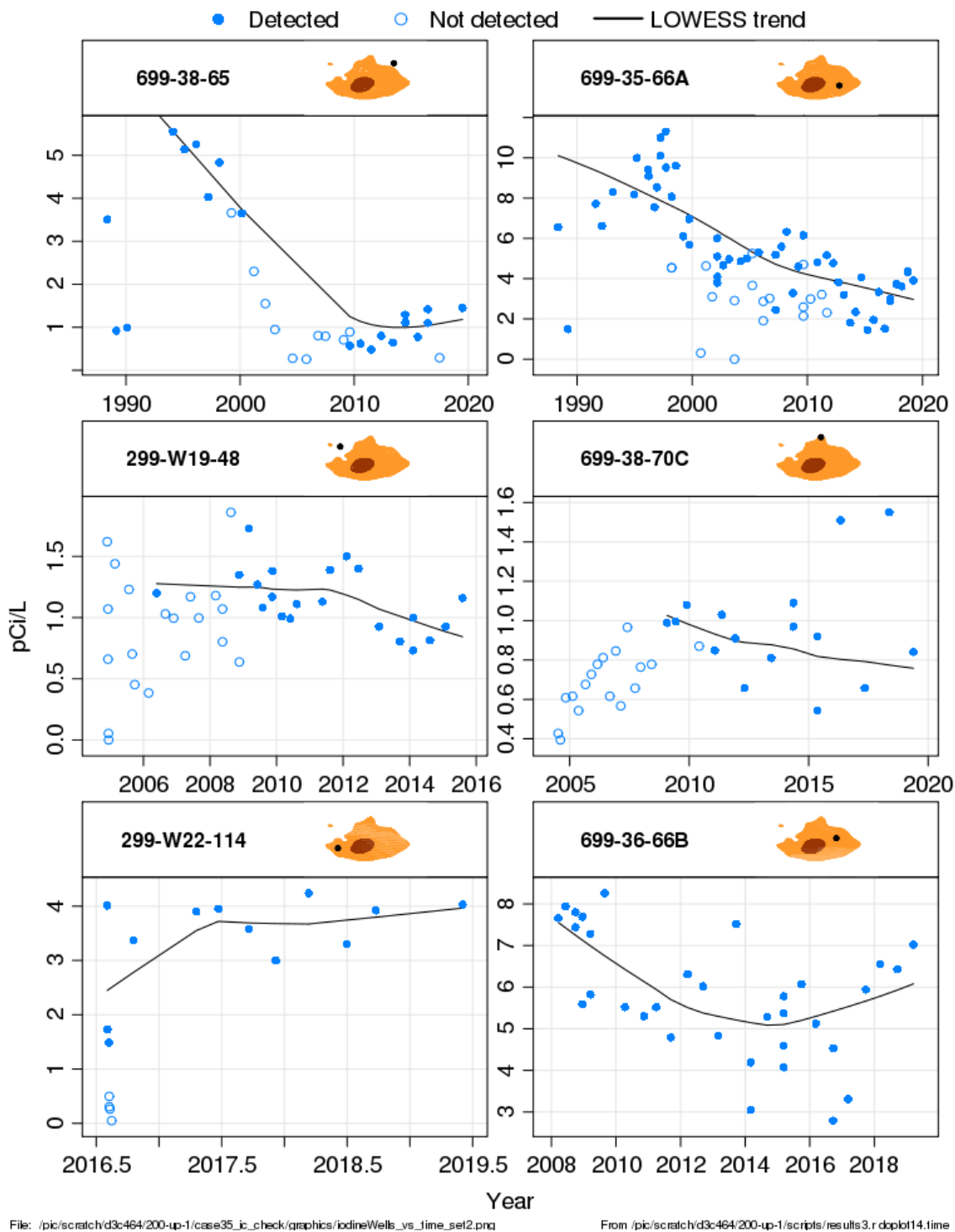


Figure 2.11. Iodine-129 Concentration versus Time at Selected Wells—Set 2. Solid blue dots are measured values, open circles are non-detects (which are reported with a value). Black line is a locally-weighted regression (LOWESS) line to suggest an approximate trend over time (fit excludes non-detects). Well location in relation to the 2018 plume is shown as a black dot in the panel strip. Wells are arranged in order of decreasing value of the most recent point in time of the trend line, continuing from set 1 wells in Figure 2.10.



### 3.0 Site Conceptual Model

The conceptual model for the 200-UP-1 OU is being developed to describe the nature and extent of subsurface iodine-129 contamination, evaluate processes that control behavior of the iodine-129 plume, and identify factors relevant to potential remediation processes in the 200-UP-1 OU. Iodine-129 is an uncommon contaminant, and relevant remediation experience and scientific literature are limited. Different iodine species exhibit unique transport behavior with respect to solid phase and aqueous phase interactions. Plume behavior and iodine transport are influenced by subsurface geology, hydrology, redox minerals, organic material, carbonate, and microorganisms. Water chemistry components such as dissolved organic matter and pH can affect transformation reactions and transport. In addition, co-contaminants, such as nitrate or other compounds that participate in redox reactions, may influence iodine transformation reactions and sorption (Truex et al. 2017). The conceptual model for iodine transport and fate in the 200-UP-1 OU considers the factors affecting plume behavior and remediation, including the following:

- Hydrogeology affecting water movement and iodine transport in the subsurface (Section 3.1)
- Geochemical and biological processes that can influence iodine reactions and iodine-129 transport (Section 3.2)
- Iodine-129 sources and estimated release volumes in 200-UP-1 OU (Section 3.3)
- Prediction of the distribution, transport, and fate of iodine-129 in 200-UP-1 (Section 3.4)

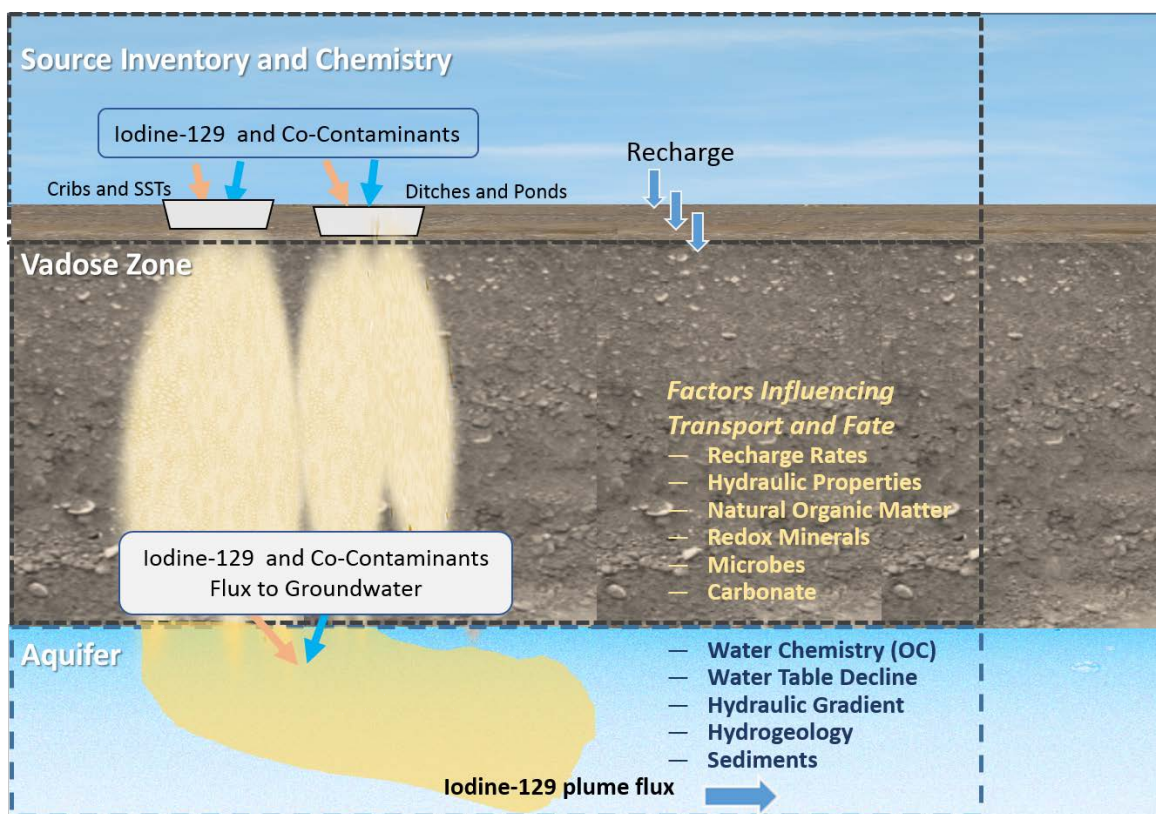


Figure 3.1. System-Level Depiction of Elements Affecting Iodine Fate and Transport (Rockhold et al. 2018b).



To the extent possible, all components of the conceptual model are based on measured data. A numerical flow and transport model, based on the conceptual model, is also used to infer behavior for regions or features where measured data are not available, such as in the vadose zone. Some results shown in subsequent sections are from the numerical model.

### 3.1 Geologic and Hydrologic Features of the 200-UP-1 OU

The Hanford Site lies within the semiarid Pasco Basin of the Columbia Plateau in southeastern Washington State (see Figure 1.1). Structural basins within the Yakima Fold Belt, including the Pasco Basin, are filled with sedimentary sequences from ancestral river systems, cataclysmic Ice Age floods, and localized deposits of colluvium and loess. The 200 Areas are located on a broad, relatively flat area that constitutes a local topographic high near the center of the Hanford Site—designated as the Central Plateau. The 200-UP-1 OU underlies the southern portion of the 200 West Area, which is on the western side of the Central Plateau. Surface elevations above the 200-UP-1 OU range from approximately 183 m (600 ft) to more than 213 m (700 ft) above mean sea level. Basalt of the Columbia River Basalt Group and a sequence of overlying sediments comprise the local geology. The overlying sediments are approximately 169 m (555 ft) thick and primarily consist of the Ringold Formation and Hanford formation, which are composed primarily of sand and gravel, with some silt layers. The unconfined aquifer is within the Ringold Formation and the depth to water table is approximately 85 m.

The sedimentary layers and underlying basalt are divided into primary geologic units that are laterally continuous across the majority of the OU (Figure 3.2). In some Hanford reports, these layers are parsed into hydrostratigraphic units (HSUs), but the original geologic names are primarily used in this document. From top to bottom, these units are as follows:

- Hanford formation (HF, HSU1) – unconsolidated sand and gravel
- Cold Creek unit (CCU, HSU 3) – silt, sand, gravel
- Ringold Formation Taylor Flats unit (Rtf, HSU4) – semi-consolidated silt, sand, and gravel
- Ringold Formation Wooded Island Unit E (Rwie, HSU5) – semi-consolidated gravel and sand
- Ringold Formation Lower Mud (Rlm, HSU8) – silt and clay
- Ringold Formation Wooded Island Unit A (Rwia, HSU9) – semi-consolidated sand and gravel
- Columbia River Basalt (Basalt, HSU5) – flood basalt lava flows and interbedded sediments

All of these units are illustrated with more detail in the stratigraphic column of Figure 3.2. The Hanford formation has also been subdivided into, from top to bottom, H1, H2, and H3 subunits (Springer 2018) (Figure 3.3).

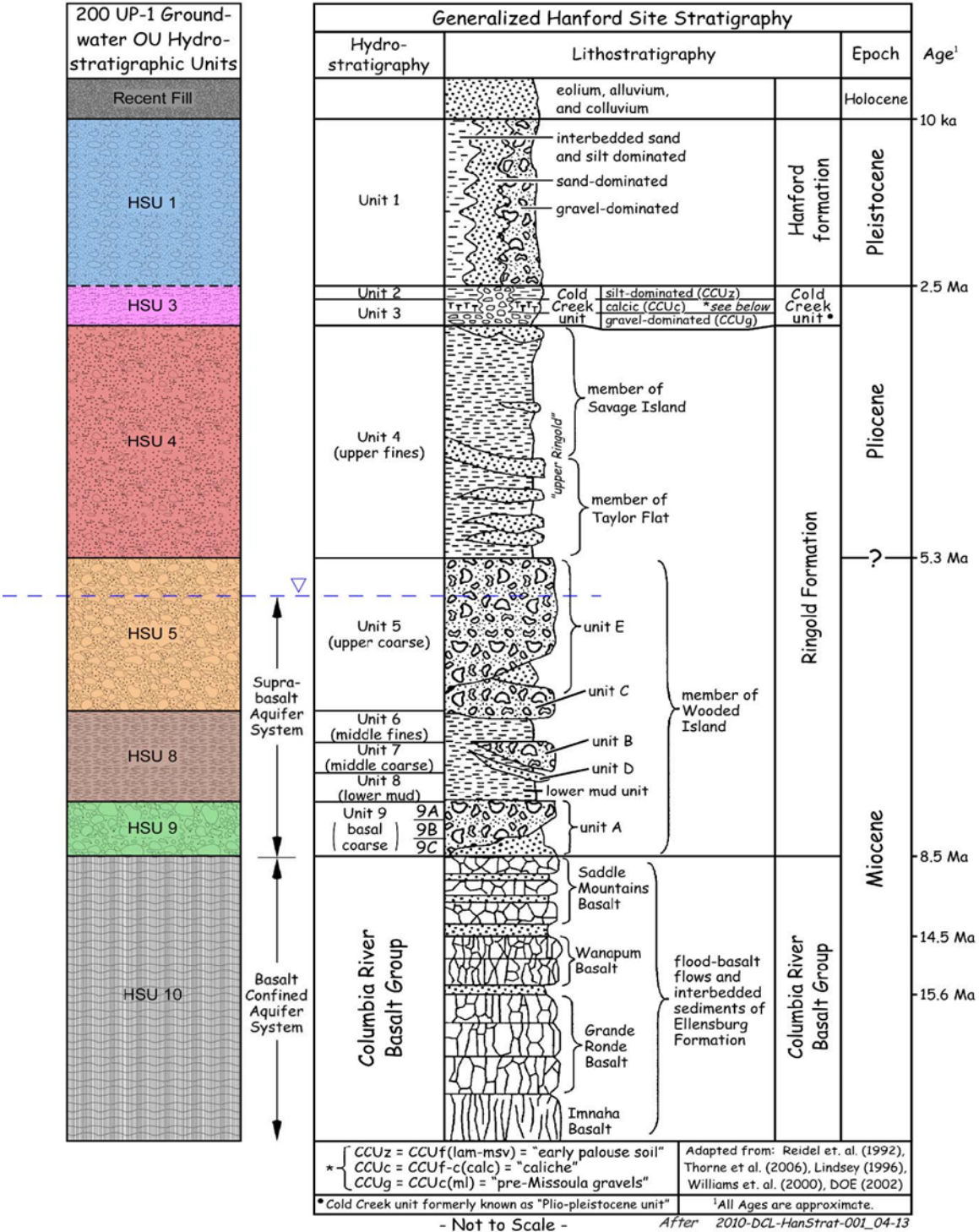


Figure 3.2. Hydrostratigraphic Units and Generalized Hanford Site Stratigraphy for 200-UP-1 Groundwater OU (Hammond and Lupton 2015).

Geologic data indicate the RIm is continuous beneath most of 200-UP-1, but is absent in the northeast quarter of the 200 West Area (Hammond and Lupton 2015). Groundwater in the unconfined aquifer flows from areas where the water table is higher (west of the Hanford Site) to areas where it is lower (the Columbia River). In general, groundwater flow through the Central Plateau occurs in a predominantly

easterly direction from the 200 West Area to the 200 East Area (Figure 3.3 through Figure 3.6). In addition to the upper, unconfined aquifer, groundwater is also found deeper in a mostly confined condition in the Rwia (HSU 9) (and the basalt).

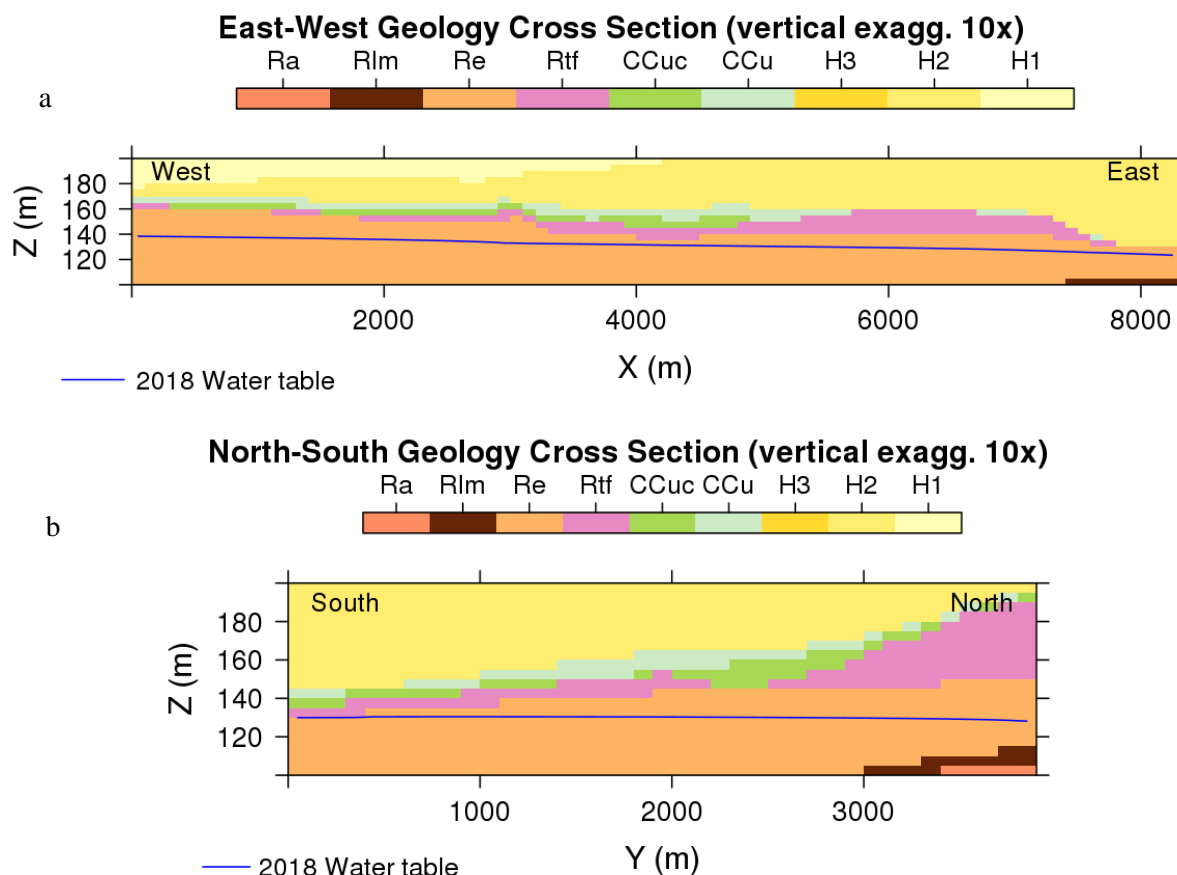


Figure 3.3. Cross Sections of Geologic Framework Model (GFM), West to East (a) (left to right) and South to North (b) through the 1 pCi/L Plume Center of the 2018 Iodine-129 Plume. Vertical exaggeration of the figure is 10x.

The Rwie unit contains the unconfined aquifer in Central Plateau and the Rlm unit is the primary confining unit that limits downward migration of groundwater and contaminants. The thickness of the unconfined aquifer varies substantially within the Central Plateau, from over 200 m (656 ft) southeast of the 200 East Area to zero where the aquifer pinches out against mud units and basalt above the water table. The water table is as deep as 106 m (348 ft) below ground surface beneath the Central Plateau. The conceptual west-to-east cross section in Figure 3.4 shows the relationship between waste sites, vadose zone, water table, and some of the geologic units underlying the 200-UP-1 OU.

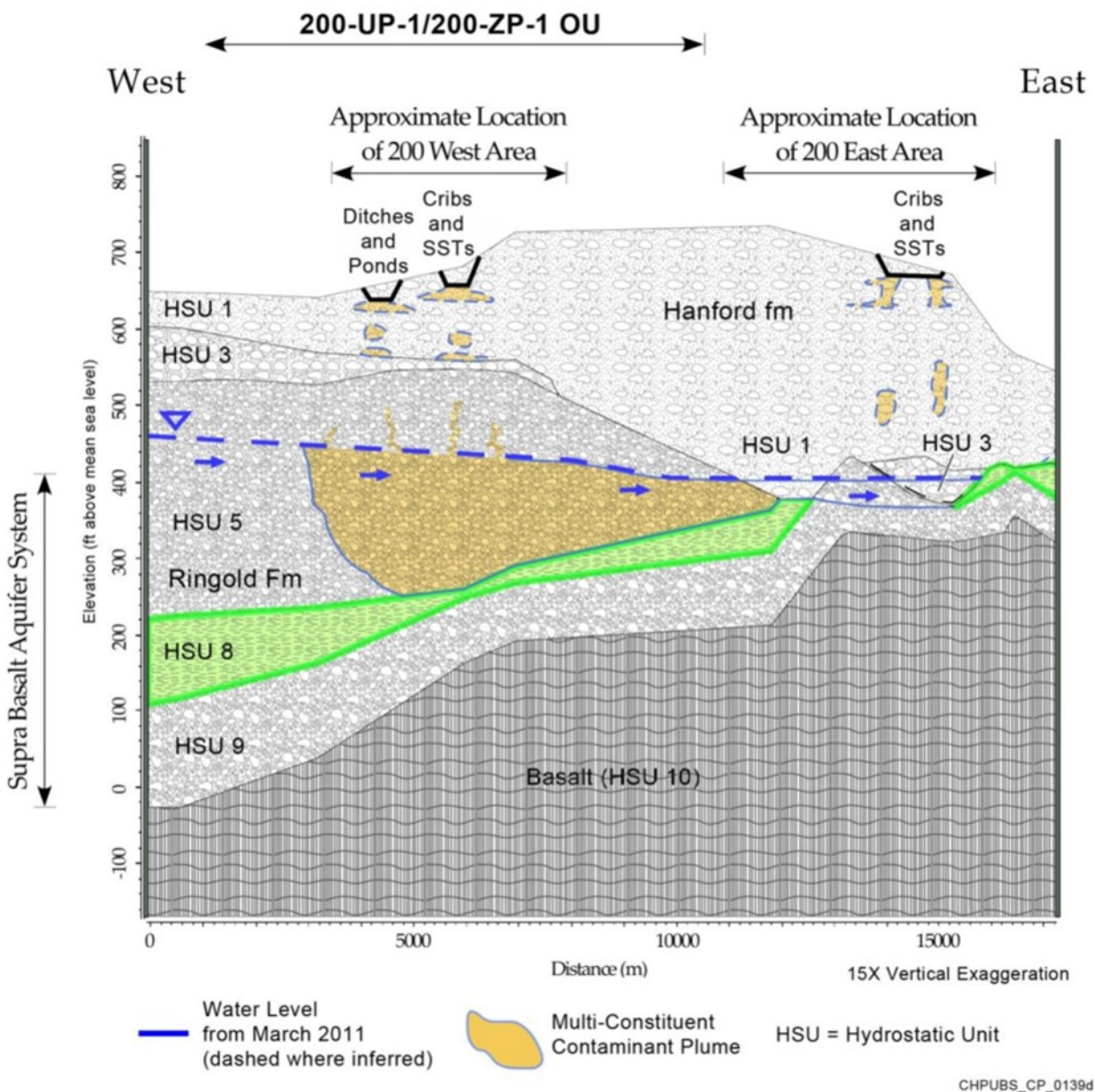


Figure 3.4. Conceptual Vertical Cross Section Showing the Extent of Contaminant Plumes with Respect to Hydrostratigraphic Units (from DOE 2013a).

### 3.1.1 Physical and Hydraulic Properties of Subsurface Materials

Physical and hydraulic properties for Hanford sediments have been determined using a variety of laboratory and field methods. Physical and hydraulic properties for Hanford saturated zone materials (aquifer sediments) have been documented in various reports (Spaine et al. 2001a,b, 2002, 2003; Spaine and Newcomer 2010a,b). Thorne and Newcomer (2002) initiated the development of a database for saturated zone hydraulic properties, but this database has not been updated since the early 2000s. Saturated zone modeling efforts that have used facies-based or other representations of the unconfined aquifer materials for which hydraulic parameters have been calibrated include Thorne et al. (2006),

Williams et al. (2006), and McDonald (2018). Vadose zone physical and hydraulic properties, including parameters describing water retention and hydraulic conductivity, have also been documented in various reports (Bergeron et al. 1987; Bjornstad 1990; Connelly et al. 1992a,b; Rockhold et al. 1993, 2015, 2018a; Khaleel and Freeman 1995; Last et al. 2006, 2009).

### **3.1.2 Depth to Groundwater**

The water table is relatively deep within the 200-UP-1 OU (Figure 3.5). Data from 2018 indicate water levels range from 59 to 97 m below ground surface for the 36 wells shown in Figure 2.9, with a mean of 78 m. Water table elevation maps are included in DOE (2019a). The eSTOMP model indicates that in the region bounded by the 2018 1 pCi/L plume, the saturated thickness of the unconfined aquifer is entirely within the  $R_{wie}$  (Figure 3.2), and ranges from approximately 20 to 65 m, with an average of 41 m.

### **3.1.3 Hydraulic Gradients (Horizontal and Vertical)**

Groundwater beneath the Central Plateau flows generally from west to east, although the 200 West P&T system disrupts this pattern locally. Natural recharge to the unconfined aquifer comes from Cold Creek Valley, Dry Creek Valley, Rattlesnake Hills, and infiltrating precipitation. The hydraulic gradient within the 2018 plume area has a northeasterly direction and a magnitude of approximately  $8.7 \times 10^{-4}$  (calculated from Figure 3.6). Directly east and northeast of the plume, the hydraulic gradient steepens markedly to approximately  $3.9 \times 10^{-3}$ . This is caused in part by a decrease in the aquifer saturated thickness and transmissivity. The hydraulic conductivity of the aquifer sediments may also decrease toward the east, which would contribute to the larger hydraulic gradient. Groundwater velocity in the Central Plateau generally ranges from a few millimeters to tenths of a meter per day. Vertical gradients within the saturated zone are small in comparison and flow is primarily lateral. Geologic structure under 200-UP-1 is low-angle layered stratigraphy, and vertical lithologic features that could provide preferential pathways are unknown.

Current treatment of iodine-129 at the 200-UP-1 OU within the Central Plateau at the Hanford Site is accomplished by hydraulic containment of the iodine-129 groundwater plume using injection wells placed at the leading edges of the plume (Figure 3.6). Groundwater flow is also locally influenced by the 200-ZP-1 OU final remedy P&T system north of the plume and the WMA S-SX interim remedial measure extraction system west of the plume. The effects of pumping and injection on the water table are shown in Figure 3.5 (DOE 2018b).



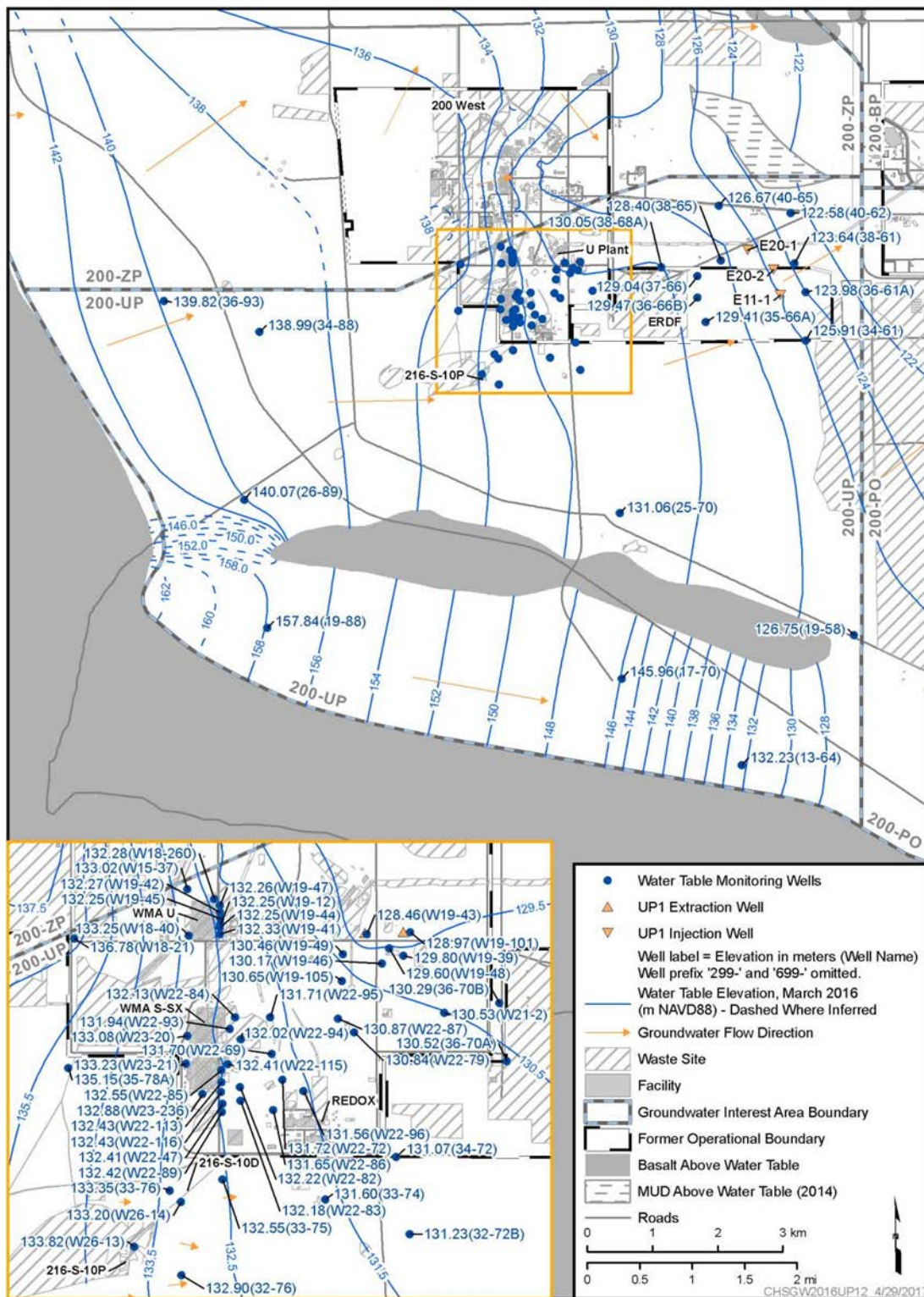


Figure 3.5. Water Table Elevation in 200-UP Interest Area from March 2016 (Figure 11-2 from DOE 2017b).

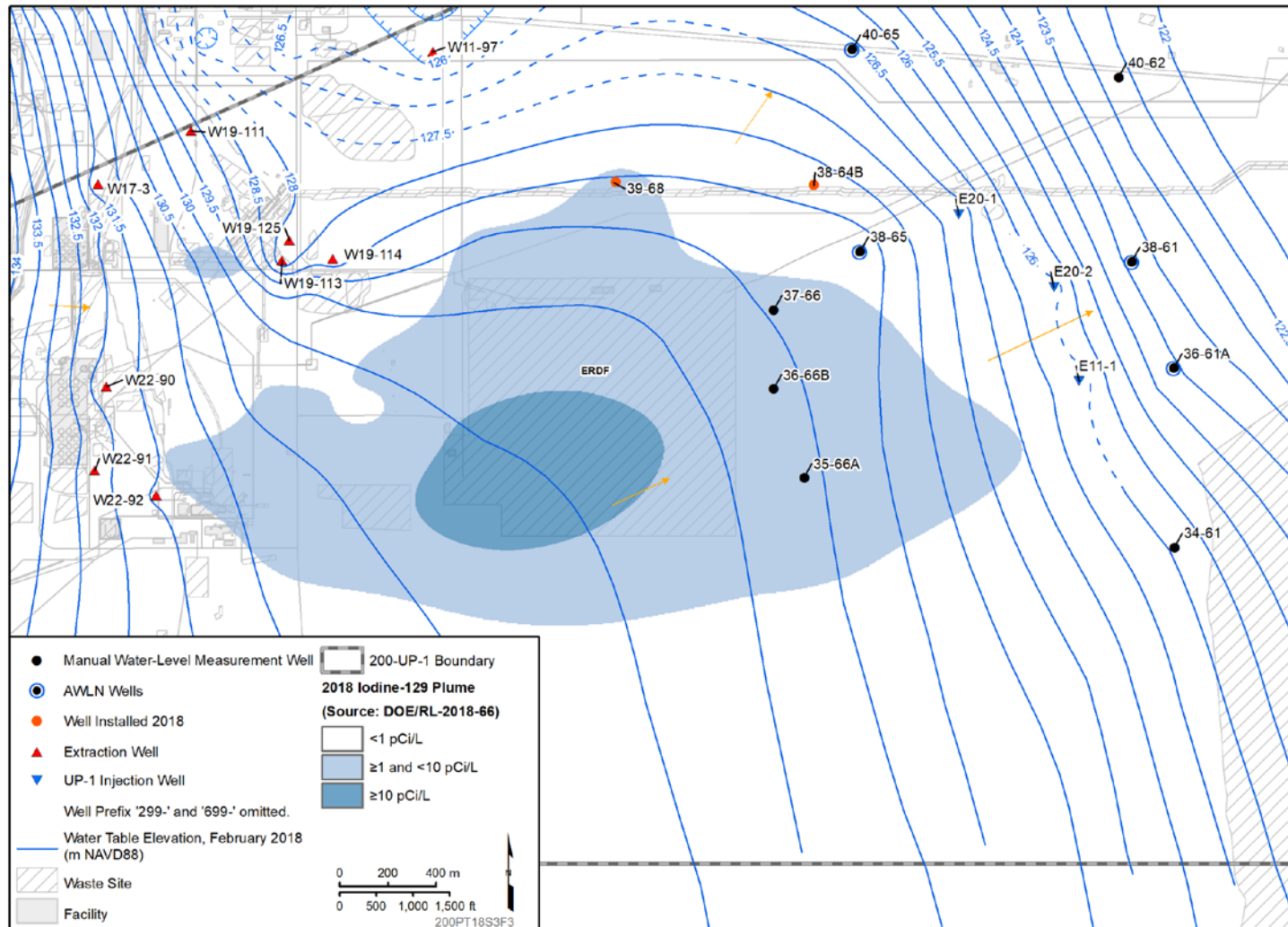


Figure 3.6. Water Level Monitoring Network and Water Table Elevations as Influenced by Iodine-129 Plume Hydraulic Containment Remedy as of December 2018 from DOE/RL-2018-66 (DOE 2019a).

### **3.1.4 Temporal Variability in Hydrologic Conditions and Contaminant Concentrations**

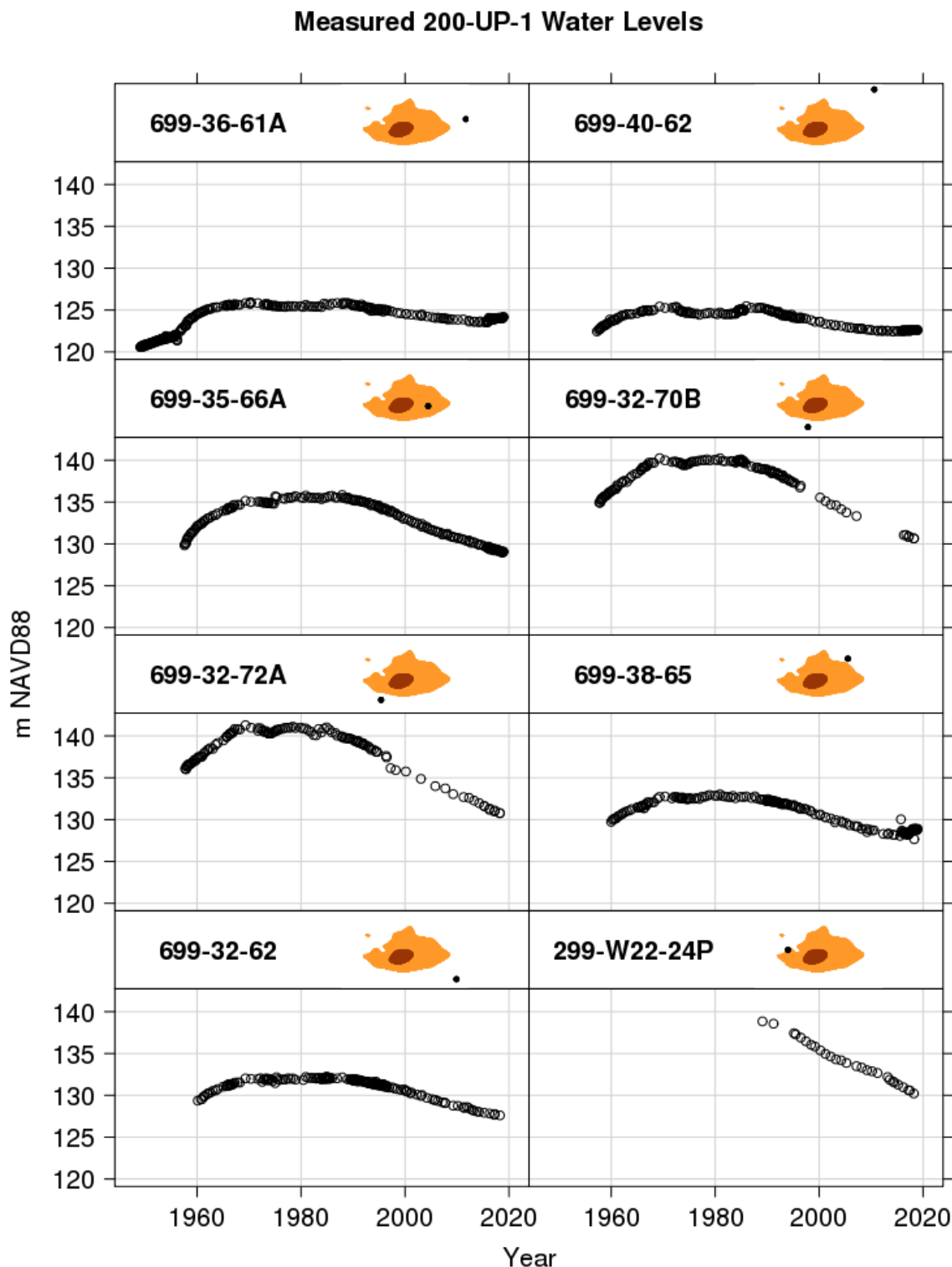
Historical liquid waste discharges to the ground (e.g., cooling water and process wastewater) during the 1940s through the 1990s significantly altered the groundwater flow regime, especially around the 216-U-10 Pond in the 200 West Area, which created a large water table mound that deflected the groundwater flow to the northeast. As drainage from these discharges has ceased, the water table has been declining, and groundwater flow direction is returning to a more easterly direction through the Central Plateau. There are currently no liquid waste discharges to the ground in 200-UP-1 (with the exception of sanitary drain fields). The 200-UP-1 P&T system has altered the hydraulic gradients locally since operation began in 2012 (Figure 3.5). The historical rise and fall of water levels at selected wells in the vicinity of the iodine-129 plume is shown in Figure 3.7.

### **3.1.5 Groundwater Recharge and Discharge Information**

Recharge is defined here as the flux of water from meteoric sources (i.e., rainfall and snowmelt) that infiltrates through the vadose zone and reaches the water table. Direct measurement of recharge at the water table is usually impractical on the Hanford Site Central Plateau due to inaccessibility; the water table is commonly located at depths of 80 m or more below ground surface, and access is influenced by historical and current Hanford operations (Fayer and Keller 2007). Instead, measurements in the shallow portion of the vadose zone and numerical and tracer analyses have been used to estimate the deep drainage flux, that is, water leaving the evapotranspiration zone and ostensibly traveling to the water table (Fayer and Walters 1995; Last et al. 2006; Fayer and Keller 2007; Rockhold et al. 2009; Fayer et al. 2010).

Recharge is the primary mechanism for ongoing transport of contaminants from the vadose zone to groundwater. Long-term average recharge rates at the Hanford Site can range from near zero to more than 100 mm/yr depending on local climate, vegetation cover, soil hydraulic properties, land use, and topography (Fayer and Walters 1995; Fayer et al. 2010). Fayer and Keller (2007) reported long-term recharge rates ranging from <0.1 for vegetated soils to 92 mm/yr for disturbed soils with graveled surface (Table 3.1). For Hanford soils or gravel surfaces without vegetation (such as the surfaces maintained above waste sites), the long-term drainage estimates range from 8.6 to 92 mm/yr.





File: /pic/scratch/d3c464/200-up-1/case35\_ic\_check/graphics/waterLevels\_vs\_time\_all.png

From /pic/scratch/d3c464/200-up-1/scripts/results3.r dplot15

Figure 3.7. Measured Water Table Elevations Over Time at Selected Wells. Water level data are from the Hanford Environmental Information System. The well location in relation to the 2017 plume is shown as a black dot in the panel strip.

Table 3.1. Estimated Long-Term Recharge Rates for Use in Hanford Assessments (Table 6.1 from Fayer and Keller 2007)

Soil Type	Estimated Long-Term Drainage Rates (mm/yr)	
	Shrub	No Plants
Rupert sand (near U.S. Ecology)	5.0	30
Rupert sand (200 East Area)	0.9	45
Rupert sand (elsewhere on Central Plateau)	1.7	45
Burbank loamy sand	1.9	53
Ephrata sandy loam	2.8	23
Hezel sand	<0.1	8.7
Esquatzel silt loam	<0.1	8.6
Hanford formation sand	Np	62
Graveled surface	Np	92
Modified RCRA C barrier	0.1	0.1
Gravel side slope on surface barrier	1.9	33 <sup>(a)</sup>

Np = Not provided by Last et al. (2006) or Fayer and Keller (2007); RCRA = *Resource Conservation and Recovery Act*.  
(a) Tentative estimate because of concerns regarding presence of some plants, road, and small section of vegetated silt-loam within the drainage collection zone.

Performance assessment calculations for Hanford waste sites usually use a combination of recharge rates to represent different areas and time periods, including pre-Hanford, operational, and post-closure periods. During the pre-Hanford period, recharge rates are usually relatively low and are assumed to be representative of undisturbed soil conditions with native shrub-steppe vegetation. Higher recharge rates are typically applied during the operational period to account for disturbance of soils for emplacement of waste storage tanks, placement of gravel over the tank farms, and maintaining the gravel-covered surfaces free of vegetation. Post-closure conditions are usually assumed to include reduced infiltration rates to account for infiltration barriers over waste sites, followed by a change in recharge rates back to assumed pre-Hanford-type conditions.

### 3.1.6 Groundwater Withdrawal and Potential Receptors

Based on the anticipated yield and natural water quality, the State of Washington has determined that the aquifer setting for the 200-UP-1 OU meets the WAC 173-340-720 definition for potable groundwater, which is the highest recognized beneficial use. EPA generally defers to state definitions of groundwater classification provided under EPA-endorsed Comprehensive State Groundwater Protection Programs (EPA 1988). Under EPA's groundwater classification program, 200-UP-1 OU groundwater would be designated Class II-B, which is groundwater that is not a current source of drinking water but is a potential future source (DOE 2017a).

Withdrawal of groundwater from 200-UP-1 OU for beneficial uses is currently prohibited by DOE institutional controls placed on groundwater. There are no drinking water supply wells and no wellhead protection areas. The existing institutional controls (specifically, prohibitions against use of groundwater for a source of drinking water) prevent human exposure. Current land use on the Central Plateau is industrial, and public access to the site is restricted.

Land use in the 200 West and 200 East Areas is anticipated to remain industrial for the foreseeable future and the areas will be used for ongoing waste disposal operations and infrastructure services (DOE 2013b). The iodine-129 contaminant plume in the 200-UP-1 OU extends less than 5 km to the east of the originating waste sources and does not interact with any surface waters within or adjacent to its

boundaries. There are no wetlands, perennial streams, or floodplains present. The iodine-129 plume currently does not extend past the OU boundary and does not extend to the groundwater discharge areas along the Columbia River to the east; thus, no ecological receptors are currently exposed to iodine-129 from the 200-UP-1 OU.

Previous investigations simulating iodine-129 transport in the OU using MODFLOW-2000 and MT3DMS indicated that iodine-129 is not expected to leave the Central Plateau within a 1000-year timeframe and would not interact with any surface waters within that period (DOE 2012b). That previous modeling indicates that iodine-129 contamination in the 200-UP-1 OU will move beyond the OU boundary at concentrations above the DWS in the absence of further remediation.

In summary, under the current withdrawal and use restrictions, there are no direct pathways for human exposures, and no ecological exposure pathways to iodine-129 contamination in the 200-UP-1 OU because the groundwater is not used for agriculture or human consumption, and does not discharge to surface water or reach the Columbia River at levels above the DWS (DOE 2017b). Due to institutional controls, groundwater within this OU is not expected to become a future source of drinking water until drinking water standards are achieved. Based on the current selected remedy, which is a combination of P&T, hydraulic containment, and MNA, it is expected that it will take 125 years for contaminants other than iodine-129 to be cleaned up to drinking water standards.

### **3.2 Geochemical and Biological Processes Affecting Iodine-129 in Soils and Groundwater**

The behavior of iodine in the environment is complicated by its multiple physical states, multiple redox states, interactions with organic matter, and microbial transformations (Truex et al. 2017). A conceptual overview showing known subsurface biogeochemical processes that affect the fate and transport of iodine at Hanford is shown in Figure 3.8. It is important to note that stable iodine-127 is found at much higher concentrations in the groundwater under 200-UP-1 OU ( $^{127}\text{IO}_3^- / ^{129}\text{IO}_3^-$  ratios ranging from 100 to 300) (Truex et al. 2017). It exhibits the same chemical behavior in the subsurface as iodine-129, and thus the presence of iodine-127 influences the biogeochemical processes for iodine-129. Most remediation technologies are not specific for a particular iodine isotope (Kaplan et al. 2012; Truex et al. 2017), and both iodine-129 and iodine-127 should be considered when evaluating contaminant transport and fate. Although the source of iodine-127 is uncertain, iodine is known to be a trace constituent of nitric acid, and enormous volumes of nitric acid were used during Hanford operations. This is considered the most likely source for the iodine-127 in Hanford groundwater.

This section summarizes information on the subsurface properties that influence reactive transport including iodine speciation and adsorption, precipitation, transformations between iodine species, and microbially mediated interactions.

Detailed discussions of the site-specific geochemical and biological processes affecting fate and transport of iodine-129 in the 200-UP-1 OU and updates to the conceptual model for iodine-129 are presented in Truex et al. (2017).

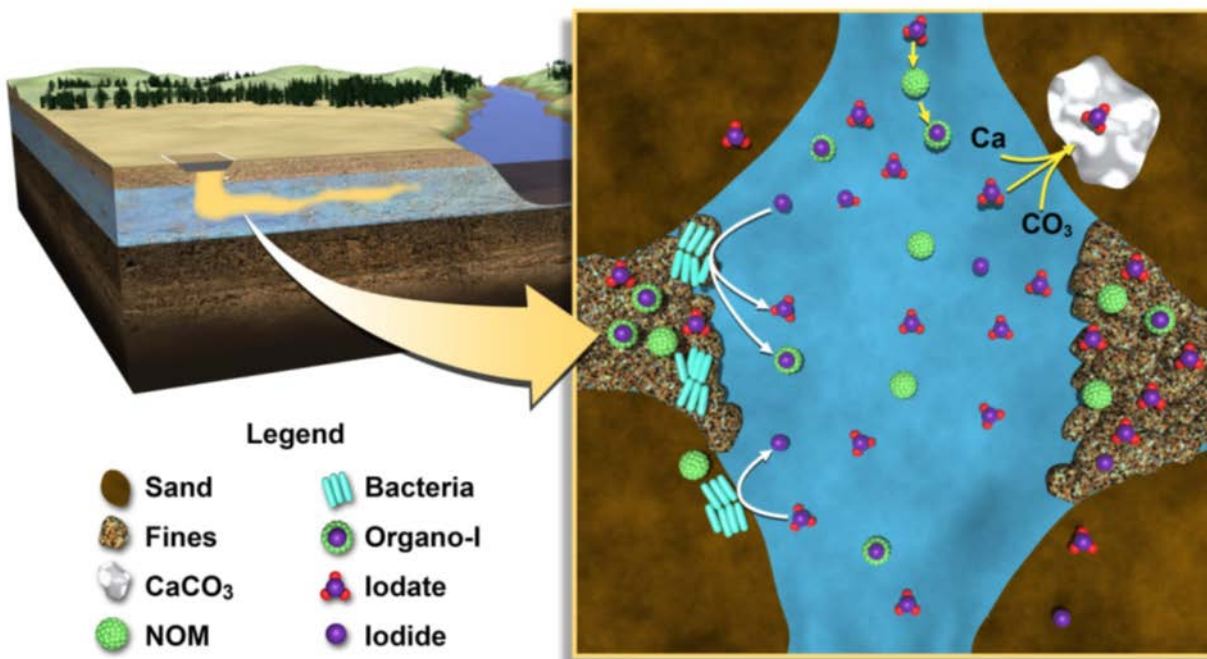


Figure 3.8. Conceptual Overview of Subsurface Biogeochemical Processes Affecting Iodine Fate and Transport (from Truex et al. 2017). Processes include biotic (bacteria) transformations between iodine species and potential transformations to other iodine species. Iodate reduction may also occur abiotically (e.g., by reactions with sediment-associated iron/manganese at the Hanford Site). Iodine species adsorb to sediment surfaces (e.g., on iron oxide deposits or phyllosilicates), with greater adsorption expected in fine-textured sediment zones (Fines). Natural organic matter may facilitate sorption and accumulation of iodine or, as a dissolved organic carbon (DOC), may form mobile Organo-I. Iodate may co-precipitate with calcium carbonate. The figure does not distinguish between iodine-129 and iodine-127 because the processes are the same for both isotopes.

### 3.2.1 Iodine Speciation

The three primary aqueous iodine species are iodate (IO<sub>3</sub><sup>-</sup>), iodide (I<sup>-</sup>), and Organo-I. Iodine can form hypiodous acid in water, and both of these species can react with natural organic matter to form Organo-I compounds (Luther 2011). The relative quantity of these three primary iodine chemical species present in the groundwater is important to predicting iodine plume behavior because each chemical species has different transport characteristics and may be subject to transformation reactions.

Iodide originally was assumed to be the dominant iodine species in Hanford groundwater. However, measurements of speciation of iodine-127 in groundwater in the 200 West Area show a mixture of iodine species (Zhang et al. 2013). Results from seven samples (two from the 200-UP-1 OU and five from the 200-ZP-1 OU) characterized in the work by Zhang et al. are presented in Table 3.2. These results indicate that iodate is the dominant species.

Table 3.2. Chemistry and Iodine-127 Speciation in Filtered Hanford Site Groundwater Samples (from Zhang et al. 2013)

Well	pH	Eh (mV)	DOC (μM)	Ca (mg/L)	Si (mg/L)	Iodide (μg/L)	Iodate (μg/L)	Organo I (μg/L)	Total I (μg/L)	Iodide (%)	Iodate (%)	Organo-I (%)
299-W14-11	7.7	250	50.2	59.4	7.5	0.35	59.50	15.18	75.03	0.5	79.3	20.2
299-W14-13	7.7	249	63.0	81.9	7.4	0.33	42.72	17.01	60.05	0.6	71.1	28.3
299-W14-15	7.9	220	25.5	35.4	5.6	0.43	32.63	5.66	38.72	1.1	84.3	14.6
299-W11-43	7.6	150	37.2	78.8	7.0	0.36	6.66	2.76	9.78	3.7	68.1	28.3
299-W11-88	7.8	321	15.6	22.1	15.0	0.17	7.08	2.08	9.33	1.8	75.9	22.3
699-36-70B	7.8	334	35.3	19.4	10.7	0.23	5.87	2.28	8.38	2.8	70.0	27.2
699-38-70B	7.8	125	21.5	29.7	8.9	1.38	4.18	3.68	9.24	15.0	45.2	39.8
Average	7.8	236	35.5	49.5	8.9	0.46	22.66	6.95	30.08	3.6	70.6	25.8

The premise that iodate was the dominant iodine species disposed to the vadose zone at Hanford also is supported by Sakurai et al. (1989). They measured iodine speciation in spent fuel solutions and their results showed that more than 90% of the added iodine volatilized to I<sub>2</sub> (g) and the remaining iodine in solution was present as iodate (47.6%), iodide (3.2%), molecular iodine (17.3%), organic iodine (6.1%), and colloidal iodine (12.4%). The average ratio of iodate to iodide in those solutions was 19.5, which agrees with that measured in Hanford groundwater (19.6) by Zhang et al. (2013), who also showed that Hanford groundwater samples contained, on average, about 70% iodate, about 26% Organo-I, and a small amount (about 4%) of iodide. Their data also indicate that iodine-127 concentrations were much greater near source terms (e.g., wells 299-W14-11, -13, and -15 in Table 3.2) than further from the source terms. There did not appear to be trends in the observed speciation with respect to either distance from the sources or whether the groundwater sample was collected from the high- or low-concentration portions of the plume, although only a limited number of samples were collected. The fact that iodine-127 exists predominantly as iodate suggests that there are natural biogeochemical drivers promoting the existence of iodine in the oxidized state. The presence of iodine in multiple oxidation states and species within a given aqueous sample is consistent with previous reports of radioiodine and stable iodine speciation measurements at other DOE sites (Kaplan et al. 2014; Otosaka et al. 2011; Truex et al. 2017; Neeway et al. 2019).

More recent sampling of groundwater wells in 200-UP-1 within the iodine-129 plume extent also shows that iodate is the prevalent species present in the groundwater. Table 3.3 shows iodine speciation data for samples collected at depth-discrete locations below the water table in well 299-W22-114. Iodate was the only iodine-127 species present in samples except for the shallowest sample depth (257.5 ft below ground surface; 7.6 ft below water table). Radioactive iodine-129 was present above drinking water standards in samples taken between 7.6 and 67.3 ft below the water table.

Table 3.3. Iodine Speciation in Groundwater Samples During Drilling Monitoring Well 299-W22-114 (August 2016) (from Truex et al. 2017).

Depth (ft bls) <sup>(a)</sup>	Depth (ft bwt) <sup>(b)</sup>	Iodine-129 (pCi/L)	Iodine-127 (µg/L)	Iodate (µg/L)	Iodide (µg/L)	Nitrate (mg/L)
257.5	7.6	4.0	6.2	2.8	3.6	79.7
284.0	34.1	1.7	13.6	17.8	ND	5.3
317.2	67.3	1.5	11.0	14.5	ND	4.4
347.6	97.7	0.3	13.0	17.1	ND	3.5
377.6	127.7	0.5	13.2	17.6	ND	3.9
427.5	177.6	0.3	16.1	21.8	ND	6.2
447.2	197.3	0.05	17.1	22.4	ND	7.5

(a) ft bls =feet below ground surface

(b) ft bwt = feet below water table

ND = non-detect; detection limits: I-127 1.26 µg/L, iodate 0.81 µg/L, iodide 1.23 µg/L

I-129 and NO<sub>3</sub> data were received from CH2M HILL Plateau Remediation Company (CHPRC).

Groundwater samples from three existing monitoring wells located in the plume along with an additional sample from 299-W22-114 also were analyzed to determine possible changes in speciation across the length of the iodine plume. Table 3.4 indicates that iodate was the only species present in the iodine-129 plume.

Table 3.4. Iodine Speciation in Groundwater Samples Collected Over the Length of the 200-UP-1 Plume (from Truex et al. 2017).

Well ID	Depth (ft bwt) <sup>(a)</sup>	Iodine-129 (pCi/L)	Iodine-127 (µg/L)	Iodate (µg/L)	Iodide (µg/L)	NO <sub>3</sub> (mg/L)
299-W22-114 <sup>(b)</sup>	7.6	4.0	NA	NA	NA	84.1
699-36-70A	34.1	8.0	10.1	13.0	ND	16.8
699-35-66A	67.3	1.5	11.0	13.0	ND	24.3
699-36-66B	97.7	2.8	12.7	17.1	ND	53.1

(a) ft bwt = feet below water table

(b) Samples from 299-W22-114 were collected in June 2017 and were not analyzed for iodine-127 or to determine speciation.

NA= Not available

ND = non-detect; detection limits: I-127 1.26 µg/L, iodate 1.62 µg/L, iodide 2.46 µg/L

I-129 and NO<sub>3</sub> data were received from CHPRC.

### 3.2.2 Iodine Sorption

Sorption is used to describe aqueous iodine partitioning to a solid phase, and may include adsorption, absorption, complexation, precipitation, co-precipitation, and ionization with organic carbon. Kaplan et al. (2014) summarized sorption behavior of the different iodine species in Hanford groundwater as follows:

“Iodine sorption is mostly reversible, but a small fraction is not. Consequently, measured (ad)sorption K<sub>d</sub> values are less than desorption K<sub>d</sub> values. Adsorption and interaction with OM are the dominant attenuation mechanisms for iodine-129 in groundwater. Iodate is typically adsorbed more strongly than iodide; adsorption is inversely related to pH. Sediment OM generally decreases iodine mobility, especially when bound to larger

organic moieties. To a lesser extent, organo-iodine complexes may increase mobility, especially when iodine is bound to smaller organic moieties. Radioiodine speciation has been measured at the SRS and Hanford Site contaminant plumes. In both cases, iodide was not the dominant species and iodate and organo-iodine aqueous species were also present. This speciation distribution is not predicted by thermodynamic considerations.”

Iodine and organic carbon form extremely strong covalent bonds, so the presence of small concentrations of dissolved organic carbon can have significant effects on iodine sorption. Organic materials in the subsurface may interact with iodine and affect its fate and transport through (1) formation of immobile sediment-associated Organo-I compounds, (2) formation of mobile soluble Organo-I compounds, (3) formation of volatile Organo-I compounds, (4) providing electron donors for microbially mediated reduction reactions that directly or indirectly affect iodine speciation, and (5) providing adsorption capacity for iodine species.

Low concentrations of Organo-I (and iodate) previously have been detected in Hanford groundwater (Santschi et al. 2012). More recent studies have detected a broad range of organic compounds in the 200-UP-1 OU aquifer groundwater (Truex et al. 2017), including lipid-like, aliphatic, olefinic, and aromatic compounds. Preliminary assessments could not confidently identify specific Organo-I complexation structures in the 200-UP-1 site at Hanford, but the results suggested that these compounds exist at Hanford. Differences in organic matter composition suggest that pore water samples have a higher abundance of aromatic compounds, which are a better target for iodine complexation (Truex et al. 2017).

Studies of sorption in shallow soils indicate that the organic matter also is a primary control on iodine sorption to sediments (Assemi and Erten 1994; Bird and Schwartz 1997; Emerson et al. 2014; Fukui et al. 1996; Kaplan 2003; Neal and Truesdale 1976; Sheppard and Thibault 1991; Whitehead 1974; Yoshida et al. 1992; Yu et al. 1996). Iodine association with natural organic matter is important in sediments, even when organic carbon concentrations are very low (e.g., <0.2% at the Hanford Site) (Santschi et al. 2017; Xu et al. 2015; Zhang et al. 2013). Xu et al. (2015) performed sequential extractions on Hanford sediment samples and showed that a substantial fraction of sediment-associated iodine was more strongly bound to sediments than expected. They noted that the iodine incorporated into calcite accounted for 2.9% to 39.4% of the total sedimentary iodine. Organic carbon appeared to control iodine binding to the sediments and was assumed to be responsible for incorporation of residual iodine (57.1% to 90.6%). Xu et al. (2015) showed that the greater the organic carbon concentrations in the sediments, the greater the values of  $K_d$  for both adsorption and desorption, and the greater residual iodine concentrations (non-exchangeable, non-calcite-incorporated and not associated with Mn or Fe-oxide).

Metal oxides and hydroxides (e.g.  $\text{Fe}(\text{OH})_3$ ,  $\text{Al}(\text{OH})_3$ ,  $\text{MnIV}\text{O}_2$ ) may play an important role in controlling iodine behavior in soils, through both adsorption of inorganic iodine and oxidation of iodide (Shetaya et al. 2012). Ferric and aluminum oxides adsorb iodate more strongly than iodide (e.g., Whitehead 1984; Kodama et al. 2006; Qafoku et al. 2018).

Iodate can co-precipitate with calcium carbonate (Zhang et al. 2013; Podder et al. 2015), which may have important implications related to iodine partitioning near the source terms, where extreme chemical conditions may promote calcite dissolution and re-precipitation. This would facilitate co-precipitation of iodate- and incorporation into the newly formed calcium carbonate. Iodate removal from the mobile aqueous phase through incorporation into  $\text{CaCO}_3$  crystal lattice was previously demonstrated under field conditions at the Hanford Site (Xu et al. 2015; Zhang et al. 2013). Results of these experiments demonstrate that iodate-precipitation more easily occurs concurrently with calcite precipitation and that the water chemistry affects this process. Recent results suggest that iodate incorporation in precipitates occurred during the calcite precipitation process and that removal of iodate was also by adsorption (Truex

et al. 2017). Co-precipitation of iodate with calcium carbonate may be important to the long-term fate of iodine in the far field, where natural calcium carbonate dissolution and precipitation cycling may occur.

Early studies of iodide sorption reported  $K_d$  with values in the range of 0 to 2 mL/g (Kaplan et al. 2000). More recently, studies in Hanford sediments have identified species-specific iodate sorption with  $K_d$  values ranging from 0.3 to 1.2 mL/g (retardation factor of 2.4 to 6.2), and iodide sorption as 0.07 to 0.1 mL/g (retardation factor 1.3 to 1.5) (Truex et al. 2017; Szecsody et al. 2017). Using subsurface sediments, desorption  $K_d$  values were much higher than the iodine adsorption  $K_d$  values, indicating that sorption was only partially reversible (Xu et al. 2015). In these studies, similar trends were noted for  $I^-$  and  $IO_3^-$ , but results indicated that iodate sorption to Hanford Site sediments was greater than iodide sorption (Truex et al. 2017; Qafoku et al. 2018). These conclusions are also supported by recent experimental data and modeling results reported in the references in Appendix B of this report. Appendix B provides a list of publications that support the iodine conceptual model, iodine technology evaluation, and data and parameter evaluations.

### 3.2.3 Iodine Transformation Processes

Transformation reactions can change the relative quantity of chemical species, result in accumulation as a solid phase, or promote volatilization of iodine (Truex et al. 2017). As shown in Figure 3.3, transformation of iodine between species is a key factor in understanding iodine fate and transport. Minerals that participate in redox reactions (e.g., iron and manganese) may mediate iodine transformation processes, either directly or coupled with microbial processes. Microorganisms and/or their cell exudates can mediate many important processes associated with iodine transformations between species, associations with organic compounds, and adsorption. Biotransformation of iodine species includes oxidation of iodide to iodate and then spontaneous formation of more oxidized species, and reduction of iodate to iodide. Iodate reduction appears to be caused by a combination of abiotic phases (e.g., ferrous iron surface phases) and microbial reduction, and the functional capacity for these abiotic and biotic processes may depend on mass of abiotic phases and available substrate for microbial processes.

Reduction of iodate in Hanford Site sediments was observed as part of partitioning experiments (Xu et al. 2015) and may have been driven by sediment-associated ferrous iron or microbial reactions. Thus, ferrous iron incorporated in minerals may be a reactive facies (as iron sulfide, if present, or other ferrous minerals) that needs to be considered relative to iodine fate and transport.

Sediments from locations within the Hanford Site 200-ZP-1 OU iodine plume with background, low, and high levels of iodine-129 were determined to contain microbial taxa (Lee et al. 2018) that have shown the ability to both oxidize  $I^-$  and reduce  $IO_3^-$ . Microbes enriched from sediments obtained from iodine-contaminated portions of the Hanford 200 West Area have demonstrated the potential for both iodide oxidation and iodate reduction (Lee et al. 2018).

Oxidation of iodide can also lead to the generation of more complex organic iodine compounds, including iodinated soil organic matter (SOM). This process may occur in Hanford groundwater since iodide-oxidation was demonstrated by Hanford bacterial isolates. Understanding this process will be important since Organo-I comprises approximately 25% of the iodine species in Hanford groundwater.

Bacteria can use iodate as an alternate electron acceptor for growth; it is converted to iodide under anaerobic or microaerobic conditions. To date, nitrate-reducing, iron-reducing, and sulfate-reducing bacteria have been found to reduce iodate. Sediments from traps incubated in iodine-contaminated groundwater at the Hanford Site have yielded a number of bacterial isolates that can oxidize or reduce different iodine species (Truex et al. 2017), and experiments were performed to determine the ability of various Hanford isolates to reduce iodate in the presence of nitrate, a common co-contaminant in the 200-



UP-1 groundwater. Results for one isolate related to *Agrobacterium tumefaciens* indicated that iodate reduction occurred under both anaerobic and micro-aerobic conditions.

Methyl iodide, CH<sub>3</sub>I, is a volatile iodine compound that plays a large role in carrying iodine from terrestrial and marine environments to the atmosphere. Recent research has shown that a variety of terrestrial bacteria volatilize iodine through the methylation of iodide (Amachi et al. 2001, 2003), and iodine-volatilizing bacteria are ubiquitous in the soil environment. Volatilization of iodine has been shown to be linked to iodide-oxidation, and this process may occur in Hanford groundwater since iodide-oxidation was demonstrated by Hanford bacterial isolates. Formation of volatile Organo-I species during the I-oxidation process was tested in the laboratory and confirmed (Qafoku et al. 2018). Work by Keppler et al. (2000) has shown also that halide ions can be alkylated during oxidation of organic matter by electron acceptors such as Fe(III), and sunlight or microbial mediation are not required. They suggest that such abiotic processes could make a significant contribution to the budget of the atmospheric compounds CH<sub>3</sub>Cl, CH<sub>3</sub>Br, and CH<sub>3</sub>I. This mechanism for volatilization of iodine has not been previously considered for Hanford.

### 3.3 Iodine-129 Source and Release Information

As described in Section 2 of this report, iodine-129 in the 200-UP-1 OU originated primarily from the 216 U 1 and 216 U 2 Cribs near U Plant and from the REDOX Plant waste sites in the southern portion of the 200 West Area. A summary of estimated total iodine-129 activities and liquid effluent volumes and calculated mean concentrations that were released to the most significant of the 200-UP-1 waste sites is presented in Table 3.5. The REDOX Plant cribs (216-S-1/2, 216-S-7, and 216-S-9) were the primary sources with the largest discharge volumes and highest iodine-129 concentrations in 200 UP-1; greater than 100 times the 1 pCi/L cleanup level.

Table 3.5. Primary Waste Sites with Highest Iodine-129 Activity and Liquid Effluent Releases in 200-UP-1 (Eslinger et al. 2006a,b).

Site	Total Activity (Ci)	Liquid Effluent Volume (m <sup>3</sup> )	Mean Concentration (pCi/L)
216-S-1/2	1.37E-01	160,426	855
216-S-7	3.55E-01	389,901	911
216-U-1/2	2.27E-06	15,929	0.14
216-S-9	2.98E-02	49,580	601
216-U-10	2.14E-01	159,859,379	1.34

Concentration trends of iodine-129 in groundwater show no clear evidence of a continuing source of iodine-129 from the vadose zone to the groundwater aquifer at concentrations above 1 pCi/L. (Truex et al 2017).

The 200-UP-1 RAWP (DOE 2013a) estimated a total activity of 0.1 Ci for iodine-129 in groundwater (Table 3.6) based on data from the 2011 Hanford Groundwater Monitoring report (DOE 2012b). The total estimated release of iodine-129 from the five sites listed in Table 3.5 was 0.73 Ci. This difference could be attributed to several factors, including uncertainty in inventory estimates, loss to volatilization, and some fraction of total disposed amount of iodine-129 still residing in the vadose zone above the unconfined aquifer. Given the general lack of depth-discrete groundwater monitoring data, and the paucity of data for vadose zone pore water samples, any further insights into the spatial distribution of iodine-129 in the aquifer and vadose zone, and potential future transport and fate, will require the use of numerical models.

Table 3.6. Characteristics of the Iodine-129 Plume Within 200-UP-1 (from 200-UP-1 RAWP; DOE 2013a)

Porosity <sup>(a)</sup>	Iodine-129 Plume Area ha (ac) <sup>(b)</sup>	Iodine-129 Estimated Average Plume Thickness, m (ft) <sup>(b)</sup>	Iodine-129 Plume Pore Volume, Billion L (gal)	90 <sup>th</sup> Percentile Concentration <sup>(b)</sup>	Estimated Iodine-129 Mass (Ci)
0.2	383 (948)	30 (100)	23 (6.2)	3.5 pCi/L	0.1
(a) Source: Record of Decision for Interim Remedial Action, Hanford 200 Area Superfund Site, 200-UP-1 Operable Unit (EPA et al. 2012). Information was generated in 2009 as part of the RI/FS Report (DOE 2012a).					
(b) Based on Hanford Site Groundwater Monitoring for 2011 (DOE 2012b).					

### 3.4 Simulation of Iodine-129 Transport and Fate

Groundwater monitoring data indicate that the size of the iodine-129 plume is decreasing (Section 2). However, the size and depth of the affected area and nature of the subsurface make characterization and monitoring challenging. Available observations are also relatively sparse in space and time. In this section, simulated iodine-129 plumes generated using a numerical flow and transport model are compared with plume maps generated by the Hanford Groundwater Monitoring Program. Simulations were performed using the eSTOMP simulator (Fang et al. 2018), a parallel version of the STOMP simulator (White et al. 2018; White and Oostrom, 2006).

The distribution and history of iodine-129 in the unconfined aquifer system has been described using measured values from well sampling (see Section 2). The distribution of iodine-129 in the vadose zone is more difficult to determine because core sampling is very sparse, but an initial assessment was provided by Rockhold et al. (2018b). In this section, a revised subsurface flow and transport model for the area of the 200-UP-1 OU was used to evaluate the potential transport, fate, and distribution of iodine-129 in the aquifer.

The model domain (Figure 3.9) covers the 200-UP-1 OU area. This represents a revision to an earlier, larger model that covered both 200-UP-1 and 200-ZP-1 (Rockhold et al. 2018b). The model includes multiple injection and extraction wells within the 200-UP-1 OU associated with P&T operations, including the three hydraulic containment wells located downgradient of the iodine-129 plume (299-E20-1, 299-E20-2, and 299-E11-1) that were installed as part of the interim remedy. The preferred alternative in the interim ROD (EPA et al. 2012) for groundwater cleanup in the 200 West Area of Hanford included 35 years of operation of the P&T system, which spans the time frame from 2012 to 2047. That pumping schedule is included in the model, which assumes removal of iodine-129 dissolved in groundwater, and injection of clean water devoid of iodine-129.

The revised flow and transport model uses the Central Plateau Vadose Zone Geologic Framework Model (GFM) (Springer 2018), and measured water levels through 2018 to determine water table boundary conditions. Water levels at the end of 2018 are assumed to persist unchanged into the future, although some further decline of the water table elevation is expected (Figure 3.7). Simulation results from Rockhold et al. (2018b) and the GFM suggest that the groundwater iodine-129 plume is located primarily within the Ringold E unit of the unconfined aquifer system. Aquifer test results for wells within the 200-UP-1 OU were reviewed (Spane and Newcomer 2008, 2004; Spane et al. 2003, 2002, 2001a,b) to estimate a saturated hydraulic conductivity value of 6 m/d and a porosity value of 0.294 for the Ringold E unit.

Rockhold et al. (2018b) modeled liquid effluent discharges and iodine-129 releases from Corbin et al. (2005) and Eslinger et al. (2006a,b) for the primary 200-UP-1 OU waste sites identified by Truex et al. (2015), as well as P&T records provided by CHPRC. Revised inventory estimates have been developed (Zaher and Agnew 2018), but the estimated time-dependent liquid effluent and contaminant release information was not available for use in this report. Therefore, instead of modeling historical liquid effluent discharges and iodine-129 releases, model simulations used the 1993 groundwater iodine-129 plume map for initial conditions (provided by CHPRC). Although this treatment discounts any continuing source of iodine-129 from the vadose zone, both field evidence (Truex et al. 2017) and simulations (Rockhold et al. 2018b) indicate that the groundwater iodine-129 plume in 200-UP-1 is largely disconnected from vadose zone sources and that any continuing flux of iodine-129 from vadose zone sources to groundwater in the 200-UP-1 OU will result in groundwater concentrations below the DWS.

Regarding iodine volatilization, in the experiments reported by Qafoku et al. (2018), iodomethane was produced and was attributed to microbially-mediated processes. However, specific mechanisms for iodomethane production were not explicitly identified, and samples were also heated to promote volatilization and facilitate gas sampling. Keppler et al. (2000) proposed an oxidation-reduction mechanism for formation of the volatile species iodomethane from an organic carbon source and iodide in the presence of iron. However, available data indicate that iodate is the predominant iodine species under the oxic conditions of the Hanford vadose zone and unconfined aquifer systems. Relatively little iodomethane generation is expected from the groundwater iodine-129 plume under current site conditions. Volatilization as a mechanism for iodine loss from the unconfined aquifer was assumed to be negligible and was therefore not considered further for the modeling reported here.

Laboratory column experiments described by Qafoku et al. (2018) were used to evaluate different models of iodine sorption in sediments from the 200-UP-1 OU area. A linear equilibrium Freundlich isotherm (a.k.a.  $K_d$ ) model, and one- and two-site kinetic Langmuir sorption models were evaluated (Fetter 1993). The  $K_d$  model assumes a linear relationship between aqueous and sorbed species concentrations. The kinetic Langmuir sorption equation can be written as

$$\frac{\partial q}{\partial t} = k_f c(b - q) - k_b q \quad (3.1)$$

where  $q$  and  $c$  are the adsorbed and aqueous phase concentrations, respectively,  $k_f$  is a sorption rate constant,  $k_b$  is a desorption rate constant, and  $b$  is a maximum sorption capacity. Under local equilibrium conditions (i.e.,  $\partial q / \partial t = 0$ ), (3.1) becomes

$$q = \frac{k_f b c}{k_b + k_f c}, \quad (3.2)$$

which is the Langmuir isotherm. Figure 3.10 shows simulation results obtained using the  $K_d$  model, and the one- and two-site kinetic Langmuir sorption models, with observed iodate breakthrough curve data (iodate aqueous concentration versus pore volume) for the Column 1 experiment reported by Qafoku et al. (2018). The kinetic Langmuir models are shown to provide better fits to the laboratory experimental data relative to the  $K_d$  model. The one-site kinetic Langmuir sorption model was selected for use in field-scale modeling based on its ability to fit laboratory experimental data for iodate and to produce simulation results that are consistent with field observations.

Figure 3.11 and Figure 3.12 show the plan-view extents of the iodine-129 plume at different times based on maps produced by the Groundwater Monitoring Program (contour lines), and simulated plumes (filled contours) generated using the one-site kinetic Langmuir sorption model. Parameters used in the kinetic Langmuir model for field-scale modeling were based on those determined from the laboratory

experiments ( $k_f = 10.09 \text{ m}^3/(\text{kg}\cdot\text{s})$ ,  $k_b = 0.02 \text{ 1/s}$ ), except for the maximum sorption capacity ( $b$  parameter) which was reduced by 10x (from  $6.5\text{e-}7 \text{ mol/kg}$  for lab experiment, to  $6.5\text{e-}8 \text{ mol/kg}$  for field-scale model). No quantitative correlations were developed between surface area or gravel fraction and maximum sorption capacity. However, this change in maximum sorption capacity has physical justification because laboratory experiments were performed using the <2-mm size fraction of the sediments, which have a larger specific surface area and thus more sorption sites than the coarser, field-textured sediments.

Simulations of field-scale transport were also performed with the  $K_d$  model, using  $K_d$  values of 0.02 and  $0.2 \text{ cm}^3/\text{g}$ . Both cases produce simulated iodine-129 plumes that are similar to those observed in the field, but results with  $K_d = 0.2 \text{ cm}^3/\text{g}$  qualitatively match field observations slightly better. With  $K_d = 0.02 \text{ cm}^3/\text{g}$ , the simulated iodine-129 plume reaches the eastern boundary of the 200-UP-1 OU by year 2100. With  $K_d = 0.2 \text{ cm}^3/\text{g}$ , the simulated plume is still well within the boundary of the 200-UP-1 OU by year 2100, similar to the results obtained with the kinetic Langmuir model. The kinetic Langmuir model is qualitatively more consistent with field observations in terms of the apparent shrinking of the core of the iodine-129 plume over time.

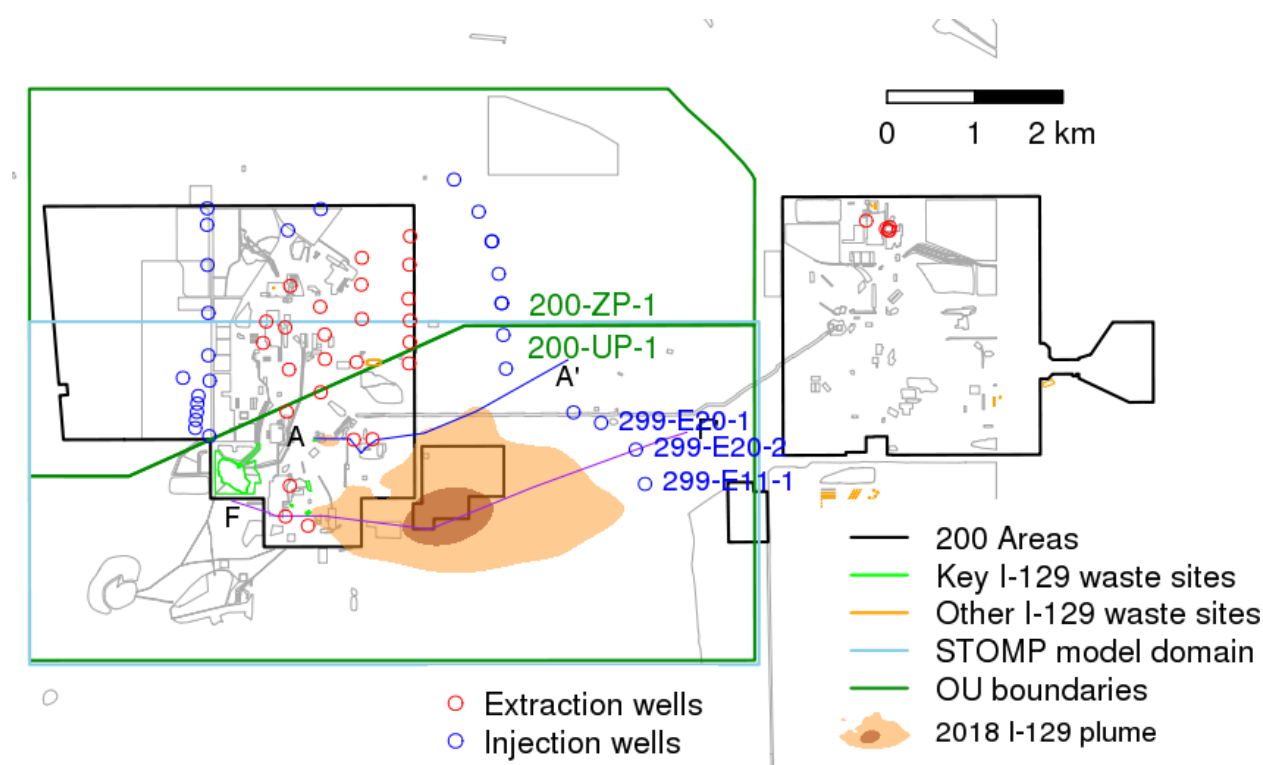


Figure 3.9. Reference Map Showing eSTOMP Model Domain. Transect lines A-A' and F-F' are same as those in Figure 2.6.

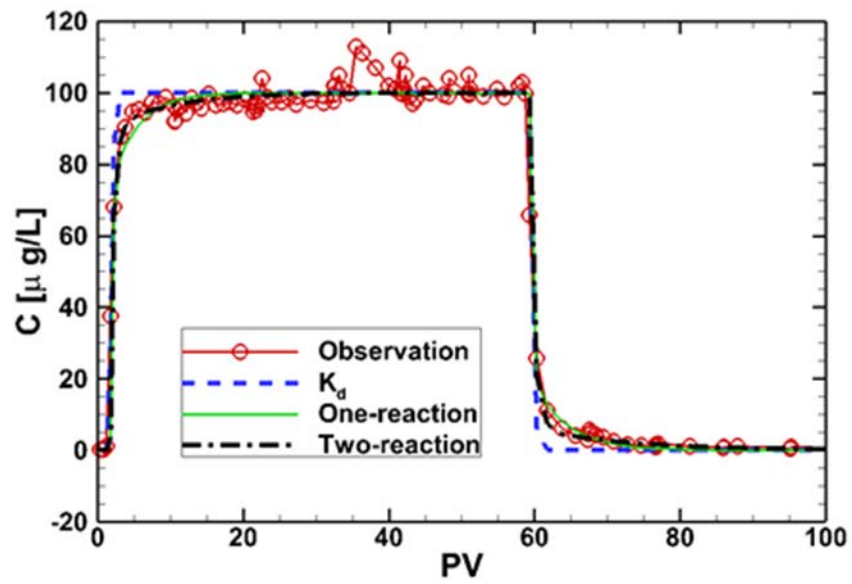
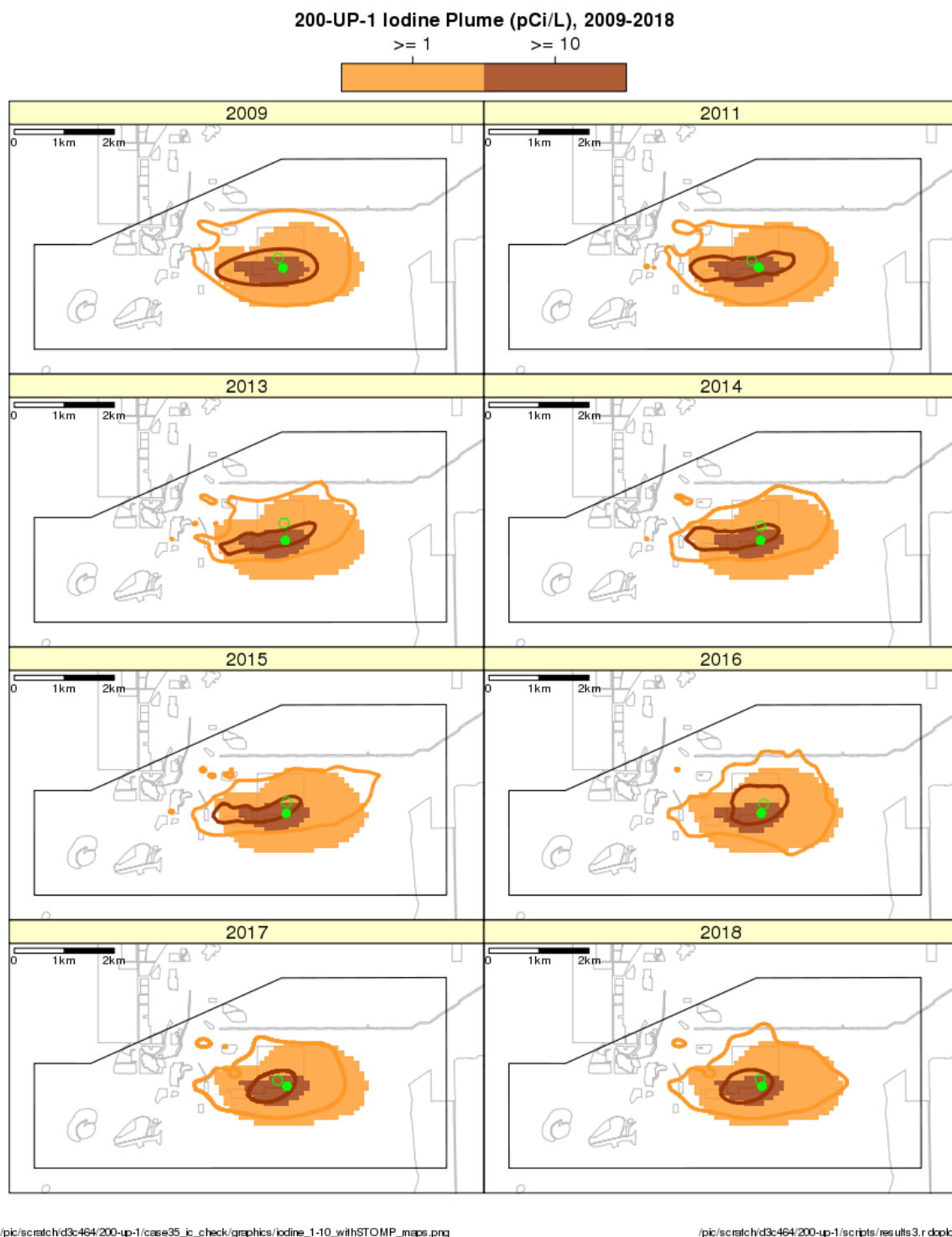


Figure 3.10. Simulation results and observed iodate breakthrough curve data for the Column 1 experiment from Qafoku et al. (2018).



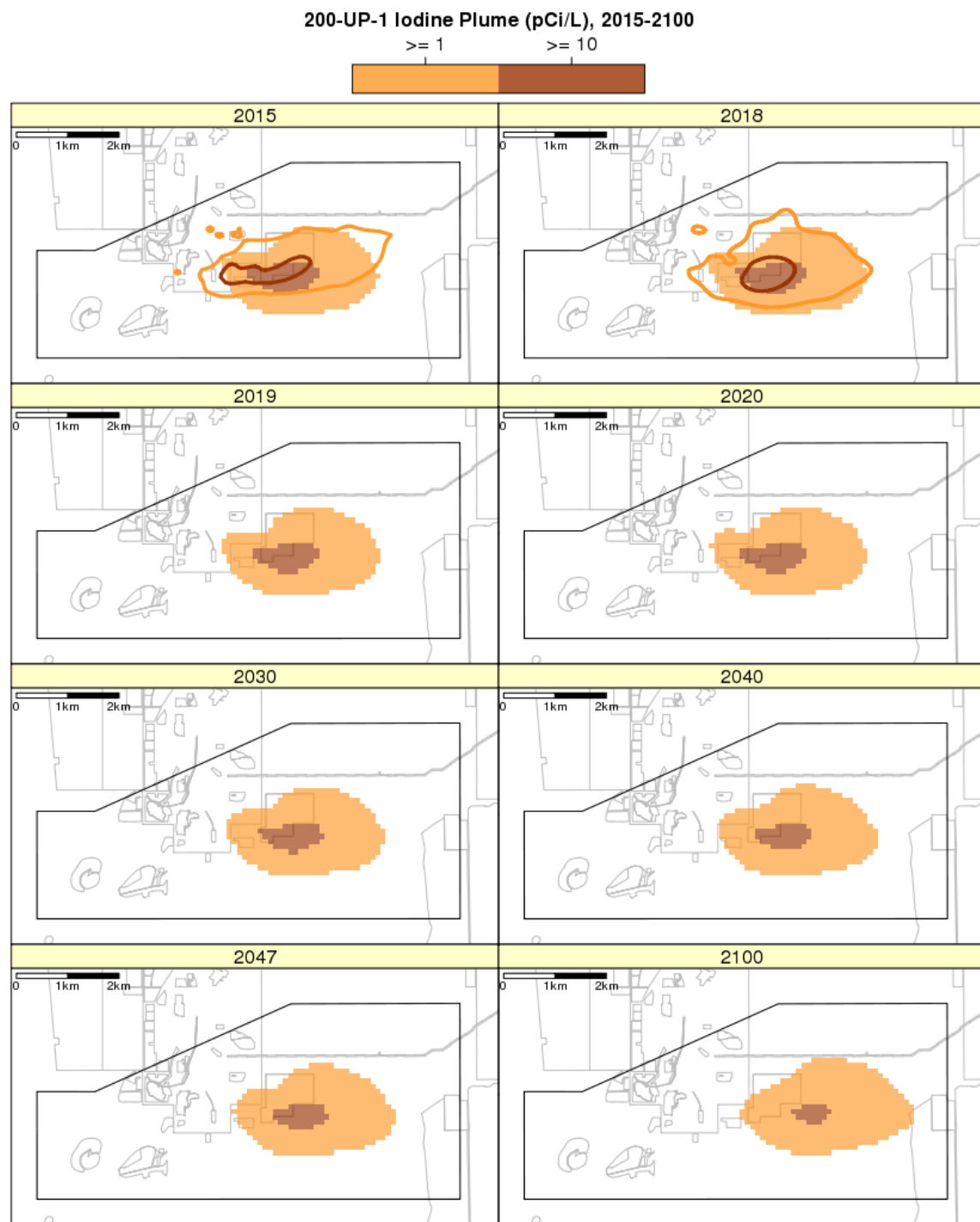


Figure 3.12. eSTOMP Simulation Results (filled contours) Using a One-Site Kinetic Langmuir Sorption Model, and Geographic Information System (GIS) Maps of Field Data (contour lines) for Years 2015-2100.

The plume maps produced by the Hanford Groundwater Monitoring Program represent interpolated results based on sparse well data while the model results represent a horizontal slice through the modeled domain. The sparsity of well monitoring results is due in part to the fact that the core of the iodine-129 groundwater plume is located immediately below the Environmental Restoration Disposal Facility (ERDF). Restrictions on drilling new wells through an active waste disposal facility impose some limitations on how well the plume is defined in the field.

The current 200 West Area P&T system began operation in 2012. The injection wells being used for hydraulic containment of the iodine-129 plume in the 200-UP-1 began pumping in 2015. Simulations were run out to year 2100, with the P&T system operating until 2047 (35 years after the start of the P&T system). At that point the source terms used to represent all extraction and injection wells were turned off. The results shown in Figure 3.12 suggest that the iodine-129 plume will remain within the 200-UP-1 OU through year 2100.

Table 3.7. Estimated and Modeled Migration of Iodine-129 Groundwater Plume. Movement of the plume as documented by the Groundwater Monitoring Program (DOE 2018a) is calculated from the centroids of the GIS polygons representing the 1 pCi/L plume. Movement of the simulated plume is calculated from the center of mass for dissolved iodine-129 in the  $z = 110\text{-}120$  m horizon.

Time Period	Groundwater Monitoring GIS		eSTOMP Model	
	Distance and Direction	Rate (m/yr)	Distance and Direction	Rate (m/yr)
1993-2008	99 m N	6.6	201 m E	13.4
2008-2018	141 m E	14.1	95 m E	9.5
2018-2047	N/A	N/A	259 m E	8.9



## 4.0 Evaluation of Restoration Potential

Restoration options for remediation of the iodine-129 contamination beneath the 200-UP-1 OU currently are limited by the size of the plume, the biogeochemistry of iodine-129 and natural stable iodine-127, and tested, viable treatment technologies. The potential remediation technologies identified can be categorized into three classes: in situ groundwater remediation, ex situ groundwater remediation, and vadose zone remediation. The evaluation of the range of treatment technologies with potential applications for iodine-129 is provided in Truex et al. (2019).

As described in Sections 2.1 and 3.2 of this document, discharge of waste waters to the cribs, ponds, and ditches that were the original sources of iodine-129 in 200-UP-1 groundwater have been discontinued. There are no current discharges of wastewater containing iodine-129 to the ground surface. Continued downward flux of iodine-129 through the vadose zone may continue to contribute contamination to the groundwater at a very low rate, but groundwater monitoring well data suggest that no significant, ongoing sources of iodine-129 exist within the OU. More accurately stated, the concentrations and fluxes of iodine-129 moving from the vadose zone into the groundwater may be low enough that when sampled over a 5-m well screen, the sampled iodine-129 concentrations may be below the DWS.

Section 4.1 provides relevant information on operation of the injection wells installed to provide hydraulic containment of the iodine-129 plume and suitability and performance of the groundwater monitoring program for 200-UP-1 OU. Section 4.2 provides context regarding the current state of knowledge on restoration, and the potential timeframe for restoration. The ongoing evaluations of remediation technologies identified as potentially viable treatments for iodine-129 in groundwater are discussed in Section 4.3.

### 4.1 Remedial Action Performance Analysis

The 200 West P&T system operates the injection wells for hydraulic containment of the iodine-129 plume. Section 4.1.1 describes implementation of the hydraulic containment remedy. Section 4.1.2 presents additional data indicating that iodine-129 concentrations in groundwater are decreasing.

In addition to the iodine-129 plume, technetium-99, uranium, tritium, nitrate, chromium, and carbon tetrachloride also form groundwater plumes in the OU. During 2016, the 200 West P&T system treated a total volume of 3038.7 million L (802.2 million gal), removing 1721 kg of carbon tetrachloride, 330,877 kg of nitrate, 69.7 kg of chromium (total and hexavalent), 8.6 kg of trichloroethene, and 147 g (2.52 Ci) of technetium-99 (DOE 2017c). Iodine-129 removal was negligible, as the influent and effluent concentrations throughout 2016 were less than the detection limit of 0.6 pCi/L, owing to mixing of waters extracted from different areas.

An extensive groundwater monitoring program is operated across the Hanford Site (DOE 2019a) and contaminant concentrations were monitored in 1076 wells across the site in 2018. Within the 200 UP-1, groundwater monitoring is conducted under CERCLA for the 200-UP-1 OU and ERDF, and under RCRA for WMA S-SX, WMA U, and the 216 S-10 pond and ditch. More than 1400 groundwater samples collected from more than 80 wells located in 200-UP-1 have been analyzed for iodine-129 during monitoring since 2003. As described in Section 2 of this document, concentrations of iodine-129 are decreasing in most of the monitored wells within the OU. Comparisons of inferred plume contours from 1993 to 2018 also indicate that the plume areal extent is shrinking (Figure 2.3, Figure 2.4, and Figure 2.5).

#### 4.1.1 Hydraulic Containment Remedy for Iodine-129

The iodine-129 plume remedy is implemented as part of the 200 West P&T design, which includes a total of 26 extraction and 27 injection wells, with an installed capacity to treat up to 9464 L/min (2500 gpm) of extracted groundwater. At the end of 2016, three active remedies were operating in 200 UP-1: WMA S-SX groundwater extraction system, U Plant area P&T system, and the hydraulic containment system for the iodine-129 plume. The U Plant area P&T and the iodine-129 plume hydraulic containment system began operating in 2015 as part of the 200-UP-1 remedy (DOE 2017c).

The iodine-129 plume hydraulic containment system consists of three hydraulic control wells for injecting treated water from the 200 West P&T system to the east of the iodine-129 plume boundary (between the 200 West and 200 East Areas). Operation of these wells provides a degree of hydraulic containment by increasing the water table elevation downgradient of the plume to slow its eastward migration while treatment technologies are further evaluated. The three injection wells (299-E11-1, 299-E20-1, and 299-E20-2) were established approximately 375 to 550 m east (downgradient) of the leading edge of the plume. Previous numerical modeling indicated that three wells located downgradient of the plume with injection rates of 189 to 379 L/min (50 to 100 gpm) per well would be sufficient for hydraulic containment. The injected water is post-treatment effluent from the treatment system, and average concentrations in the treated water meet all of the cleanup levels specified in the 200-UP-1 ROD (EPA et al. 2012; DOE 2017c). In 2018, the total average flow rate for all three wells was 843 L/min (223 gal/min), or 149% of the minimum nominal flow rate. The total volume of water injected into the aquifer during 2018 was 443 million L (117 million gal), and the total volume of water injected since system startup was 1.187 billion L (313.5 million gal) (DOE 2019b, 2018b).

Operation of the hydraulic containment injection wells began on October 28, 2015. Monthly water level measurements began in September 2015 from a network of monitoring wells near the injection wells. Potentiometric surface maps prepared using multi-event universal kriging from the water level measurements show small groundwater mounds around the injection wells (DOE 2017c, 2018b, 2019b). The groundwater flow direction is toward the east-northeast, and the magnitude of the hydraulic gradient is large in the area just to the east of the hydraulic containment injections wells, as shown by the close spacing of the water table contours (Figure 4.1). The increased magnitude in the hydraulic gradient is caused, at least in part, by a decrease in aquifer thickness to the east, and a resulting decrease in transmissivity (DOE 2017c). The R1m unit, which forms the base of the unconfined aquifer, increases in elevation toward the east, resulting in a thinner aquifer. The hydraulic conductivity of the aquifer sediments may also decrease toward the east, which would also contribute to the reduced transmissivity and larger hydraulic gradient.

The 2018 Hanford Groundwater Pump and Treat (DOE 2019b) report presents an evaluation of the hydraulic control remedy by comparing water table maps and hydraulic gradients for pre- and post-injection conditions. The available data suggest that the migration rate of the iodine-129 plume has been reduced.

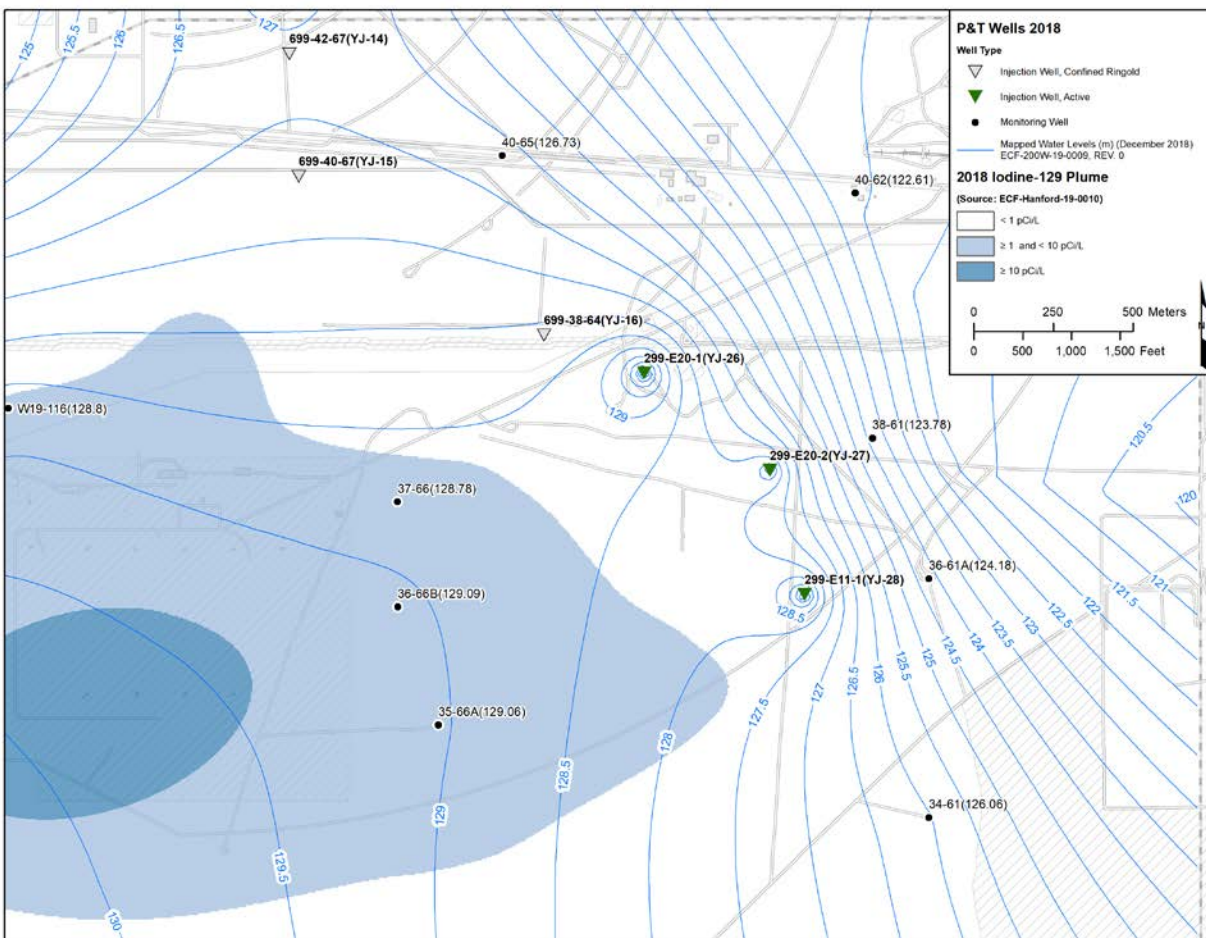


Figure 4.1. Water Table for the Iodine 129 Plume Hydraulic Containment Remedy, December 2018 (from DOE 2019b).

#### 4.1.2 Trends in Subsurface Iodine-129 Concentrations

As illustrated in Section 2, the areal extent of the iodine-129 plume has contracted since initial estimation of plume boundaries in 1993. In addition, concentrations of iodine-129 show a decreasing trend in most wells that are sampled. Maps illustrating the iodine-129 plume extent over a 20-year period beginning in 1993 shown in Truex et al. (2017) and Section 2.2 of this document indicate that plume has fluctuated in shape, but declined overall, in areal extent. Well data, in conjunction with the plume maps, are consistent with influences from (1) historical pulses of iodine into the groundwater that have now diminished in magnitude and (2) declining hydraulic gradients from dissipation of the historical 200 West Area groundwater mound created during processing operations. The data imply that the current plume was generated from a historical source that has diminished, and that a discrete plume is now migrating in the aquifer.

The overall decline in plume area and concentration are consistent with natural attenuation processes affecting the plume. Increases in concentrations for discrete locations in the central portion of the plume are consistent with movement of a higher concentration core along a flow path. A higher concentration core may still be attenuating, but temporal data at individual wells may be showing the progression of a plume core past the location of the well. The water table and inferred groundwater movement as shown in Figure 4.1 indicates a strong overall gradient to the east. The effect of the hydraulic containment wells

appears to be localized, but the wells have only been operating since 2015, so their full effect is still under evaluation (DOE 2019b). Predictive modeling results suggest that the hydraulic containment wells are effective in slowing plume migration (Table 3.7).

## **4.2 Restoration Timeframe Analysis**

The half-life of iodine-129 is 15.7 million years. MNA is generally not a viable remedy for such a long-lived radionuclide unless the hydraulic regime, transport distance, and/or other attenuation processes are such that mixing, dispersion, sorption, and/or reactions can be shown to reduce groundwater concentrations to less than the MCL in a reasonable timeframe. The model results shown in the previous section, generated using an integrated model of the combined vadose zone-aquifer system with a kinetic Langmuir sorption model, suggest that under current and expected future conditions, groundwater plume concentrations will remain above the MCL through year 2100. At later times, the iodine-129 plume will likely move further to the east, outside of the 200-UP-1 OU boundaries. Evaluation of longer term behavior will require the use of a model that considers a larger area of the central plateau.

## **4.3 Other Applicable Technologies**

As noted in the 200-UP-1 Evaluation Plan (DOE 2017a), field-tested, mature remediation technologies were not readily available to use in remediating the iodine-129 plume in 200-UP-1 OU. However, investigations have been conducted to identify potential remediation technologies and are reported in Truex et al. (2019).

## 5.0 Summary and Conclusions

The preferred alternative described in the 2012 ROD for the 200-UP-1 OU Interim Remedial Action includes active remediation using a combination of (1) groundwater P&T and (2) MNA for portions of the contaminated groundwater, followed by institutional controls until cleanup levels are met for unrestricted use. As noted in the 200-UP-1 OU interim ROD, no treatment technology for iodine-129 had been found that could achieve the DWS of 1 pCi/L for the iodine-129 concentrations present in the 200-UP-1 OU groundwater. Therefore, the 200-UP-1 OU interim ROD specified hydraulic containment of the iodine-129 plume, update of the conceptual model for iodine-129, and further evaluation of potentially applicable iodine-129 treatment technologies. The 200-UP-1 OU ROD further stated that in the event a viable treatment technology is not available, the use of a TI waiver be considered as part of the final remedy.

Available data and modeling results indicate that the groundwater iodine-129 plume in the 200-UP-1 OU can be hydraulically contained, but this action will not reduce iodine-129 concentrations to below the DWS. Natural attenuation mechanisms can reduce the plume concentrations, as evidenced by field data that show a shrinking iodine-129 plume footprint over time. However, predictive modeling results, which assume current P&T operations will continue through year 2047, suggest that the plume will remain within the 200-UP-1 OU at concentrations above the DWS through year 2100. This means that a TI waiver may only be appropriate for the more recalcitrant regions of the 200-UP-1 plume, as natural attenuation mechanisms and targeted remedies (that are still under evaluation) may reduce the more distal regions of the iodine-129 plume to below the DWS.

## 6.0 Quality Assurance

This work was performed in accordance with the Pacific Northwest National Laboratory (PNNL) Nuclear Quality Assurance Program (NQAP). The NQAP complies with the United States Department of Energy Order 414.1D, *Quality Assurance*, and 10 CFR 830 Subpart A, *Quality Assurance Requirements*. The NQAP uses NQA-1-2012, *Quality Assurance Requirements for Nuclear Facility Application* as its consensus standard and NQA-1-2012 Subpart 4.2.1 as the basis for its graded approach to quality.

## 7.0 References

- 10 CFR 830 Subpart A, *Quality Assurance Requirements*. U.S. Code of Federal Regulations.
- Amachi S, M Kasahara, S Hanada, Y Kamagata, H Shinoyama, T Fujii, and Y Muramatsu. 2003. "Microbial Participation in Iodine Volatilization from Soils." *Environmental Science & Technology* 37(17):3885-3890.
- Amachi S, Y Kamagata, T Kanagawa, and Y Muramatsu. 2001. "Bacteria Mediate Methylation of Iodine in Marine and Terrestrial Environments." *Applied and Environmental Microbiology* 67(6):2718-2722.
- ASME NQA-1-2012, *Quality Assurance Requirements for Nuclear Facility Applications*. American Society of Mechanical Engineers, New York, NY.
- Assemi S and HN Erten. 1994. "Sorption of Radioiodine on Organic Rich Soil, Clay Minerals, and Alumina." *Journal of Radioanalytical and Nuclear Chemistry* 178:193-204.
- Bergeron MP, GV Last, AE Reisenauer. 1987. *Geohydrology of a Commercial Low-Level Radioactive Waste Disposal Facility near Richland, Washington*. Prepared for US Ecology, Inc., Louisville, Kentucky under Contract 2311207358, by Battelle – Pacific Northwest National Laboratory, Richland, WA.
- Bird GA and W Schwartz. 1997. "Distribution Coefficients, Kds, for Iodide in Canadian Shield Lake Sediments under Oxidic and Anoxic Conditions." *Journal of Environmental Radioactivity* 35(3):261-279.
- Bjornstad BN. 1990. *Geohydrology of the 218-W-5 Burial Ground, 200-West Area, Hanford Site*. PNL-7336, Pacific Northwest Laboratory, Richland, WA.
- Connelly MP, BH Ford, and JV Borghese. 1992a. *Hydrogeologic Model of the 200 West Groundwater Aggregate Area*. WHC-SD-EN-TI-014, Westinghouse Hanford Company, Richland, WA.
- Connelly MP, JV Borghese, CD Delaney, BH Ford, JW Lindberg, and SJ Trent. 1992b. *Hydrogeologic Model for the 200 East Groundwater Aggregate Area*. WHC-SD-EN-TI-019, Westinghouse Hanford Company, Richland, WA.
- Corbin RA, BC Simpson, MJ Anderson, WF Danielson III, JG Field, TE Jones, and CT Kincaid. 2005. *Hanford Soil Inventory Rev. 1*. RPP-26744, Rev. 0, CH2M Hill Hanford Group, Inc. Richland, WA.
- DOE. 2012a. *Remedial Investigation/Feasibility Study for the 200-UP-1 Groundwater Operable Unit*. DOE/RL-2009-122, U.S. Department of Energy, Richland Operations Office, Richland, WA.
- DOE. 2012b. *Hanford Site Groundwater Monitoring for 2011*. DOE/RL-2011-118, Rev. 0, U.S. Department of Energy, Richland Operations Office, Richland, WA.
- DOE. 2012c. *Proposed Plan for Remediation of the 200-UP-1 Groundwater Operable Unit*. DOE/RL-2010-05, Rev. 0, U.S. Department of Energy, Richland Operations Office, Richland, WA.
- DOE. 2013a. *200-UP-1 Groundwater Operable Unit Remedial Design/Remedial Action Work Plan*. DOE/RL-2013-07, Rev. 0, U.S. Department of Energy, Richland, WA.

DOE. 2013b. *Hanford Site Cleanup Completion Framework*. DOE/RL-2009-10, Rev. 1, U.S. Department of Energy, Richland Operations Office, Richland, WA.

DOE. 2017a. *UP-1 Evaluation Plan for Iodine*. DOE/RL-2015-69, Rev. 0, U.S. Department of Energy, Richland Operations Office, Richland, WA.

DOE. 2017b. *Hanford Site Groundwater Monitoring Report for 2016*. DOE/RL-2016-67, Rev. 0, U.S. Department of Energy, Richland, WA.

DOE. 2017c. *Calendar Year 2016 Annual Summary Report for the 200-ZP-1 and 200-UP-1 Operable Unit Pump-and-Treat Operations*. DOE/RL-2016-69, Rev. 0, U.S. Department of Energy, Richland, WA.

DOE. 2018a. *Hanford Site Groundwater Monitoring Report for 2017*. DOE/RL-2017-66, Rev. 0, U.S. Department of Energy, Richland, WA.

DOE. 2018b. *Calendar Year 2017 Annual Summary Report for the 200-ZP-1 and 200-UP-1 Operable Unit Pump-and-Treat Operations*. DOE/RL-2017-68, Rev. 0, U.S. Department of Energy, Richland, WA.

DOE. 2019a. *Hanford Site Groundwater Monitoring Report for 2018*. DOE/RL-2018-66, Rev. 0, CH2M Hill Plateau Remediation Company, U.S. Department of Energy, Richland, WA.

DOE. 2019b. *Calendar Year 2018 Annual Summary Report for the 200-ZP-1 and 200-UP-1 Operable Unit Pump-and-Treat Operations*. DOE/RL-2018-68, Rev. 0, U.S. Department of Energy, Richland, WA.

DOE Order 414.1D, *Quality Assurance*. U.S. Department of Energy, Washington, D.C.

Emerson HP, C Xu, Y Feng, M Lilley, DI Kaplan, PH Santschi, and BA Powell. 2014. "Geochemical Controls of Iodine Transport in Savannah River Site Subsurface Sediments." *Chemical Geology* 45:105-113.

EPA. 1988. *Guidelines for Ground-Water Classification Under the EPA Ground-Water Protection Strategy*. U. S. Environmental Protection Agency, Office of Ground-water Protection, Washington D.C.

EPA, Ecology, and DOE. 2012. *Record of Decision for Interim Remedial Action Hanford 200 Area Superfund Site 200-UP-1 Operable Unit*. U.S. Environmental Protection Agency, Washington State Department of Ecology, and U.S. Department of Energy, Olympia, WA.

Eslinger PW, CT Kincaid, WE Nichols, and SK Wurstner. 2006a. *A Demonstration of the System Assessment Capability (SAC) Rev. 1 Software for the Hanford Remediation Assessment Project*. PNNL-16209, Pacific Northwest National Laboratory, Richland, WA.

Eslinger PW, DW Engel, LH Gerhardstein, CA Lopresti, TB Miley, WE Nichols, DL Strenge, and SK Wurstner. 2006b. *Updated User Instructions for the Systems Assessment Capability, Rev. 1, Computer Codes – Volume 1: Inventory, Release, and Transport Modules*. PNNL-16115, Volume 1, Pacific Northwest National Laboratory, Richland, WA.

Fang Y, D Appriou, DH Bacon, V Freedman, ML Rockhold, C Ruprecht, G Tartakovsky, MD White, SK White, and F Zhang. 2018. *eSTOMP Online User Guide*. Accessed on September 15, 2018 at [http://stomp.pnnl.gov/estomp\\_guide/eSTOMP\\_guide.stm](http://stomp.pnnl.gov/estomp_guide/eSTOMP_guide.stm) (last update March 2015).



- Fayer MJ and JM Keller. 2007. *Recharge Data package for Hanford Single-Shell Tank Waste Management Areas*. PNNL-16688, Pacific Northwest National Laboratory, Richland, WA.
- Fayer MJ, DL Saunders, RS Herrington, and D Felmy. 2010. *Soil Water Balance and Recharge Monitoring for the Hanford Site – FY 2010 Status Report*. PNNL-19945, Pacific Northwest National Laboratory, Richland, WA.
- Fayer MH and TB Walters. 1995. *Estimated Recharge Rates at the Hanford Site*. PNL-10285, Pacific Northwest National Laboratory, Richland, WA.
- Fetter CW. 1993. *Contaminant Hydrogeology*. MacMillan Publishing Company, New York.
- Fukui M, Y Fujikawa, and N Satta. 1996. “Factors Affecting Interaction of Radioiodide and Iodate Species with Soil.” *Journal of Environmental Radioactivity* 31(2):199-216.
- Hammond TB and D Lupton. 2015. *Development of the Hanford South Geologic Framework Model, Hanford Site, Washington*. ECF-HANFORD-13-0029, Rev. 2, CH2M Hill Plateau Remediation Company, Richland, WA.
- Kaplan DI. 2003. “Influence of Surface Charge of an Fe-Oxide and an Organic Matter Dominated Soil on Iodide and Perchnetate Sorption.” *Radiochimica Acta* 91(3):173-178.
- Kaplan DI, ME Denham, S Zhang, C Yeager, C Xu, KA Schwehr, H-P Li, YF Ho, D Wellman, and PH Santschi. 2014. “Radioiodine Biogeochemistry and Prevalence in Groundwater.” *Critical Reviews in Environmental Science & Technology* 44(20):2287-2335. doi: 10.1080/10643389.2013.828273.
- Kaplan DI, RJ Serne, KE Parker, and IV Kutnyakov. 2000. “Iodide Sorption to Subsurface Sediments and Illitic Minerals.” *Environmental Science & Technology* 34(3): 399-405, doi:10.1021/es990220g.
- Kaplan DI, C Yeager, ME Denham, S Zhang, C Xu, KA Schwehr, H-P Li, R Brinkmeyer, and PH Santschi. 2012. *Biogeochemical Considerations Related to the Remediation of <sup>129</sup>I Plumes*. SRNL-STI-2012-00425, Rev. 0 (RPT-DVZ-AFRI-002), Savannah River National Laboratory, Aiken, SC.
- Keppler F, R Eiden, V Niedan, J Pracht, and HF Schöler. 2000. “Halocarbons Produced by Natural Oxidation Processes During Degradation of Organic Matter.” *Nature* 403(6767):298-301.
- Khaleel R and EJ Freeman. 1995. *Variability and Scaling of Hydraulic Properties for 200 Area Soils, Hanford Site*. WHC-EP-0883, Westinghouse Hanford Company, Richland, WA.
- Kodama S, Y Takahashi, K Okumura, and T Uruga. 2006. “Speciation of Iodine in Solid Environmental Samples by Iodine K-edge XANES: Application to Soils and Ferromanganese Oxides.” *Science of the Total Environment* 363(1-3):275-284.
- Last GV, ML Rockhold, CJ Murray, and KJ Cantrell. 2009. *Selection and Traceability of Parameters to Support Hanford-Specific RESRAD Analyses – Fiscal Year 2008 Status Report*. PNNL-18564, Pacific Northwest National Laboratory, Richland, WA.
- Last GV, EJ Freedman, KJ Cantrell, MJ Fayer, GW Gee, WE Nichols, BN Bjornstad, DG Horton. 2006. *Vadose Zone Hydrogeology Data Package for the 2004 Composite Analysis*. PNNL-14702, Rev. 1, Pacific Northwest National Laboratory, Richland, WA.

Lee BD, JT Ellis, A Dodwell, EER Eisenhauer, DL Saunders, and MH Lee. 2018. “Iodate and Nitrate Transformation by Agrobacterium/Rhizobium Related Strain Dvz35 Isolated from Contaminated Hanford Groundwater.” *Journal of Hazardous Materials* 350:19-26. <https://doi.org/10.1016/j.jhazmat.2018.02.006>

Luther GW III. 2011. “Thermodynamic Redox Calculations for One and Two Electron Transfer Steps: implications for Halide Oxidation and Halogen Environmental Cycling.” In Tratnyek P, T Grundl, and SB Haderlein (eds). *Aquatic Redox Chemistry*, Vol. 1071. Washington, D.C: American Chemical Society, pp. 15-35.

McDonald JP. 2018. *Capture –Zone and Particle-Tracking Analysis for the WMA S-SX Pump and Treat System Using a Sub Model from the 2017 Updated Central Plateau Model*. ECF-200W-17-0045, Rev. 0. CH2M Plateau Remediation Company, Richland, WA.

Neal C and VW Truesdale. 1976. “Sorption of Iodate and Iodide by Riverine Sediments – Its Implications to Dilution Gauging and Hydrochemistry of Iodine.” *Journal of Hydrology* 31(3-4):281-291.

Neeway, JJ, DI Kaplan, CE Bagwell, ML Rockhold, JE Szecsody, MJ Truex, and NP Qafoku. 2019. “A review of the behavior of radioiodine in the subsurface at two DOE sites.” *Science of the Total Environment* 691:466-475.

Otosaka S, KA Schwehr, DI Kaplan, KA Roberts, S Zhang, C Xu, H Li, Y Ho, R Brinkmeyer, CM Yeager, PM Santschi. 2011. “Factors controlling mobility of <sup>127</sup>I and <sup>129</sup>I species in an acidic groundwater plume at the Savannah River Site.” *Science of the Total Environment* 409(10):3857-3865.

Podder J, J Line, W Sun, Y Pan, SM Botis, J Tse, N Chen, Y Hu, D Li, and J Seaman. 2015. “Uptake and speciation of iodine in calcium carbonate.” In Proceedings of the 35<sup>th</sup> Annual Canadian Nuclear Society (CNS) Conference, Saint John, NB, Canada, May 31- June 3 2015.

Qafoku NP, C Bagwell, AR Lawter, MJ Truex, JE Szecsody, O Qafoku, L Kovarik, L Zhong, A Mitroshkov, V Freedman. 2018. *Conceptual Model of Subsurface Processes for Iodine at the Hanford Site*. PNNL-28053; DVZ-RPT-0004, Rev. 0, Pacific Northwest National Laboratory, Richland, WA.

Rockhold ML, JL Downs, SR Waichler, CMR Yonkofski, VL Freedman, and MJ Truex. 2018b. *Draft Technical Impracticability Evaluation for Iodine-129 in Groundwater at Hanford: 200-UP-1 Operable Unit*. PNNL-28057; DVZ-RPT-0016, Rev. 0, Pacific Northwest National Laboratory, Richland, WA.

Rockhold ML, MJ Fayer, and PR Heller. 1993. *Physical and Hydraulic Properties of Sediments and Engineered Materials Associated with Grouted Double-Shell Tanks Waste Disposal at Hanford*. PNL-8813, Pacific Northwest Laboratory, Richland, WA.

Rockhold ML, DL Saunders, CE Strickland, SR Waichler, RE Clayton. 2009. *Soil Water Balance and Recharge Monitoring at the Hanford Site – FY09 Status Report*. PNNL-18807, Pacific Northwest National Laboratory, Richland, WA.

Rockhold ML, FA Spane, TW Wietsma, DR Newcomer, RE Clayton, I Demirkanli, DL Saunders, MJ Truex, MM Valenta-Snyder, and CJ Thompson. 2018a. *Physical and Hydraulic Properties of Sediments from the 200-DV-1 Operable Unit*. PNNL-27846; RPT-DVZ-CHPRC 0005, Rev. 0, Pacific Northwest National Laboratory, Richland, WA.

Rockhold ML, ZF Zhang, PD Meyer, and JN Thomle. 2015. *Physical, Hydraulic, and Transport Properties of Sediments and Engineered Materials Associated with Hanford Immobilized Low-Activity Waste*. PNNL-23711; RPT-IGTP-004, Rev. 0, Pacific Northwest National Laboratory, Richland, WA.

Sakurai T, A Takahashi, N Ishikawa, and Y Komaki. 1989. "The Behavior of Iodine in a Simulated Spent-Fuel Solution." *Nuclear Technology* 85:206-212.

Santschi PH, C Xu, S Zhang, KA Schwehr, R Grandbois, DI Kaplan, and CM Yeager. 2017. "Iodine and Plutonium Association with Natural Organic Matter: A Review of Recent Advances." *Applied Geochemistry* 85:121-127.

Santschi PH, C Xu, S Zhang, Y –F Ho, H P Li, KA Schwehr, and DI Kaplan. 2012. *Laboratory Report on Iodine <sup>129</sup>I and <sup>127</sup>I Speciation, Transformation, and Mobility in Hanford Groundwater, Suspended Particle, and Sediments*. SRNL-STI-2012-00592, Rev. 0, Savannah River National Laboratory, Aiken, SC.

Sheppard MI and DH Thibault. 1991. "A 4-Year Mobility Study of Selected Trace-Elements and Heavy-Metals." *Journal of Environmental Quality* 20(1):101-114.

Shetaya WH, SD Young, MJ Watts, EL Ander, and EH Bailey. 2012. "Iodine dynamics in soils." *Geochimica et Cosmochimica Acta* 77:457-473.

Spane FA and DR Newcomer. 2004. *Results of Detailed Hydrologic Characterization Tests Fiscal Year 2003*. PNNL-14804, Pacific Northwest National Laboratory, Richland, WA.

Spane FA and DR Newcomer. 2008. *Results of Detailed Hydrologic Characterization Tests – Fiscal and Calendar Year 2005*. PNNL-17348, Pacific Northwest National Laboratory, Richland, WA.

Spane FA and DR Newcomer. 2010a. *Slug Test Characterization Results for Multi-Test/Depth Intervals Conducted During the Drilling of CERCLA Operable Unit OU UP-1 Wells 299-W19-48, 699-30-66, and 699-36-70B*. PNNL-19482, Pacific Northwest National Laboratory, Richland, WA.

Spane FA and DR Newcomer. 2010b. *Slug Test Characterization Results for Multi-Test/Depth Intervals Conducted During the Drilling of CERCLA Operable Unit OU ZP-1 Wells 299-W11-43, 299-W15-50, and 299-W18-16*. PNNL-19491, Pacific Northwest National Laboratory, Richland, WA.

Spane FA, Jr., PD Thorne, and DR Newcomer. 2001a. *Results of Detailed Hydrologic Characterization Tests – Fiscal Year 1999*. PNNL-13378, Pacific Northwest National Laboratory, Richland, WA.

Spane FA, Jr., PD Thorne, and DR Newcomer. 2001b. *Results of Detailed Hydrologic Characterization Tests – Fiscal Year 2000*. PNNL-13514, Pacific Northwest National Laboratory, Richland, WA.

Spane FA, Jr., PD Thorne, and DR Newcomer. 2002. *Results of Detailed Hydrologic Characterization Tests – Fiscal Year 2001*. PNNL-14113, Pacific Northwest National Laboratory, Richland, WA.

Spane FA, Jr., PD Thorne, and DR Newcomer. 2003. *Results of Detailed Hydrologic Characterization Tests – Fiscal Year 2002*. PNNL-14186, Pacific Northwest National Laboratory, Richland, WA.

Springer SD. 2018. *Model Package Report: Central Plateau Vadose Zone Geoframework, Version 1.0*. CP-60925, Rev. 0, CH2MHill Plateau Remediation Company, Richland, WA.

Szecsody JE, BD Lee, AR Lawter, NP Qafoku, CT Resch, SR Baum, II Leavy, VL Freedman. 2017. *Effect of Co-Contaminants Uranium and Nitrate on Iodine Remediation*. PNNL-26955; RPT-DVZ-AFRI-048, Rev. 0.0, Pacific Northwest National Laboratory, Richland, WA.

Thorne PD and DR Newcomer. 2002. *Prototype Database and User's Guide of Saturated Zone Hydraulic Properties for the Hanford Site*. PNNL-14058, Pacific Northwest National Laboratory, Richland, WA.

Thorne PD, MP Bergeron, MD Williams, and VL Freedman. 2006. *Groundwater Data Package for Hanford Assessments*. PNNL-14753, Rev. 1, Pacific Northwest National Laboratory, Richland, WA.

Truex MJ, VL Freedman, JE Szecsody, and CI Pierce. 2019. *Assessment of Technologies for I-129 Remediation in the 200-UP-1 Operable Unit*. PNNL-29148, Pacific Northwest National Laboratory, Richland, WA.

Truex MJ, BD Lee, CD Johnson, NP Qafoku, JE Szecsody, JE Kyle, M Tfaily, MMV Snyder, KJ Cantrell, DL Saunders, AR Lawter, M Oostrom, G Tartakovsky, II Leavy, EM Mcelroy, D Appriou, R Sahajpal, MM Carroll, RK Chu, EA Cordova, GV Last, MH Lee, DI Kaplan, W Garcia, S Kerisit, O Qafoku, M Bowden, F Smith, JG Toyoda, and AE Plymale. 2017. *Conceptual Model of Iodine Behavior in the Subsurface at the Hanford Site*. PNNL-24709, Rev. 2, Pacific Northwest National Laboratory, Richland, WA.

Truex MJ, VR Vermeul, D Adamson, M Oostrom, L Zhang, RD Mackley, BG Fritz, JA Horner, TC Johnson, JN Thomle, DR Newcomer, CD Johnson, M Rysz, TW Wietsma, and CJ Newell. 2015. "Field Test of Enhanced Remedial Amendment Delivery Using a Shear-Thinning Fluid." *Ground Water Monitoring and Remediation* 35(3):34-45.

White MD and M Oostrom. 2006. *STOMP – Subsurface Transport Over Multiple Phases, Version 4.0, User's Guide*. PNNL-15782, Pacific Northwest National Laboratory, Richland, WA.

White MD, D Appriou, DH Bacon, Y Fang, V Freedman, ML Rockhold, C Ruprecht, G Tartakovsky, SK White, and F Zhang. 2018. *STOMP Online User Guide*. Accessed on September 15, 2018 at [http://stomp.pnnl.gov/user\\_guide/STOMP\\_guide.stm](http://stomp.pnnl.gov/user_guide/STOMP_guide.stm).

Whitehead DC. 1974. "The Sorption of Iodide by Soil Components." *Journal of the Science of Food and Agriculture* 25:73-79.

Whitehead D. 1984. "The Distribution and Transformations of Iodine in the Environment." *Environment International* 10(4):321-339.

Williams MD, PD Thorne, MP Bergeron, and DL Ward. 2006. *Transient Inverse Calibration of a Facies-Based Groundwater Flow and Transport Model using Contaminant Concentration and Hydraulic Head Data*. PNNL-16425 (Limited Distribution), Pacific Northwest National Laboratory, Richland, WA.

Xu C, D Kaplan, S Zhang, M Athon, Y Ho, H Li, C Yeager, K Schwehr, R Grandbois, D Wellman, and P Santschi. 2015. "Radioiodine sorption/desorption and speciation transformation by subsurface sediments from the Hanford Site." *Journal of Environmental Radioactivity* 139:43-55.

Yoshida S, Y Muramatsu, and S Uchida. 1992. "Studies on the Sorption of I- (iodide) and IO<sub>3</sub>- (iodate) onto Andosols." *Water Air and Soil Pollution* 63(3-4):321-329.

Yu Z, JA Warner, RA Dahlgren, and WH Casey. 1996. "Reactivity of Iodine in Volcanic Soils and Noncrystalline Soil Constituents." *Geochimica et Cosmochimica Acta* 60:4945-4956.

Zaher U and S Agnew. 2018. *Hanford Soil Inventory Model (SIM-v2) Calculated Radionuclide Inventory of Direct Liquid Discharges to Soil in the Hanford Site's 200 Areas*. ECF-HANFORD-17-0079, Rev. 0. CH2M Plateau Remediation Company, Richland, WA.


Zhang S, C Xu, D Creeley, Y -F Ho, H -P Li, R Grandbois, K A Schwehr, DI Kaplan, CM Yeager, D Wellman, and PH Santschi. 2013. "Iodine-129 and Iodine-127 Speciation in Groundwater at the Hanford Site, U.S.: Iodate Incorporation into Calcite." *Environmental Science & Technology* 47(17):9635-9642.  
<https://doi.org/10.1021/es401816e>


## Appendix A

### Summary Checklist for Groundwater Technical Impracticability Evaluation

The U.S. Environmental Protection Agency (EPA) Checklist for evaluating a Superfund site for consideration of a groundwater technical impracticability waiver is provided in this Appendix for convenience. For each applicable section of the EPA Checklist, the relevant sections of this document that address the checklist issue are identified.

Items in the checklist for which the required information is considered complete are marked .

Items that are considered to be not applicable for iodine-129 in the 200-UP-1 OU are marked .





















Items related to alternative remedial strategies, feasibility studies, and costs associated with remedies that have not been implemented are marked .

This checklist is not considered to be final, but is provided as an example and reference.
















## RECOMMENDED SUMMARY CHECKLIST FOR A SUPERFUND GROUNDWATER TECHNICAL IMPRACTICABILITY EVALUATION










Regions should consider the recommended checklist below when evaluating whether they have sufficient information to support a TI evaluation for the administrative record. [EPA 1993, 4.4]:

<b>A. Specific ARARs or Media Cleanup Standards [EPA 1993, 4.4.1]</b>		
<input checked="" type="checkbox"/>	Identifies the specific ARARs for which the TI waiver is sought	Section 1.0
<input checked="" type="checkbox"/>	Identifies the technical feasibility of restoring some of the groundwater contaminants	Section 1.1
<input checked="" type="checkbox"/>	Identifies potential benefits of attaining ARARs for some of the specific COCs	Section 1.1
<b>B. Spatial Extent of TI Decisions [EPA 1993, 4.4.2]</b>		
<input checked="" type="checkbox"/>	Specifies the spatial distribution (vertical and horizontal) of subsurface contaminants in the unsaturated and saturated zones where the TI is sought	Section 2.2 and 2.3
<input checked="" type="checkbox"/>	Identifies the spatial extent of the TI zone as small as possible	Section 2.2 and 2.3
<input checked="" type="checkbox"/>	Identifies the vertical limit of the TI zone in either absolute (e.g., mean sea level) or relative (e.g., aquifer system) terms	Section 2.3
<b>C. Development and Purpose of the Site Conceptual Model [EPA 1993, 4.4.3, Figure 4]</b>		
	<b>1. Background Information [EPA 1993, 4.4.3]</b>	
<input checked="" type="checkbox"/>	Groundwater classification	Section 3.1.6
<input checked="" type="checkbox"/>	Location of potential environmental receptors	Section 3.1.6
<input checked="" type="checkbox"/>	Nearby wellhead protection areas or sole-source aquifers	Section 3.1.6
<input checked="" type="checkbox"/>	Location of water supply wells	Section 3.1.6
	<b>2. Geologic and Hydrologic Information [EPA 1993, 4.4.3]</b>	
<input checked="" type="checkbox"/>	Description of regional and site geology	Section 3.1
<input checked="" type="checkbox"/>	Physical properties of subsurface materials	Section 3.1.1
<input checked="" type="checkbox"/>	Stratigraphy, including thickness, lateral extent, continuity of units, and presence of depositional features, such as channel deposits, that may provide preferential pathways for, or barriers to, contaminant transport	Section 3.1
<input checked="" type="checkbox"/>	Hydraulic gradients (horizontal and vertical)	Section 3.1.3
<input checked="" type="checkbox"/>	Geologic structures or other subsurface features that may form preferential pathways for NAPL migration or zones of accumulation	Section 3.1.3
<input checked="" type="checkbox"/>	Hydraulic properties of subsurface materials	Section 3.1.1

	Temporal variability in hydrologic conditions	Section 3.1.4
	Groundwater recharge and discharge information	Section 3.1.5
	Groundwater/surface water interactions	Section 3.1.6
	Characterization of secondary porosity features (e.g., fractures, karst features) to the extent practicable	Not applicable
	Depth to groundwater	Section 3.1.2
	<b>3. Contaminant Source and Release Information [EPA 1993, 4.4.3]</b>	
	Location, nature, and history of previous contaminant releases or sources	Sections 2.1 and 3.3
	Locations and characterizations of continuing releases or sources	Section 2.1
	Locations of subsurface sources (e.g., NAPLs)	Sections 2.1 and 3.3
	<b>4. Contaminant Distribution, Transport, and Fate Parameters [EPA 1993, 4.4.3]</b>	
	Temporal trends in contaminant concentrations in each phase	Sections 2.4 and 4.1.2
	Estimates of subsurface contaminant mass	Section 3.3
	Phase distribution of each contaminant in the unsaturated and saturated zones (e.g., gaseous, aqueous, sorbed, free-phase NAPL, or residual NAPL)	Section 3.4.1
	Spatial distribution of subsurface contaminants in each phase in the unsaturated and saturated zones	Section 3.4.1
	Sorption information, including contaminant retardation factors	Section 3.2.2
	Contaminant transformation processes and rate estimates	Section 3.2.3
	Contaminant migration rates	Section 3.4.1
	Assessment of facilitated transport mechanisms (e.g., colloidal transport)	Section 3.2
	Properties of NAPLs that affect transport (e.g., composition, effective solubility, density, viscosity)	Not applicable
	Geochemical characteristics of subsurface media that affect contaminant transport and fate	Section 3.2
	Other characteristics that affect distribution, transport, and fate (e.g., vapor transport properties)	Section 3.2
	<b>D. Evaluation of Restoration Potential [EPA 1993, 4.4.4]</b>	
	<b>1. Source Control Measures [EPA 1993, 4.4.4.1]</b>	
	Demonstrates that contamination sources have been located and will employ removal, migration control or containment, or treatment, to the extent practicable	Sections 2.1, 3.3, and 4.1



	<b>2. Remedial Action Performance Analysis [EPA 1993.4.4.4.2]</b>	
	Demonstrates that the groundwater monitoring program within and outside the aqueous contaminant plume is of sufficient quality and detail to fully evaluate remedial action performance (e.g., to analyze plume migration or containment and identify concentration trends within the remediation zone)	Section 4.1
	Demonstrates that the existing remedy has been effectively operated and adequately maintained	Section 4.1.1
	Describes and evaluates the effectiveness of any remedy modifications (whether variations in operation, physical changes, or augmentations to the system) designed to enhance its performance	Section 4.1.1
	Evaluates trends in subsurface contaminant concentrations. Consider such factors as whether the aqueous plume has been contained, whether the areal extent of the plume is being reduced, and the rates of contaminant concentration decline and contaminant mass removal. Further considerations include whether aqueous-phase concentrations rebound when the system is discontinued, whether dilution or other natural attenuation processes are responsible for observed trends, and whether contaminated soils on site are contaminating groundwater	Section 4.1.2
	Analyzes performance of any ongoing or completed remedial actions: Operational information	Section 4.1.1
	Analyzes performance of any ongoing or completed remedial actions: Enhancements to original remedy (including optimization efforts)	Not applicable
	<b>3. Restoration Timeframe Analysis [EPA 1993.4.4.4.3]</b>	
	Estimates timeframe for groundwater restoration	Section 4.2
	Documents predictive analyses of the timeframes to attain required cleanup levels as part of the overall demonstration using available technologies and approaches laying out the associated modeling inputs and uncertainties	Section 3.4
	<b>4. Other Applicable technologies [EPA 1993.4.4.4.4]</b>	
	Conducted and documented a literature search to determine what cleanup approaches are possible based on the contaminants and geology at the site	Truex et al. 2019
	Lists technologies and approaches that were evaluated	Truex et al. 2019
	Analyzed chemical and hydrogeologic data to support any technology capable of achieving cleanup levels	
	Evaluated treatability study data (bench, pilot or full-scale)	
	Demonstrates that no other remedial technologies (conventional or innovative) could reliably, logically, or feasibly attain the cleanup levels at the site within a reasonable timeframe	Truex et al. 2019
	<b>5. Cost Estimates [EPA 1993, 4.4.5]</b>	
	Provides cost estimates for the potentially viable remedial alternatives included in the Evaluation of Restoration Potential, including construction, operation and maintenance costs	
	Provides cost estimates of selected remedy(s) for continued operation of existing remedy including operation and maintenance costs (if a remedy has been implemented)	

	Provides cost estimates for the proposed Alternative Remedial Strategy (ARS)	
	<b>6. Alternate Remedial Strategies (ARS) [EPA 1993, 5.0]</b>	
	Selects and summarizes an ARS that is technically practicable, protective of human health and the environment, and satisfies Superfund statutory and regulatory requirements [EPA 1993, 5.1]	
	Demonstrates that the ARS addresses exposure prevention [EPA 1993, 5.1.1]	
	Demonstrates that the ARS addresses source control and remediation [EPA 1993, 5.1.2]	
	Demonstrates that the ARS addresses aqueous plume remediation [EPA 1993, 5.1.3]	
	<b>7. Additional Remedy Selection Considerations [EPA 1993, 5.2.3]</b>	
	Aggressive action for shorter timeframes than other options	
	Shorter timeframe to reduce potential human exposures	
	Shorter timeframe to reduce impacts to environmental receptors	
	Discusses additional information or analyses considered for the TI evaluation	

## Appendix B

### **Compendium of References on Iodine-129 at Hanford**

This appendix is a compendium of references related to groundwater iodine-129 contamination at Hanford. References are divided into four categories: 1) Iodine Conceptual Model, 2) Ex Situ Remedy Screening, 3) In Situ Remedy Screening, and 4) Characterization and Modeling.

## Iodine Conceptual Model

Neeway JJ, DI Kaplan, CE Bagwell, ML Rockhold, JE Szecsody, MJ Truex and NP Qafoku. 2019. “A review of the behavior of radioiodine in the subsurface at two DOE sites.” *Science of The Total Environment* 691:466-475.

The differences in the iodine behavior are described for the both the Hanford and Savannah River Sites. Due to differences in climate and biogeochemical conditions, predominant iodine species and subsequent remedies differ between the two sites.

Qafoku N, C Bagwell, AR Lawter, MJ Truex, JE Szecsody, O Qafoku, and L Kovarik, L Zhong, A Mitroshkov and V Freedman. 2018. *Conceptual Model of Subsurface Processes for Iodine at the Hanford Site*. PNNL-28053, Pacific Northwest National Laboratory, Richland, WA.

This final report on the iodine conceptual model provides summary level information on processes that affect  $^{129}\text{I}$  behavior in the subsurface and provides information needed to support fate and transport modeling and remedy evaluations.. Dominant biogeochemical processes are summarized in a comprehensive diagram that describes the interrelationship of these processes and the associated iodine chemical speciation. More detailed information on laboratory experiments conducted to identify this information is largely found in PNNL-24709, Rev. 2.

Truex MJ, BD Lee, CD Johnson, N Qafoku, JE Szecsody, JE Kyle, and MM Tfaily, MMV Snyder, KJ Cantrell, DL Saunders, AR Lawter, M Oostrom, G Tartakovsky, II Leavy, EM McElroy, D Appriou, R Sahajpal, MM Carroll, RK Chu, EA Cordova, GV Last, MH Lee, DI Kaplan, W Garcia, S Kerisit, O Qafoku, M Bowden, F Smith, JG Toyooda and AE Plymale. 2017. *Conceptual Model of Iodine Behavior in the Subsurface at the Hanford Site*. PNNL-24709, Rev. 2, Pacific Northwest National Laboratory, Richland, WA.

Revision 2 of this report describes the conceptual model elements for iodine behavior in the subsurface to support  $^{129}\text{I}$  fate and transport modeling, risk assessment, remedy decisions, and remedy design and implementation. Information describing the relative quantity of three primary iodine chemical species present in the groundwater (iodide, iodate, and organic-iodine complexes) is provided, and data describing iodine species transport properties and transformation reactions have been compiled. In addition, technical gaps are identified associated with the need to refine this information in support of future remedy decisions.

## Ex Situ Remedy Screening

Cordova EA, V Garayburu-Caruso, CI Pearce, KJ Cantrell, JW Morad, EC Gillispie, BJ Riley, FC Colon, TG Levitskaia, SA Saslow, O Qafoku, CT Resch, MJ Rigali, JE Szecsody, SM Heald, M Balasubramanian, P Meyers, VL Freedman. “Hybrid Sorbents for  $^{129}\text{I}$  Capture from Contaminated Groundwater.” *ACS Applied Materials & Interfaces*. To be submitted.

Compares the immobilization capacity of  $^{129}\text{I}$  across commercially available resins and silica beads and PAN beads with three different materials (ferrihydrite, bismuth oxy(hydroxide), and bismuth subnitrate. Evaluation is based on the resin and bead capacity to remove at least 97% of iodate from solution, thereby reducing the concentration of  $^{129}\text{I}$  from 30 pCi/L (average groundwater concentration in the Hanford site) to 1 pCi/L (primary drinking water standard). Although batch tests showed significant uptake capacity for iodate, column experiments

demonstrated marginal to poor performance for all resins tested, indicating further development is needed to optimize their performance.

Cantrell KJ, CI Pearce, EA Cordova, JW Morad, V Garayburu-Caruso, SA Saslow, BN Gartman, O Qafoku, TG Levitskaia, SM Heald, MJ Rigali, and VL Freedman. “Influence of Comingled Contaminants on Removal of <sup>99</sup>Tc and <sup>129</sup>I and from Contaminated Groundwater by Ion Exchange Resins.” *Journal of Environmental Radioactivity*. To be submitted.

Batch and flow-through column experiments evaluate the performance of different ion exchange resins with respect to 1) breakthrough capacity for pertechnetate, iodate and iodide; 2) impact of high co-contaminant concentrations; and 3) confounding effects of particulates and microbial activity at low, environmentally-relevant contaminant concentrations. The Purolite A530E was demonstrated to have a high affinity for iodide only (and possibly organo-iodine), but not iodate, the species that predominates in Hanford groundwater.

Campbell EL, TG Levitskaia, MS Fujimoto, VE Holfeltz, S Chatterjee, and GB Hall. 2018. *Analysis of Uranium Ion Exchange Resin from the 200 West Pump-and-Treat Facility*. PNNL-28062, Pacific Northwest National Laboratory, Richland, WA.

Analysis of Dowex 21K spent resin from the 200 West Pump-and-Treat facility was analyzed with respect to its loading for uranium and other constituents adhering to the resin. Results demonstrated that a significant amount of non-radioactive iodine was being retained on the resin, and radioactive iodine to a much lesser extent.

Campbell, EL, M Carlson, GB Hall, SD Chatterjee, O Qafoku and TG Levitskaia. “Characterization of Purolite A530E post removal of Pertechnetate from Contaminated Hanford Groundwater and Evaluation of Iodine Uptake.” To be submitted to *Chemical Engineering Journal*.

Analysis of Purolite A530E spent resin from the 200 West Pump-and-Treat facility was analyzed with respect to its loading for technetium-99 and other constituents adhering to the resin. The mechanism of iodine retention by the Purolite A530E resin for both iodide and iodate was identified.

Levitskaia TG, EL Campbell, SD Chatterjee and GB Hall. 2017. *Analysis of Technetium Ion Exchange Resin from the 200 West Pump-and-Treat Facility*. PNNL-26933, Pacific Northwest National Laboratory, Richland, WA.

Analysis of Purolite A530E spent resin from the 200 West Pump-and-Treat facility was analyzed with respect to its loading for technetium-99 and other constituents adhering to the resin. Information on total loading of stable and radioiodine retention, which exceeded the total loading technetium-99, is also provided in this report. The concentration ratio of stable to radioiodine on the resin is about 1000.

## **In Situ Remedy Screening**

Kerisit SN, FN Smith, S Saslow, M Hoover, A Lawter and N Qafoku. 2018. “Incorporation Modes of Iodate in Calcite.” *Environmental Science & Technology*. 52.10.1021/acs.est.8b00339.

To identify the potential for iodate sequestration in calcite, molecular dynamics simulations and extended X-ray absorption fine structure spectroscopy were used to determine the local

coordination environment of iodate in calcite. The pH was found to strongly affect the extent of iodate incorporation, that iodate accumulated on calcite surface, and that these particles may undergo mobilization under conditions that promote calcite dissolution.

Lawter AR, WL Garcia, RK Kukkadapu, O Qafoku, ME Bowden, SA Saslow and NP Qafoku. 2018. “Technetium and iodine aqueous species immobilization and transformations in the presence of strong reductants and calcite-forming solutions: Remedial action implications.” *Science of the Total Environment* 636:588-595.

Reductants (zero-valent iron and sulfur modified iron) and calcite-forming solutions were tested to simultaneously remove aqueous technetium-99 and iodate via reduction and incorporation, respectively. Although technetium-99 could be rapidly removed from the aqueous phase via reduction, the reduction caused iodate to transform to iodide, and therefore has the potential to mobilize radioiodine in groundwater.

Lawter AR, O Qafoku, FC Colon, CI Pearce, TG Levitskaia and NP Qafoku. “Simultaneous immobilization of aqueous co-contaminants using a bismuth layered material.” *Environmental Science & Technology Letters*. To be submitted.

Batch experiments were used to test the effectiveness of a bismuth layered oxide material remove co-located contaminants, including technetium-99, chromium, uranium, nitrate and iodine. The results of these batch tests demonstrated that the bismuth based oxy-hydroxide material is a promising material for sequestering multiple contaminants in situ, without an unintended consequence of iodine (or other contaminant) mobilization.

McElroy EM, AR Lawter, D Appriou, FN Smith, ME Bowden, O Qafoku, and L Kovarik, JE Szecsody, MJ Truex and NP Qafoku. “Iodate interactions with calcite: Implications for natural attenuation.” *Environmental Earth Sciences*. Submitted.

A series of macroscale batch experiments with solid phase characterization were conducted to identify various factors impacting time-dependent aqueous removal of iodate via calcite precipitation. Incorporation was identified as the main removal mechanism, although slower precipitation and/or adsorption in later times may have also contributed to iodate removal.

Moore, RC, CI Pearce, JW Morad, S Chatterjee, TG Levitskaia, R M Asmussen, AR Lawter, JJ Neeway, NP Qafoku, MJ Rigali, SA Saslow, JE Szecsody, PK Thallapally, G Wang, and VL Freedman. 2019. “Iodine immobilization by materials through sorption and redox-driven processes: A literature review.” *Science of The Total Environment*. <https://doi.org/10.1016/j.scitotenv.2019.06.166>. In Press.

Scientific literature was reviewed to compile information on materials that could potentially be used to immobilize  $^{129}\text{I}$  through sorption and redox-driven processes, with an emphasis on ex-situ processes. Compiled information includes material performance in terms of (i) capacity for  $^{129}\text{I}$  uptake; (ii) long-term performance; (iii) technology maturity; (iv) cost; (v) available quantity; (vi) environmental impact; (vii) ability to emplace the technology for in situ use at the field-scale; and (viii) ex situ treatment.

Pearce CI, EA Cordova, WL Garcia, SA Saslow, KJ Cantrell, JW Morad, O Qafoku, J Matyáš, AE Plymale, S Chatterjee, J Kang, FC Colon, TG Levitskaia, MJ Rigali, JE Szecsody, S Heald, M Balasubramanian, G Wang, DT Sun, WL Queen, R Bontchev, RC Moore and VL Freedman. “Evaluation of materials for iodine and technetium immobilization through sorption and redox-driven processes.” *Science of The Total Environment*. Submitted.

Based on the literature reviews, a suite of natural and engineered materials were selected for evaluation in terms of iodate and pertechnetate uptake capacity, selectivity and affinity. Material performance is compared with materials currently in use at the 200W P&T system, the Purolite A530E ion exchange resin and Carbon Activated Corporation 011-55 granulated activated carbon. Several materials were evaluated, including iron oxides, bismuth-based materials, organoclays, and metal organic frameworks.

Saslow SA, SN Kerisit, T Varga, KC Johnson, NM Avalos, AR Lawter, and NP Qafoku. 2019. "Chromate effects on iodate incorporation into calcite." *ACS Earth and Space Chemistry* 3(8):1624-1630.

Demonstrated that a decrease in iodate removal during calcite precipitation would occur when chromate was present, although its incorporation mode remained the same. Iodate readily substituted for carbonate but iodate and chromate clustering was unlikely when co-incorporated into calcite.

Strickland CE, CD Johnson, BD Lee, N Qafoku, JE Szecsody, MJ Truex, and VR Vermeul. 2017. *Identification of Promising Remediation Technologies for Iodine in the UP-1 Operable Unit*. PNNL-26934, Pacific Northwest National Laboratory, Richland, WA.

Identifies the broad set of potentially applicable iodine remediation methods for radioiodine. Technologies were reviewed and their evaluation categorized as 1) geochemical/biological sequestration, 2) microbial volatilization, and 3) enhanced pump-and-treat. A detailed description is provided for each of these promising remediation technologies, including discussion of data needs that allow for the evaluation of the technologies as part of a remediation alternatives assessment.

Szecsody JE, BD Lee, AR Lawter, N Qafoku, CT Resch, SR Baum, and II Leavy and VL Freedman. 2017. *Effect of Co-Contaminants Uranium and Nitrate on Iodine Remediation*. PNNL-26955, Pacific Northwest National Laboratory, Richland, WA.

Batch experiments were conducted to quantify coupled uranium-iodate behaviors and the influence of bio-reductive processes on iodine. Although the presence of uranium did not influence iodate removal from solution, uranium incorporation into iodate was more favorable and that iodine mass is mainly incorporated into a different surface phase than calcite. Abiotic processes were also found to control most of the observed iodate reduction at the sediment/water ratios relevant to the field.

Szecsody JE, HP Emerson, CI Pearce, CT Resch, and S Di Pietro. "Use of An Aqueous Reductant, Na-Dithionite, to Enhance Iodine Mobility from Aquifer Sediments." *Journal of Environmental Radioactivity*. Submitted.

Reports on the laboratory testing of an aqueous reductant (Na-dithionite) as a potential remedial approach for enhancing pump-and-treat extraction for iodine-contaminated sediments at 200-UP-1. This work investigated the treatment technology viability by examining iodine mass release, its release rate, and accelerated surface phase dissolution during groundwater flushing. The Na-dithionite enhances pump-and-treat by mobilizing solid-phase iodide. However, iodide precipitated within a few pore volumes, suggesting a limited long-term use of dithionite at the field scale for enhancing iodine pump-and-treat extraction through iodine mobilization.

Szecsody JE, G Wang, CI Pearce, AR Lawter, KJ Cantrell, EA Cordova, CF Brown, NP Qafoku, HP Emerson, EC Gillispie, BN Gartman, SR Kimming and V Garayburu-Caruso. 2019. *Evaluation of In Situ and Ex Situ Remediation Technologies for Iodine-129: Final Bench Scale Results*. PNNL-28064, Rev. 1, Pacific Northwest National Laboratory, Richland, WA.

This report provides detailed description of all technologies evaluated for radioiodine treatment that passed initial laboratory screening evaluations. This revision provides information on the most promising approaches, including both in situ and ex situ applications (calcite incorporation, iron oxide incorporation and sorption, enhancing pump-and-treat through mobilization of iodine with Na-dithionite, and various resin capacities).

Truex, MJ, VL Freedman, CI Pearce and JE Szecsody. 2019 *Assessment of Technologies for I-129 Remediation in the 200-UP-1 Operable Unit*. PNNL-29148. Pacific Northwest National Laboratory, Richland, WA.

This report provides an overview of all of the technologies evaluated for radioiodine treatment in terms of effectiveness, implementability, and relative cost similarly to how the screening evaluation is conducted for a CERCLA feasibility study. This evaluation also accounted for the maturity of the technologies with respect to the ability for viable consideration in a feasibility study.

Wang G, NP Qafoku, JE Szecsody, CE Strickland, CF Brown, and VL Freedman. 2019. "Time-Dependent Iodate and Iodide Adsorption to Fe Oxides." *ACS Earth and Space Chemistry*. doi:10.1021/acsearthspacechem.9b00145.

A series of macroscopic batch tests were conducted to test aqueous iodine removal via adsorption onto iron oxides. Time-dependent iodate was found to occur via multiple geochemical reactions, but iodide adsorption was determined to be insignificant.

Wang, G, JE Szecsody, NM Avalos, NP Qafoku, and VL Freedman. "In situ precipitation of hydrous ferric oxide (HFO) for remediation of subsurface iodine contamination." *Journal of Contaminant Hydrology*. To be submitted.

Injection of a hydrous ferric oxide (HFO) solution was injected into bench-scale column experiments packed with Hanford sediments to sequester iodine through both adsorption and co-precipitation processes. Although the transport of iodate in the HFO-amended sediments was strongly retarded through both adsorption and co-precipitation processes, reversible adsorption was observed and was not a permanent sequestration mechanism for iodate.

### **Characterization and Modeling**

Lee, B, J Szecsody, N Qafoku, E McElroy, S Baum, M Snyder, A Lawter, M Truex, B Gartman, L Zhong, D Saunders, B Williams, J Horner, I Leavy, C Resch, B Christiansen, R Clayton, and K Johnson. 2017. *Contaminant Attenuation and Transport Characterization of 200-UP-1 Operable Unit Sediment Samples*. PNNL-26894, Pacific Northwest National Laboratory, Richland, WA.

Through a data quality objectives process, sediment cores from the 200-UP-1 operable unit were drilled and evaluated for attenuation and transport processes for mobile contaminants, including radioiodine. Information on contaminant distributions, hydrologic and biogeochemical settings, attenuation processes and transport parameters are identified for use in evaluating future remedies.



Rockhold ML, JL Downs, SR Waichler, C Yonkofski, VL Freedman, and MJ Truex. 2019. Information on *Technical Impracticability for Remediation of Iodine-129 Contamination – Summary of Data and Modeling for Hanford Site 200-UP-1 Operable Unit*. PNNL-28057, Rev. 1, Pacific Northwest National Laboratory, Richland, WA.

This report provides information needed to support consideration of a technical impracticability (TI) waiver for iodine for 200-UP-1 groundwater. This includes the EPA's recommended summary checklist for Superfund site groundwater TI evaluation. Using conceptual model information on iodine fate and transport reported in PNNL-28053, the technical basis for iodine subsurface transport parameters at Hanford is also provided in this report.

He X, ML Rockhold, Y Fang, AL Lawter, NP Qafoku. "Evaluation of Attenuation Mechanisms for a Groundwater Radioiodine Plume." *To be submitted to J. Contaminant Hydrol. or J. Environ. Radioactivity*

Laboratory experimental data on transport and sorption of different iodine species are used with field observations and modeling to evaluate the relative importance of different mechanisms on radioiodine plume attenuation at the field scale.

Szecsody J, M Truex, B Lee, C Strickland, J Moran, M Snyder, C Resch, L Zhong, B Gartman, D Saunders, S Baum, I Leavy, J Horner, B Williams, B Christiansen, E McElroy, M Nims, R Clayton, and D Appriou, 2017. *Geochemical, Microbial, and Physical characterization of 200-DV-1 Operable Unit B-Complex Cores from Boreholes C9552, C9487, and C9488 on the Hanford Site Central Plateau*. PNNL-26266, Pacific Northwest National Laboratory, Richland, WA.

Through a data quality objectives process, 200-DV-1 waste sites at the B-Complex were selected for evaluation of attenuation and transport processes for mobile contaminants, including radioiodine. Information on contaminant distributions, hydrologic and biogeochemical settings, attenuation processes and transport parameters are identified for use in evaluating future remedies, and may be relevant to iodine in the 200-UP-1 groundwater.

Truex M, J Szecsody, N Qafoku, C Strickland, J Moran, B Lee, M Snyder, A Lawter, C Resch, B Gartman, L Zhong, M Nims, D Saunders, B Williams, J Horner, I Leavy, S Baum, B Christiansen, R Clayton, E McElroy, D Appriou, K Tyrell, M Striluk. 2017. *Contaminant Attenuation and Transport Characterization of 200-DV-1 Operable Unit Sediment Samples*. PNNL-26208, Pacific Northwest National Laboratory, Richland, WA.

Through a data quality objectives process, 200-DV-1 waste sites at S- and T- Complexes were selected for evaluation of attenuation and transport processes for mobile contaminants, including radioiodine. Information on contaminant distributions, hydrologic and biogeochemical settings, attenuation processes and transport parameters are identified for use in evaluating future remedies, and may be relevant to iodine in the 200-UP-1 groundwater.

# **Pacific Northwest National Laboratory**

902 Battelle Boulevard  
P.O. Box 999  
Richland, WA 99354  
1-888-375-PNNL (7665)

***[www.pnnl.gov](http://www.pnnl.gov)***